INFORMATION TO USERS

This manuscript has been reproduced from the microfilm master. UMI films the text directly from the original or copy submitted. Thus, some thesis and dissertation copies are in typewriter face, while others may be from any type of computer printer.

The quality of this reproduction is dependent upon the quality of the copy submitted. Broken or indistinct print, colored or poor quality illustrations and photographs, print bleedthrough, substandard margins, and improper alignment can adversely affect reproduction.

In the unlikely event that the author did not send UMI a complete manuscript and there are missing pages, these will be noted. Also, if unauthorized copyright material had to be removed, a note will indicate the deletion.

Oversize materials (e.g., maps, drawings, charts) are reproduced by sectioning the original, beginning at the upper left-hand corner and continuing from left to right in equal sections with small overlaps. Each original is also photographed in one exposure and is included in reduced form at the back of the book.

Photographs included in the original manuscript have been reproduced xerographically in this copy. Higher quality 6" x 9" black and white photographic prints are available for any photographs or illustrations appearing in this copy for an additional charge. Contact UMI directly to order.

UMI

A Bell & Howell Information Company
300 North Zeeb Road, Ann Arbor MI 48106-1346 USA
313/761-4700 800/521-0600

A method for determining mixed mode stress intensity factors using strain gage data

by

Gregory Roger Swanson

A dissertation submitted to the graduate faculty
in partial fulfillment of the requirements for the degree of
DOCTOR OF PHILOSOPHY

Major: Engineering Mechanics
Major Professor: Loren W. Zachary

Iowa State University
Ames, Iowa
1997

Graduate College

Iowa State University

This is to certify that the Doctoral dissertation of

Gregory Roger Swanson

has met the dissertation requirements of Iowa State University

Signature was redacted for privacy.

Major Professor

Signature was redacted for privacy.

For the Major Program

Signature was redacted for privacy.

For the Graduate College

TABLE OF CONTENTS

CHAPTER 1. INTRODUCTION

Fracture mechanics life has become a design requirement for advanced aerospace structures. The basic requirement is that a structure survive its design life with no compromise in fit, form, or function, using an assumed initial flaw of the size that could escape detection by the non-destructive testing (NDT) imposed on the component [1,2]. Additionally, fracture mechanics is used to assess the use of components that have detected flaws that were introduced during fabrication or service [3]. Normally, cracked hardware is subject to limited use with frequent inspections to monitor the growth of the defect. A limitation of the fracture mechanics analysis procedures and software used in the aerospace industry is the restriction to load control only problems [4]. This means that the load is conservatively assumed to be constant and unrelieved by growth of a defect. However, for many applications the load in a component is due to displacement control, or a mixture of load and displacement control, and a crack will relieve the displacement load reducing the load on the net section. This is a non-trivial problem to model since a crack has to be included in the analysis of the part to understand the load redistribution due to the crack and is the reason why the conservative load control assumption is made. Otherwise all possible cracks in all sections of all components would need to be analyzed.

Therefore a need exists for an experimental technique that can measure the crack size and stress intensity factors on a structure as the crack propagates. This will allow the analyst to determine if the crack is relieving the load in a component and therefore is a safe condition for continued service.

A strain gage method for measuring the opening mode

stress intensity factor, KI, has been presented by Dally and Sanford [5]. An extension of this to an overdeterministic method using multiple strain gages was presented by Dally and Berger [6]. Dally and Berger [7] extended the opening mode work to include mixed modes KI and KII. The overdeterministic method eliminated some of the constraints on gage orientation and location of the original method, however, knowledge of the crack tip location and orientation relative to the strain gages must still be known.

In this paper the strain gage method is extended to determine crack tip location and angular orientation relative to the strain gages in addition to the mixed-mode stress intensity factors. The theory for the strain fields near a crack tip and the relation to KI and KII is briefly reviewed. A generalized coordinate system introducing crack tip location and orientation variables is presented. Significance testing of the coefficients in the strain field equations is performed to establish practical limits for the infinite series used to model the strain fields. A weighted multiple linear least squares routine is developed to calculate stress intensity factors and crack tip location and orientation.

Experimental strain gage data for two test specimens is presented along with numerical modeling of the specimens. The first specimen is a standard compact tension specimen with a crack-like notch introduced by electro-discharge machining (EDM). The second is a mixed mode plate specimen which allows the ratio of KII to KI to be varied from 0 to 2.2, and is based on a specimen used by Sanford and Dally [8].

CHAPTER 2. LITERATURE REVIEW ON DETERMINING CRACK STRESS INTENSITY FACTORS

The strain fields in the immediate vicinity of a crack are influenced by both the crack geometry and the state of stress in the component. For any given geometry and stress state the strain can be determined experimentally and/or numerically. If the strain state near the crack tip is correlated to the stress intensity factors acting on the crack tip then the growth rate of the crack and potential for catastrophic failure when critical stress intensity factors are exceeded can be determined. Unfortunately, it is very difficult to determine analytically the stress state in complex structures in the presence of a crack since most structures see a combination of load and displacement controlled loading.

Experimental Methods

For the purposes of determining strain information and crack stress intensity information in the vicinity of a crack tip, the experimental techniques can be divided into the two broad categories of optical and strain gage.

Optical

The optical methods applicable to existing structures are photoelasticity, moiré, and caustics. The basic photoelastic technique requires a birefringent material as a model of the component or as a coating on the component, a polaroscope, a source of light, and an optical recording device [9]. This method provides the difference between the principal in-plane stresses (or strains if the photoelastic material is linear elastic). Sanford and Dally [8], Sanford, Chona, Farney, and Irwin [10], Sanford [11], and Dally and Etheridge [12] have

conducted experiments using this technique to determine mixed mode stress intensity parameters. The method has been shown to yield high quality results on models but has the inherent limitation of optical viewing of the test article by the polaroscope. Paris, Picon, Marin, and Cana [13] provide a methodology for processing photoelastic data to determine accurate values of KI and KII. The difficulties associated with obtaining reliable convergence of iterative schemes is addressed with an overdeterministic Newton-Raphson least squares method. In this paper a similar difficulty while processing strain gage data is overcome with an iterative least squares method.

The moiré technique is capable of measuring displacements with a resolution in the sub-wavelength of light. The method uses a reference grid, or array, of lines or points and an identical grid, or array, placed on the specimen to be analyzed [9]. MacKenzie, Walker, and Giannettoni [14], Post and Baracat [15], Weissman and Post [16], and Post [17] have demonstrated the accuracy and sensitivity of this method to measure the in-plane mixed mode stress intensity factors, KI and KII. The method requires an interferometer to achieve the high sensitivity and special optical filtering techniques to remove initial differences between the reference grid and the specimen. Although the method has been demonstrated to have very high resolution, it still requires visible access to the component and knowledge of the crack location and orientation.

In the method of caustics the information about the stress intensity factors is derived from the sharp strain and stress gradient at the crack tip. The caustic pattern is caused by the lens shape of the gradient at the crack tip interacting with light reflected from or transmitted through the specimen. The shape and size of the pattern can be used

to determine stress intensity parameters. Younis [18], Theocaris and Gdoutos [19], Theocaris and Papadopoulas [20], and Theocaris [21] have applied this technique to determining the mixed mode stress intensity factors. There are several limitations to this technique, namely that the crack tip is obscured by the caustic pattern, the specimen must be illuminated, and, for some techniques, a transparent specimen is required.

Nigam and Shukla [22]and Sanford [23] compare the optical methods for determining the stress intensity factors of fracture. Sanford summarizes that a general procedure using full field optical fringe patterns with a high degree of data redundancy (6 or more data points for each unknown) will provide accurate results. The difficulty of implementing the general method proposed is overcome with modern computers and digitization equipment. Nigam and Shukla concluded that the caustic and photoelastic techniques give reasonable results for static problems provided the caustic initial curve radius is at least half the plate thickness. For dynamic experiments photoelastic and caustic methods did not compare well. The error was believed to be a result of the higher order terms in the stress function being included in the photoelastic method but not in the caustic method.

The optical methods provide the analyst with methods to use the full field of information surrounding a crack tip if the limitations of the methods can be accepted. In cases where the component is not transparent the optical methods become restricted. In cases where the area of interest is hidden from view, the optical methods do not apply. Further, the methods do not lend themselves to a fully automated technique without digitization of an image.

Strain Gage

The electrical resistance strain gage is based in the discovery by Lord Kelvin in 1856 that the resistance of copper and iron wire changes with applied strain [9, 24]. Further, Lord Kelvin also applied the Wheatstone bridge circuit to accurately measure the resistance of the wire. Commercially available bondable strain gages are based on this basic concept but with specialized alloys and packaging for easier use and interpretation of the data. Strain gages near a crack tip have been successfully used to determine static KI and KII [5-7]. Dally and Sanford [25,26] and Sanford, Dally, and Berger [27] have also applied the strain gage technique to measuring stress intensity factors of propagating cracks. The strain gage averages the strain measured over the area it covers on the component. Small gages are required in regions of rapidly varying strain. Dally and Berger [28] have addressed this issue and shown that small gages located appropriately near a crack tip will have negligible error. As an extension to the static problem, Swanson and Zachary [29] have generalized the solution to also locate the crack tip along with the mixed mode stress intensity factors. The strain gage method suffers from a limit on the data available since each gage covers a portion of the area near the crack tip and the method is restricted from the plastic zone near the crack tip. However, the strain gage technique does not require the component be viewed while loaded, and strain gages are commercially available that can endure very harsh environments so the technique lends itself to many more applications than optical techniques.

Analytical Methods

The analytical methods used to determine the stress intensity factors acting on a crack tip can be broadly categorized as closed form (exact or approximate) or numerical.

Closed Form

The closed form solutions for stress intensity factors presented in the literature are either exact or approximate solutions. Tada, Paris and Irwin [30] and Rooke and Cartwright [31] contain compilations of stress intensity factors for crack geometries with imposed loads and displacements. Parker [32] and Wilson [33] provide techniques for superimposing the solutions found elsewhere to solve a specific problem. A useful form for representing the strain field near a crack tip which contains the mixed mode stress intensity factors is shown in [7] and is elaborated on in Chapter 3.

Finite Element

The Finite Element Method [FEM] for solution of crack stress intensity factors takes two forms, the stress or displacement matching form, or the energy approach [33, 34]. The FEM method takes advantage of the fact that the square-root strain singularity at a crack tip can be modeled using quadratic isoparametric elements by placing the mid side nodes adjacent to the crack tip at the quarter points. Further, by using triangular instead of rectangular elements at the crack tip the singularity is also maintained over the element interior.

Stress or displacement matching uses the stresses or

displacements near the modeled crack tip. These are fit to the stress or displacement equations for the singularity dominated zone at the crack tip and the limit, as the distance to the crack tip goes to zero, is taken. The displacement matching form is conveniently available in commercial FEM software.

The energy approach is based on the amount of work required to extend a crack a small amount. The measure is made with either the energy release rate using virtual or actual crack extension or by taking the J-integral about a boundary surrounding the crack tip.

The FEM method is applicable to any geometry and loading condition the analyst wishes to model. Specific guidelines for consistent and accurate results are discussed with each of the FEM models presented in Chapter 5.

CHAPTER 3. STRAIN FIELD EQUATIONS

Mode I

Dally and Sanford [5] have shown the derivation of strain equations from the stress field for the mode one loading of a single crack in the vicinity of the tip, and Dally and Berger [7] have extended this for the mode two case. The stress field near a mode one loaded crack, based on the Westergaard equations, is:

$$\sigma_{xx} = \text{Re } Z - y \text{ Im } Z' - y \text{ Im } Y' + 2 \text{ Re } Y$$

$$\sigma_{yy} = \text{Re } Z + y \text{ Im } Z' + y \text{ Im } Y'$$

$$\tau_{xy} = - y \text{ Re } Z' - y \text{ Re } Y' - \text{Im } Y \qquad (1)$$

where the stress functions Z and Y can be represented by

$$Z(z) = \sum_{n=0}^{\infty} A_n z^{n-1/2}$$

$$Y(z) = \sum_{m=0}^{\infty} B_m z^{m} \qquad (2)$$

and where, for both mode I and II,

$$z = x + i y \qquad (3)$$

Dally and Sanford have reduced the mode I case, for plane stress conditions, to the following four parameter strain field.

$$
\begin{aligned}
2\,\mu\,\varepsilon_{x'x'} = {} & A_0\, r^{-1/2}\,[k\cos(\theta/2) \\
& - (1/2)\sin(\theta)\sin(3\theta/2)\cos(2\alpha) \\
& + (1/2)\sin(\theta)\cos(3\theta/2)\sin(2\alpha)] \\
& + B_0\,[\,k + \cos(2\alpha)] \\
& + A_1\, r^{1/2}\cos(\theta/2)[k + \sin^2(\theta/2)\cos(2\alpha) \\
& - (1/2)\sin(\theta)\sin(2\alpha)] \\
& + B_1\, r\,[(k + \cos(2\alpha))\cos(\theta) \\
& - 2\sin(\theta)\sin(2\alpha)]
\end{aligned}
\tag{4}
$$

where,

μ = Shear modulus

$\varepsilon_{x'x'}$ = Stain gage reading

r = Distance to gage

θ = Angle to gage

α = Gage angle relative to crack tip

A_0 = Constant

B_0 = Constant

A_1 = Constant

B_1 = Constant

ν = Poisson's ratio

For the plane stress conditions on the free surface that a strain gage could be mounted on,

$$k = (1 - \nu) / (1 + \nu) \tag{5}$$

and,

$$KI = \sqrt{2\Pi}\ A_0 \qquad (6)$$

Mode II

The stress field near a mode two loaded crack, based on the Westergaard equations, is:

$$\sigma_{xx} = \text{Im } Y + y \text{ Re } Y' + y \text{ Re } Z' + 2 \text{ Im } Z$$

$$\sigma_{yy} = \text{Im } Y - y \text{ Re } Y' - y \text{ Re } Z'$$

$$\tau_{xy} = - y \text{ Im } Y' - y \text{ Im } Z' + \text{Re } Z \qquad (7)$$

where the stress functions Z and Y can be represented by

$$Z(z) = \sum_{n=0}^{\infty} C_n\ z^{n-1/2}$$

$$Y(z) = \sum_{m=0}^{\infty} D_m\ z^{m} \qquad (8)$$

Dally and Berger have reduced the mode II case, for plane stress conditions, to the following four parameter strain field. Note that the D_0 term drops out of the following equations. Also, minor errors in the reference have been corrected here.

$$E\,\varepsilon_{x'x'} = C_0\ r^{-1/2}\ \{\sin(\theta/2)[\sin^2(\alpha)$$
$$((1+\nu)\cos(\theta/2)\cos(3\theta/2)+2\nu)$$
$$-\cos^2(\alpha)((1+\nu)\cos(\theta/2)\cos(3\theta/2)+2)]$$
$$+2(1+\nu)\sin(\alpha)\cos(\alpha)\cos(\theta/2)$$

$$(1-\sin(\theta/2)\sin(3\theta/2))\}$$
$$+ C_1\, r^{1/2}\{\sin(\theta/2)[\cos^2(\alpha)((1+\nu)\cos^2(\theta/2)+2)$$
$$-\sin^2(\alpha)((1+\nu)\cos^2(\theta/2)-2\nu)]$$
$$+2(1+\nu)\sin(\alpha)\cos(\alpha)\cos(\theta/2)$$
$$(1+\sin^2(\theta/2))\}$$
$$+ 2\, D_1\, r\, [\sin(\theta)(\cos^2(\alpha)-\nu\sin^2(\alpha)] \qquad (9)$$

where,

C_0 = Constant

C_1 = Constant

D_1 = Constant

and,

$$KII = \sqrt{2\Pi}\ C_0 \qquad (10)$$

Collecting the terms in Equation 9 into a form similar to Equation 4:

$$2\,\mu\,\varepsilon_{x'x'} = C_0\, r^{-1/2}\,[\sin(\theta/2)(-k-\cos(2\alpha)(1+\cos(\theta/2)$$
$$\cos(3\theta/2)))+\sin(2\alpha)(\cos(\theta/2)-0.5\sin(\theta)\sin(3\theta/2)))$$
$$+C_1\, r^{1/2}[\sin(\theta/2)(k+\cos(2\alpha)(1+\cos^2(\theta/2)))$$
$$+\sin(2\alpha)\cos(\theta/2)(1+\sin^2(\theta/2))]$$
$$+ D_1\, r\, \sin(\theta)(k+\cos(2\alpha)) \qquad (11)$$

Mixed Modes

Combined, the mixed mode strain equations are:

$$
\begin{aligned}
2\,\mu\,\varepsilon_{x'x'} = {} & A_0\, r^{-1/2}\,[k\cos(\theta/2) \\
& - (1/2)\sin(\theta)\sin(3\theta/2)\cos(2\alpha) \\
& + (1/2)\sin(\theta)\cos(3\theta/2)\sin(2\alpha)] \\
& + B_0\,[\,k + \cos(2\alpha)] \\
& + A_1\, r^{1/2}\cos(\theta/2)[k + \sin^2(\theta/2)\cos(2\alpha) \\
& - (1/2)\sin(\theta)\sin(2\alpha)] \\
& + B_1\, r\,[(k + \cos(2\alpha))\cos(\theta) \\
& - 2\sin(\theta)\sin(2\alpha)] \\
& + C_0\, r^{-1/2}\,[\sin(\theta/2)(-k-\cos(2\alpha)(1 + \cos(\theta/2) \\
& \cos(3\theta/2))) + \sin(2\alpha)(\cos(\theta/2) - 0.5\sin(\theta)\sin(3\theta/2))) \\
& + C_1\, r^{1/2}[\sin(\theta/2)(k + \cos(2\alpha)(1+\cos^2(\theta/2))) \\
& + \sin(2\alpha)\cos(\theta/2)(1+\sin^2(\theta/2))] \\
& + D_1\, r\sin(\theta)(k+\cos(2\alpha))
\end{aligned}
\qquad (12)
$$

Generalized Coordinate System

Figure 1 shows the generalized coordinate system for the crack tip location, orientation, and the strain gage locations and orientations. The location of each strain gage relative to the crack tip is defined by:

$$r = \sqrt{(X_G - X_C)^2 + (Y_G - Y_C)^2} \qquad (13)$$

$$\theta = \mathrm{ArcTan}\left[\frac{-(X_G - X_C)\sin(\beta) + (Y_G - Y_C)\cos(\beta)}{(X_G - X_C)\cos(\beta) + (Y_G - Y_C)\sin(\beta)}\right] \qquad (14)$$

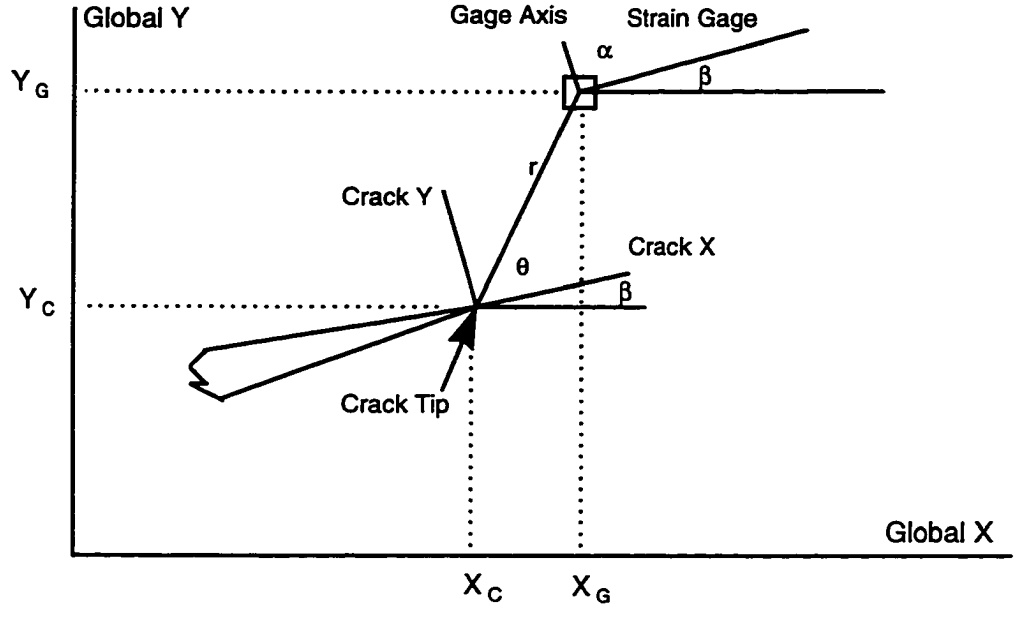

Figure 1. Crack Tip General Coordinate System

r = Distance to gage from crack tip

θ = Angle to gage from crack tip

β = Crack tip orientation angle

Significance Testing of Coefficients

Since the number of terms in the strain field equation is potentially infinite a multiple regression analysis of the significance of the higher order terms is performed for the mode one loaded crack tip. Applying the methods of Cox [35] on experimental data from a 10 element strain gage on a mode one compact tension (CT) specimen and also numerical data at the gage locations from a finite element model (FEM) of the same CT specimen, the significance of the higher order terms is tested. The data and statistical model are cast in the

form:

$$(\varepsilon_i\ ,\ X_{1i},\ X_{2i},\ .\ .\ .\ ,\ X_{pi}) \quad i = 1,\ .\ .\ .\ ,\ n \qquad (15)$$

$$\varepsilon_i = \beta_0 + \beta_1 X_{1i} + \beta_2 X_{2i} + .\ .\ . + \beta_p X_{pi} + \xi_I \qquad (16)$$

where,

ε_i = Strain

Xn_i = Functions of r, θ, and α

β_i = Coefficients A_i and B_i

ξ_I = Individual deviation from model

Equation 16 is used to represent the mode one only case of Equation 12. The statistical tests are, first, whether or not all $\beta_i = 0$ and, second, do higher order terms significantly improve the fit of the equation to the data. The first test is:

$H_T : \beta_1 = \beta_2 = .\ .\ . = \beta_p = 0$

H_A : not all $\beta_i = 0$; 0.005

$F_{\alpha 1} = F\ (p\ ,\ n - 1 - p;\ 0.005)$

$$F_{T1} = \left[\frac{(\text{sum of squares due to model parameters})(n-1-p)}{(\text{residual sum of squares})(p)}\right]$$

If $F_{T1} < F_{\alpha 1}$ accept H_T

If $F_{T1} > F_{\alpha 1}$ accept H_A

In all cases $F_{T1} > F_{\alpha 1}$ so not all $\beta_i = 0$. This means, for both the experimental and FEM data, the equations to which

the data is being fit are a significant improvement over the simple equation $\varepsilon_i = \varepsilon_{ave} + \xi_i$. The test is performed with up to four terms (A_0, B_0, A_1 and B_1) used in Equation 16. The second statistical test used is:

$$H_T : \beta_j \neq 0, \quad j = 1, \ldots, r$$

$$\text{and } \beta_j = 0, \quad j = r+1$$

$$H_A : \beta_j \neq 0, \quad j = 1, \ldots, r$$

$$\text{and } \beta_j \neq 0, \quad j = r+1$$

$$F_{T2} = \left[\frac{(\text{sum of squares due to additional term})(n-2-r)}{(\text{residual sum of squares})}\right]$$

$$F_{\alpha 2} = F\ (1\ ,\ n - 2 - r;\ 0.005)$$

If $F_{T2} < F_{\alpha 2}$ accept H_T

If $F_{T2} > F_{\alpha 2}$ accept H_A

This test is used to see if adding a higher order term to Equation 16 significantly improves the fit. The test is applied by sequentially adding higher order terms. Up to r^1.5 is tested. For the experimental strain gage data the A_0, B_0, and A_1 terms provide significant improvement in the equation's fit to the data. The B_1 term is marginally accepted, meaning F_{T2} nearly equals $F_{\alpha 2}$. For the FEM data the A_0, B_0, and A_1 terms provide significant improvement in the equation's fit and the B_1 term is rejected. For both data sets terms beyond the B_1 term are rejected. The conclusion drawn is the first three terms provide useful information. The remainder may be discarded since they provide no significant improvement in the fit. The rejection of higher order terms is also empirically pleasing since the strain field near a crack tip is expected to be dominated by singular

behavior. The rejected higher order terms represent functions that increase with increasing distance from the crack tip. Additional support for the truncated series is found in Berger and Dally [36] where a study of a compact tension specimen using up to a six parameter solution showed that the accuracy of the KI solution degraded with the addition of terms past the third (A_1). This occurred even though the higher order terms reduced the residual sum of the squares. Sanford et al. [10] also report that the six term series can exhibit instability causing convergence to erroneous solutions.

CHAPTER 4. WEIGHTED MULTIPLE LINEAR LEAST SQUARES ROUTINE

Mode I Only

To solve Equations 12, 13, and 14 simultaneously with overdeterministic strain gage data, the following method using multiple linear least squares and weighted residuals is developed. Equation 12 is cast in the following form for mode one only loading keeping only the terms statistically significant for the CT specimen, where the index i is for the i^{th} strain gage:

$$2\,\mu\varepsilon_i = A_0\,F_{0i}\,(r_i,\theta_i,\alpha_i) + B_0\,[\,k + \cos(2\,\alpha_i)\,] + A_1\,F_{1i}\,(r_i,\theta_i,\alpha_i) \qquad (17)$$

For 10 element strip strain gages the orientation angle α_i is the same for each gage, so let:

$$B'_0 = B_0\,[\,k + \cos(2\,\alpha)\,] \qquad (18)$$

Note that B'_0 is now a constant for all gages. If the crack tip location and orientation are known Equation 17 has only 3 unknown parameters, A_0, B_0, and A_1. The equation is now linear in the sense that all of the first order partial derivatives with respect to the unknown parameters are independent of the parameter values and, consequently, all higher order derivatives are zero [36]. Now a linear least squares routine [35, 37] is used to solve for the unknown terms, and Equation 6 is used to determine the stress intensity. In matrix form for N total strain gages:

$$\begin{bmatrix} 2\mu\varepsilon_1 \\ \cdot \\ \cdot \\ 2\mu\varepsilon_N \end{bmatrix} = \begin{bmatrix} 1 & (F_{01} - \bar{F}_0) & (F_{11} - \bar{F}_1) \\ \cdot & \cdot & \cdot \\ \cdot & \cdot & \cdot \\ 1 & (F_{0N} - \bar{F}_0) & (F_{1N} - \bar{F}_1) \end{bmatrix} \begin{bmatrix} B_0' \\ A_0 \\ A_1 \end{bmatrix} \tag{19}$$

$$\mathbf{Y} = \mathbf{X}\,\mathbf{B} \tag{20}$$

so,

$$\mathbf{B} = \left[\mathbf{X}^t\mathbf{X}\right]^{-1}\mathbf{X}^t\mathbf{Y} \tag{21}$$

The strain predicted by the least squares coefficients A_0, B_0, and A_1 is

$$\begin{bmatrix} 2\mu\varepsilon_1' \\ \cdot \\ \cdot \\ 2\mu\varepsilon_N' \end{bmatrix} = \begin{bmatrix} 1 & (F_{01} - \bar{F}_0) & (F_{11} - \bar{F}_1) \\ \cdot & \cdot & \cdot \\ \cdot & \cdot & \cdot \\ 1 & (F_{0N} - \bar{F}_0) & (F_{1N} - \bar{F}_1) \end{bmatrix} \begin{bmatrix} B_0' \\ A_0 \\ A_1 \end{bmatrix} \tag{22}$$

where,

$$\bar{F}_i = \frac{1}{N}\sum_{1}^{N} F_{ij} \tag{23}$$

To also solve for the crack tip location and orientation a non-linear technique is required. Several techniques and codes (Newton-Raphson [8 ,38], GAUSSFIT [39]) are found to be unreliable in consistently converging to a correct solution when input data with a known solution are used. In order to understand why the routines have difficulty converging, the

residual sum, r_o, is computed for 625 cases using linear least squares over a range of initial crack tip offsets in x and y while holding the crack orientation, β, constant.

$$r_o = \sum_{i=1}^{N} (\varepsilon_i - \varepsilon_i') \tag{24}$$

Figure 2 shows the contour plot of r_o over a crack tip offset range of $-0.025 \le x \le 0.025$ and $-0.025 \le y \le 0.025$. This surface approaches the minimum residual location of x=0 and

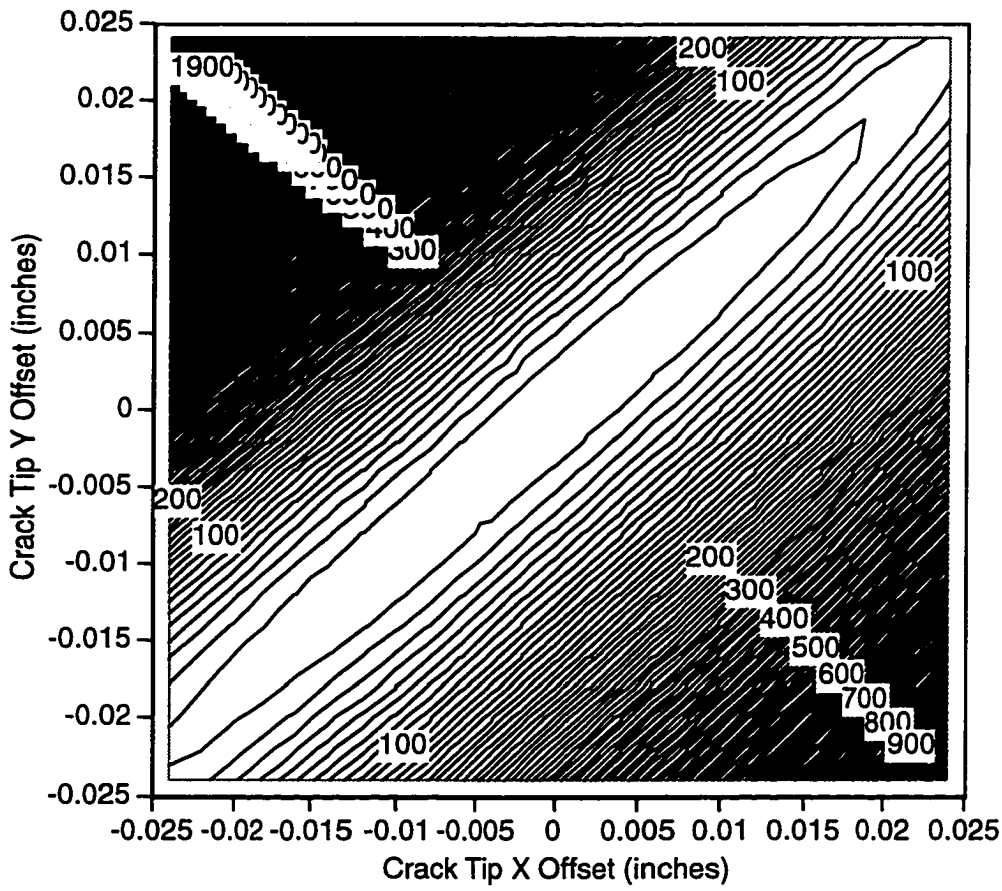

Figure 2. Contour plot of the residual sum with imposed crack tip offsets.

y=0 as a tangency. To improve the performance of the residual minimization routines weight functions, WF, are employed.

$$\text{Residual}(j) = \sum_{i=1}^{N} WF(\varepsilon_i - \varepsilon'_i) \tag{25}$$

Equations 26 through 32 list some of the functions tried. Figure 3 shows the contour plot for the square root function, and the cubic root function is shown in Figure 4.

$$\text{Absolute value function} = |\varepsilon_i - \varepsilon'_i| \tag{26}$$

$$\text{Weighted absolute value function} = \frac{|\varepsilon_i - \varepsilon'_i|}{\varepsilon_t} \tag{27}$$

where,

$$\varepsilon_t = \sum_{i=1}^{N} |\varepsilon_i| \tag{28}$$

$$\text{Square root function} = \sqrt[2]{\frac{|\varepsilon_i - \varepsilon'_i|}{\varepsilon_t}} \tag{29}$$

$$\text{Third root function} = \sqrt[3]{\frac{|\varepsilon_i - \varepsilon'_i|}{\varepsilon_t}} \tag{30}$$

$$\text{Fourth root function} = \sqrt[4]{\frac{|\varepsilon_i - \varepsilon'_i|}{\varepsilon_t}} \tag{31}$$

$$\text{Fifth root function} = \sqrt[5]{\frac{|\varepsilon_i - \varepsilon'_i|}{\varepsilon_t}} \tag{32}$$

The fractional root weighting functions provide a sharper gradient at the minimum location which improves the performance of the minimization routine. To test the weight function performance, an iterative routine is developed. The iterative routine uses initial seed guesses for crack tip

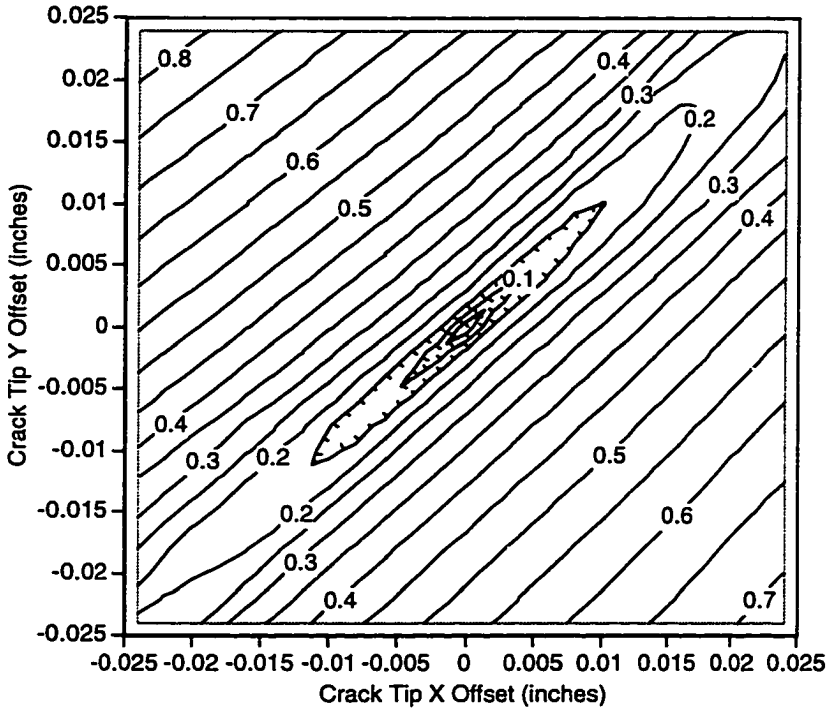

Figure 3. Contour plot of the weighted square root residual function with imposed crack tip offsets.

location X_C, Y_C and crack tip orientation angle β along with small initial seed offsets ΔX_C, ΔY_C and $\Delta\beta$. Table 1 shows the set of 27 cases that are created using the seed and offset data. The multiple linear least squares problem is then solved for the 27 cases and 27 weighted residuals are computed.

The weighted residuals are computed by using the A_0, B'_0 and A_1 calculated for each of the 27 cases as a fit to predict ε'_i for each of the N data points. The 27 cases are searched for the minimum residual case and the crack tip location and orientation are updated to this location. If the location and orientation do not require moving from the previous step, the seed offsets are reduced and the routine rerun. The routine

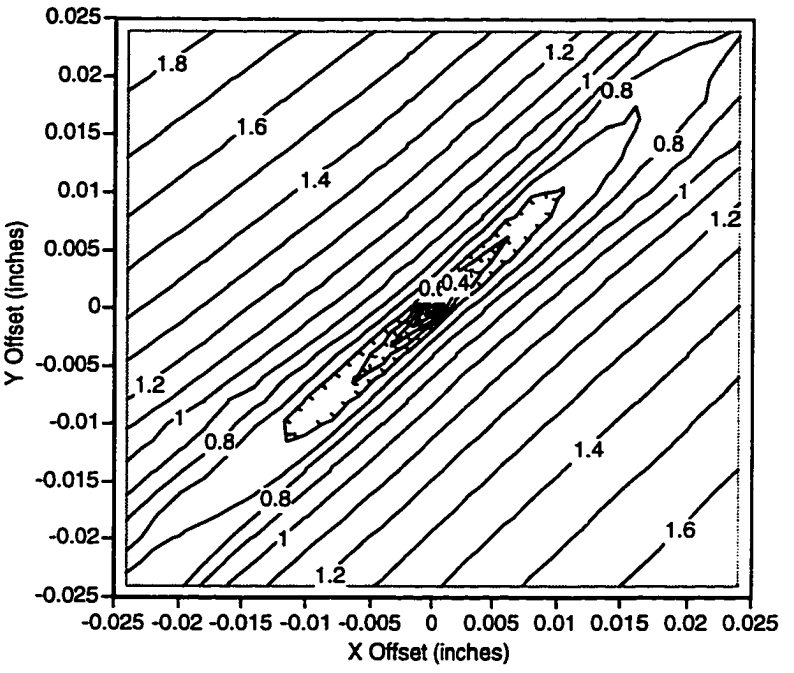

Figure 4. Contour plot of the weighted cube root residual function with imposed crack tip offsets.

is converged when the tip location and orientation are no longer moved and the seed offsets are reduced to a user defined minimum. The FORTRAN program, MLLS, to perform this is listed in Appendix A.

Many weight functions are tried while searching for the weight function that will let the routine find the location of the minimum residual quickly and with low sensitivity to experimental error. Sets of strain gage data to test weight functions are created by taking the experimental data, fitting the three term Equation 17 to it, and back calculating a set of strains. The back calculated set of strains have zero residual when fit to the three parameter equation. This "perfect fit" set of data (zero residual) has experimental noise and error simulated by randomly adding or subtracting from each reading. The random noise added to the initial values is at a fixed maximum level instead of a maximum

Table 1. List of 27 cases created around initial estimate of crack location and orientation.

Case 1	XC - Delta XC	YC - Delta YC	Beta - Delta Beta	Residual (1)
Case 2	XC - Delta XC	YC - Delta YC	Beta	Residual (2)
Case 3	XC - Delta XC	YC - Delta YC	Beta + Delta Beta	Residual (3)
Case 4	XC - Delta XC	YC	Beta - Delta Beta	Residual (4)
Case 5	XC - Delta XC	YC	Beta	Residual (5)
Case 6	XC - Delta XC	YC	Beta + Delta Beta	Residual (6)
Case 7	XC - Delta XC	YC + Delta YC	Beta - Delta Beta	Residual (7)
Case 8	XC - Delta XC	YC + Delta YC	Beta	Residual (8)
Case 9	XC - Delta XC	YC + Delta YC	Beta + Delta Beta	Residual (9)
Case 10	XC	YC - Delta YC	Beta - Delta Beta	Residual (10)
Case 11	XC	YC - Delta YC	Beta	Residual (11)
Case 12	XC	YC - Delta YC	Beta + Delta Beta	Residual (12)
Case 13	XC	YC	Beta - Delta Beta	Residual (13)
Case 14	XC	YC	Beta	Residual (14)
Case 15	XC	YC	Beta + Delta Beta	Residual (15)
Case 16	XC	YC + Delta YC	Beta - Delta Beta	Residual (16)
Case 17	XC	YC + Delta YC	Beta	Residual (17)
Case 18	XC	YC + Delta YC	Beta + Delta Beta	Residual (18)
Case 19	XC + Delta XC	YC - Delta YC	Beta - Delta Beta	Residual (19)
Case 20	XC + Delta XC	YC - Delta YC	Beta	Residual (20)
Case 21	XC + Delta XC	YC - Delta YC	Beta + Delta Beta	Residual (21)
Case 22	XC + Delta XC	YC	Beta - Delta Beta	Residual (22)
Case 23	XC + Delta XC	YC	Beta	Residual (23)
Case 24	XC + Delta XC	YC	Beta + Delta Beta	Residual (24)
Case 25	XC + Delta XC	YC + Delta YC	Beta - Delta Beta	Residual (25)
Case 26	XC + Delta XC	YC + Delta YC	Beta	Residual (26)
Case 27	XC + Delta XC	YC + Delta YC	Beta + Delta Beta	Residual (27)

percentage. This is because many of the potential problems in strain gage applications are due to experimental setup and do not vary with indicated strain so small indicated strains contain a greater percentage of error. Table 2 lists the locations and values for the perfect fit data and the maximum percent random error in each of the sets of 100 readings. This data set fits to a KI = 4623 psi $\sqrt{in}$ and a crack tip at x = 0, y = 0, and β = 0.

Figure 5 shows the performance of the tested weighting functions on the 100 sets of strain gage data for the ±5 $\mu\varepsilon$ case. Each line on the plot is one of the 100 sets. The stability of the weight functions in Equations 25-27 is poor as evidenced by the scatter and dropout of test cases. Figure

6 shows that the standard deviation of KI decreases as the order of the root increases until the fifth root which adds no additional reduction in variation. The fourth root weight function of the residuals is selected as best. If higher order terms are kept the order of the weight function should be checked, a higher order root may be required.

The fourth root weight function is further tested with all of the variations shown in Table 2. Table 3 lists the results of this test and shows that the fourth root weight function using the MLLS routine provides acceptable accuracy for careful experimenters but is sensitive to relatively large errors in strain measurement. For all cases the routine is stable and convergent.

Table 2. Strain, location, and maximum percent for each set of 100 readings.

				%Change from initial value for max error listed						
Gage	εi	X in	Y in	±1 με	±5 με	±10 με	±15 με	±20 με	±25 με	±30 με
1	349	0.010	0.2485	0.3	1.4	2.9	4.3	5.7	7.2	8.6
2	359	0.045	0.2483	0.3	1.4	2.8	4.2	5.6	7.0	8.4
3	347	0.080	0.2480	0.3	1.4	2.9	4.3	5.8	7.2	8.6
4	317	0.115	0.2478	0.3	1.6	3.2	4.7	6.3	7.9	9.5
5	275	0.150	0.2475	0.4	1.8	3.6	5.5	7.3	9.1	10.9
6	227	0.185	0.2473	0.4	2.2	4.4	6.6	8.8	11.0	13.2
7	178	0.220	0.2470	0.6	2.8	5.6	8.4	11.2	14.0	16.9
8	131	0.255	0.2468	0.8	3.8	7.6	11.5	15.3	19.1	22.9
9	87	0.290	0.2465	1.1	5.7	11.5	17.2	23.0	28.7	34.5
10	46	0.325	0.2463	2.2	10.9	21.7	32.6	43.5	54.3	65.2

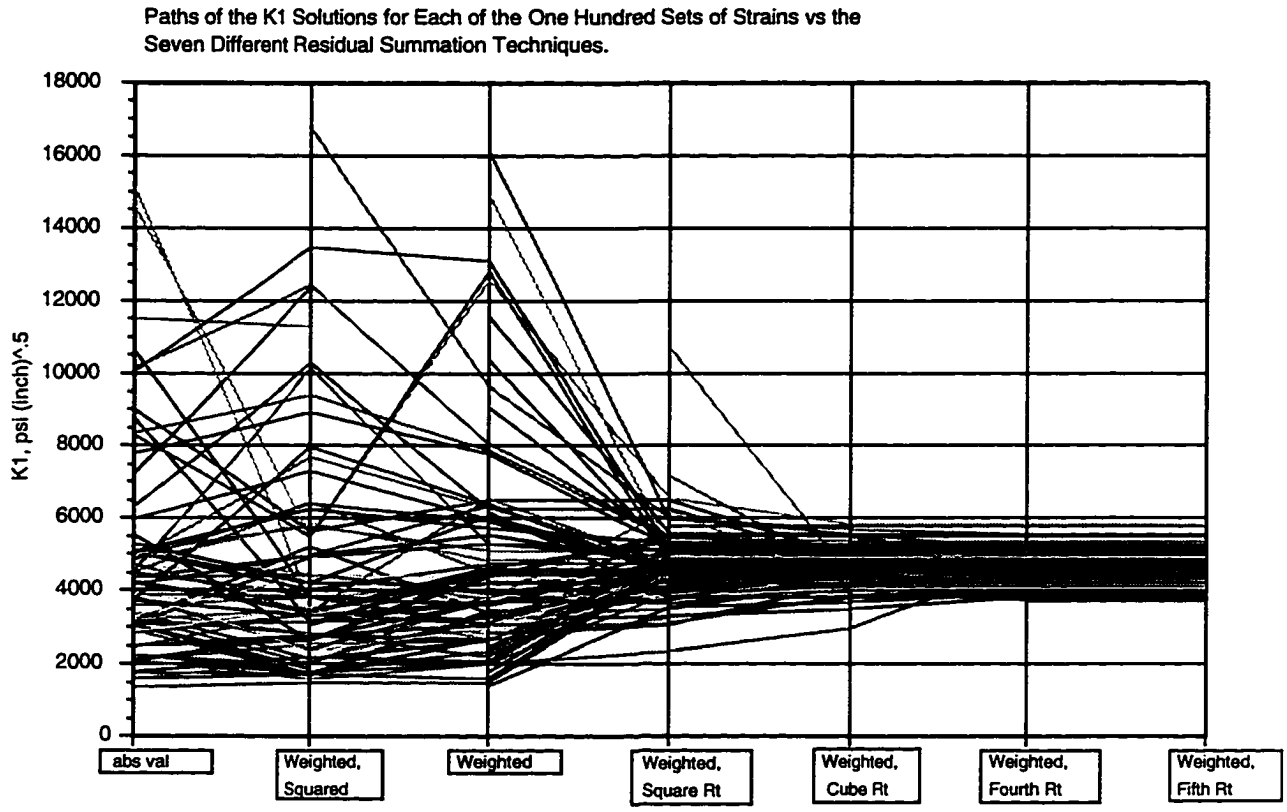

Figure 5. Converged KI solution for 100 test data sets with up to ±5 με error added and processed with different weight functions.

Table 3. Fourth root weight function performance with various levels of random noise numerically introduced.

Parameter	±1 με	±5 με	±10 με	±15 με	±20 με	±25 με	±30 με
Average X offset, in	5E-04	-2E-04	0.0003	0.0008	0.0017	0.0018	0.0018
X Standard Deviation	0.004	0.006	0.008	0.013	0.017	0.016	0.02
Average Y offset, in	4E-04	-2E-04	-4E-04	-0.001	-0.002	-9E-04	-0.002
Y Standard Deviation	0.003	0.005	0.008	0.011	0.016	0.017	0.021
Average β offset, radians	0.001	0	0	-0.002	-2E-04	-0.002	-0.002
β Standard Deviation	0.005	0.006	0.008	0.013	0.016	0.016	0.02
Average KI, psi (in)^.5	4602	4683	4689	4756	4784	4820	4963
KI Standard Deviation	256	411	532	839	980	1155	1436

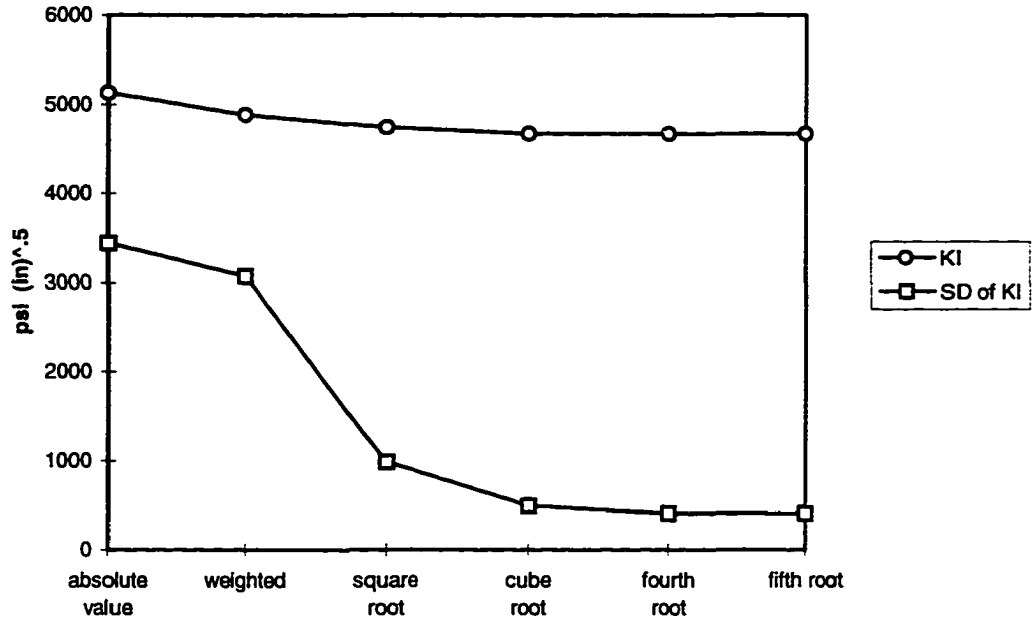

Figure 6. Mean stress intensity factor and standard deviation for 100 sets of test data with up to ±5 με error added and processed with different weight functions.

Mixed Modes

The mode 1 case is extended to mixed modes by including the C0 and C1 terms in Equation 17.

$$2\,\mu\varepsilon_i = A_0\,F_{0i}\,(r_i,\theta_i,\alpha_i) + B_0\,[\,k + \cos(2\,\alpha_i)\,] + A_1\,F_{1i}\,(r_i,\theta_i,\alpha_i) + C_0\,F_{2i}\,(r_i,\theta_i,\alpha_i) + C_1\,F_{3i}\,(r_i,\theta_i,\alpha_i) \qquad (33)$$

Now Equation 19 becomes:

$$\begin{bmatrix} 2\mu\varepsilon_1 \\ \cdot \\ \cdot \\ 2\mu\varepsilon_N \end{bmatrix} = \begin{bmatrix} 1 & (F_{01} - \bar{F}_0) & (F_{11} - \bar{F}_1) & (F_{21} - \bar{F}_2) & (F_{31} - \bar{F}_3) \\ \cdot & \cdot & \cdot & \cdot & \cdot \\ \cdot & \cdot & \cdot & \cdot & \cdot \\ 1 & (F_{0N} - \bar{F}_0) & (F_{1N} - \bar{F}_1) & (F_{2N} - \bar{F}_2) & (F_{3N} - \bar{F}_3) \end{bmatrix} \begin{bmatrix} B_0' \\ A_0 \\ A_1 \\ C_0 \\ C_1 \end{bmatrix} \quad (34)$$

and Equations 20 - 23 are used to solve for the unknown coefficients. Again, by using strip gages with parallel gage axis, the term in Equation 18 is treated as a constant for each gage reading. If the gage axes are not parallel relative to each other, Equations 33 and 34 are rewritten as:

$$\begin{aligned} 2\,\mu\varepsilon_i &= A_0\, F_{0i}\,(r_i, \theta_i, \alpha_i) + B_0\, F_{B\alpha} \\ &+ A_1\, F_{1i}\,(r_i, \theta_i, \alpha_i) + C_0\, F_{2i}\,(r_i, \theta_i, \alpha_i) \\ &+ C_1\, F_{3i}\,(r_i, \theta_i, \alpha_i) + D \end{aligned} \quad (35)$$

Where D is a constant. Equation 19 now becomes:

$$\begin{bmatrix} 2\mu\varepsilon_1 \\ \cdot \\ \cdot \\ 2\mu\varepsilon_N \end{bmatrix} = \begin{bmatrix} 1 & (F_{B\alpha 1} - \bar{F}_{B\alpha}) & (F_{01} - \bar{F}_0) & (F_{11} - \bar{F}_1) & (F_{21} - \bar{F}_2) & (F_{31} - \bar{F}_3) \\ \cdot & \cdot & \cdot & \cdot & \cdot & \cdot \\ \cdot & \cdot & \cdot & \cdot & \cdot & \cdot \\ 1 & (F_{B\alpha N} - \bar{F}_{B\alpha}) & (F_{0N} - \bar{F}_0) & (F_{1N} - \bar{F}_1) & (F_{2N} - \bar{F}_2) & (F_{3N} - \bar{F}_3) \end{bmatrix} \begin{bmatrix} D \\ B_0 \\ A_0 \\ A_1 \\ C_0 \\ C_1 \end{bmatrix}$$

(36)

which introduces another parameter into the least squares solution. Parallel strip gages are used in this paper to reduce the number of parameters in the least squares solutions. The FORTRAN code, MIXMODE, to perform mixed mode analysis is listed in Appendix B.

CHAPTER 5. STRESS INTENSITY EXPERIMENTS

EDM Compact Tension Specimen

Specimen Description

The electro discharge machined (EDM) compact tension (CT) specimen has a crack-like defect introduced by EDM machining a 0.010 inch wide slot in a CT specimen. The specimen is produced from a 1.00 inch thick 2024 T3 Aluminum plate with the dimensions shown in Figure 7.

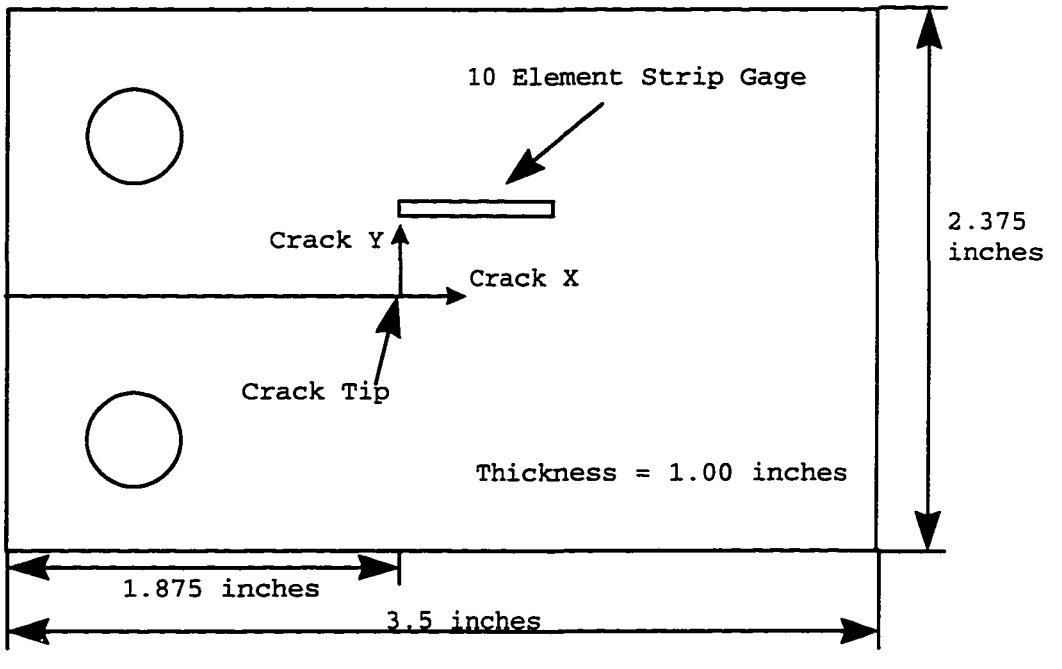

Figure 7. Compact Tension Specimen Dimensions.

Located on one face of the specimen is a ten element strip strain gage manufactured by Measurements Group, Inc. The gage manufacturers type is EA-13-020PF-120, so the length for each element is 0.020 inches. Using a Cartesian coordinate system with the origin at the crack tip as shown in

Figure 7, the locations of the 10 element gage centriods are listed in Table 4 along with the conversion to polar coordinates and the gage orientation angle, α, as shown in Figure 1.

Table 4. EDM CT Strain Gage Locations

Gage #	X (inches)	Y (inches)	r (inches)	θ (radians)	α (radians)
1	0.010	0.2485	0.2487	1.5306	1.5638
2	0.045	0.2483	0.2523	1.3915	1.5638
3	0.080	0.2480	0.2606	1.2588	1.5638
4	0.115	0.2478	0.2732	1.1363	1.5638
5	0.150	0.2475	0.2894	1.0259	1.5638
6	0.185	0.2473	0.3088	0.9258	1.5638
7	0.220	0.2470	0.3308	0.8431	1.5638
8	0.225	0.2468	0.3549	0.7691	1.5638
9	0.290	0.2465	0.3806	0.7045	1.5638
10	0.325	0.2463	0.4082	0.6478	1.5638

The strain gage placement on the specimen considered three related factors: the plastic zone at the crack tip, the error due to physical size of the gage grid in a strain gradient, and the valid extent of the three parameter solution.

Irwin's model [30] estimates the plastic zone extends to a radius of r_y from the tip

$$r_y = \frac{1}{2\pi}\left(\frac{KI}{\sigma_{yield}}\right)^2 \qquad \text{Plane Stress} \qquad (37)$$

$$r_y = \frac{1}{6\pi}\left(\frac{KI}{\sigma_{yield}}\right)^2 \qquad \text{Plane Strain} \qquad (38)$$

To restore equilibrium Irwin redistributed the stress around the crack tip as shown in Figure 8 so now

$$r_p = \frac{1}{\pi}\left(\frac{KI}{\sigma_{yield}}\right)^2 \qquad \text{Plane Stress} \qquad (39)$$

$$r_p = \frac{1}{3\pi}\left(\frac{KI}{\sigma_{yield}}\right)^2 \qquad \text{Plane Strain} \qquad (40)$$

The conditions are plane stress for strain gages mounted on a free surface. The specimens used in this paper are aluminum and the maximum plastic zone size for the tests run is

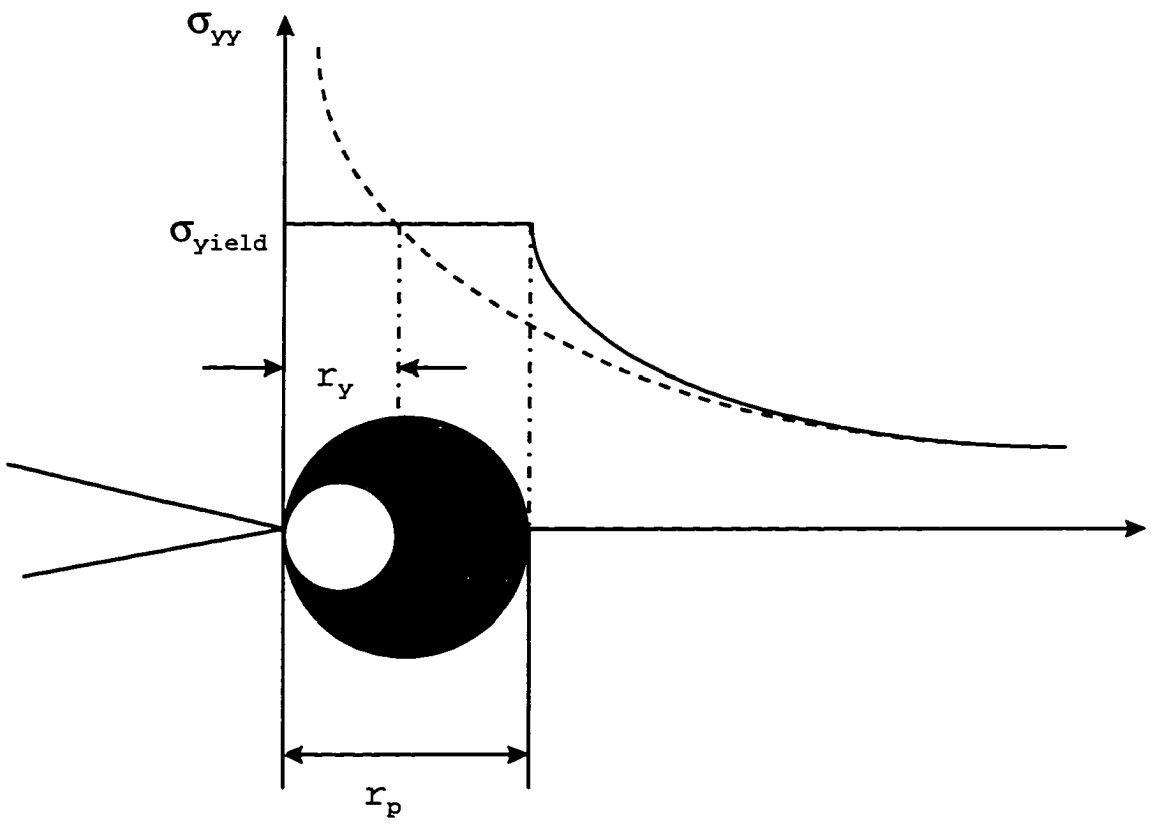

Figure 8. Approximate size of the plastic zone near a crack tip.

$KI_{max} = 12 \ Ksi\sqrt{in}$

$\sigma_{yield} = 40 \ Ksi$

$r_p = 0.028$ inches

Examination of Table 4 shows that all gages are well clear of this limitation. A further restriction on gage placement is the error caused by the physical size of the grid which averages strain over its area. In a region of high strain gradient the average strain indicated by the gage corresponds to the actual strain at a point that is different from the gage centroid. Dally and Berger [28] provide a derivation of shift in the true gage position due to strain gradient errors at the crack tip. Figure 9 illustrates the error in gage position, Δr, due to the gradient at the tip.

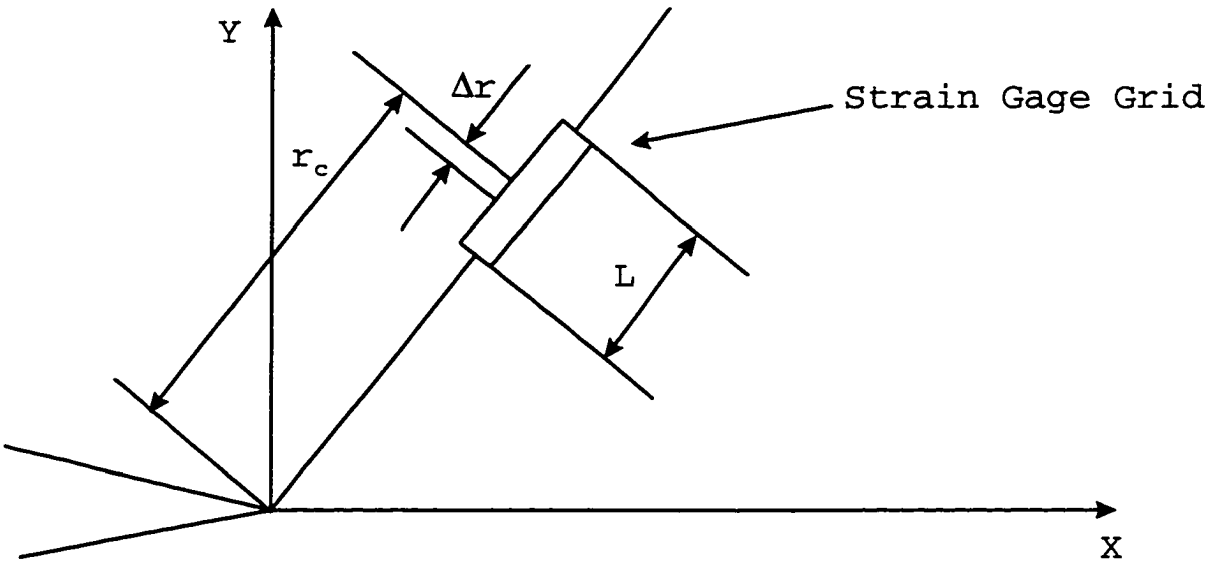

Figure 9. Strain gage position error due to strain gradient at crack tip.

$$\frac{\Delta r}{r_c} = \frac{1}{2}\left\{1 - \left[1 - \left(\frac{L}{2r_c}\right)^2\right]^{\frac{1}{2}}\right\} \tag{41}$$

where,

Δr = apparent shift in actual gage location
r_c = actual gage location
L = gage length

To shift the apparent gage position 0.001 inches, for a gage length of 0.020 inches, the gage centroid must be within 0.026 inches of the crack tip. The closest gage for all the experiments conducted is well beyond this distance so gage position error due to strain gradients will be less then 0.001 inch which is negligible.

The final question for gage placement is the extent of the valid region of the strain equations around a crack tip. In Chapter 3 it is shown that, for the gage locations listed in Table 4, additional terms beyond 3 are not significant. Dally and Berger [6, 7, 28], Berger, Dally, and Sanford [41], and Dally and Sanford [3] have mapped regions around a crack tip where a three term solution yields nearly the same results as a twelve term solution. The gage placement falls within this criteria.

Theoretical Solution

From Tada [30] a closed form solution for a compact tension specimen is:

$$KI = \sigma\sqrt{a}F_1\left(\frac{a}{b}, \frac{h}{b}, \frac{d}{h}\right) \tag{42}$$

where,

$$\sigma = \frac{P}{b}$$

P = Load

a = 1.4375 inches

b = 3.0625 inches

d = 0.8125 inches

h = 1.1875 inches

$$\frac{a}{b} = 0.4694$$

$$\frac{h}{b} = 0.3878$$

$$\frac{d}{h} = 0.6842$$

From the charts in Tada,

$$F_2 \approx 0.88$$

so,

$$F_1 = \frac{2\left(2 + \frac{a}{b}\right)}{\left(2 - \frac{a}{b}\right)^{\frac{3}{2}}} \frac{1}{\sqrt{\frac{a}{b}}} F_2$$

$$F_1 = 16.4$$

so,

$$KI = \frac{P}{b} \sqrt{a}\, F_1$$

which reduces to:

$$KI = 6.43\, P\, psi\, \sqrt{inch} \quad (P \text{ in pounds}) \tag{43}$$

This is a plane strain value. The specimen tested here differed from a standard compact tension specimen in that the corners had been rounded. To understand if this is a significant difference from the standard square edged specimen a numerical solution is run.

Numerical Solution

A quarter symmetry model of the EDM compact tension specimen is modeled using the ANSYS finite element code. The model consists of 26,458 nodes and 12,054 second order isoparametric elements. Symmetry planes are established along the crack axis and halfway through the thickness. Figures 10 and 11 show the overall grid. Selection of the grid spacing and element type at the crack tip directly influences the accuracy of the resulting stress intensity factor calculation. Gerstle and Abdalla [42], Liebowitz and Moyer [43], Mikkola and Niemi [44] and Solecki [34] discuss the use of singular elements at a crack tip. Since the strain field is dominated by the $\sqrt{r}$ singularity the elements at the crack tip must exhibit this behavior for accurate results. An isoparametric triangular element with the mid-side nodes moved from the mid-points to the quarter points nearest the crack tip, as shown in Figure 12, has the desired singularity not only along its boundaries but also throughout its areas and volume. The guidelines for tip mesh size set by Gerstle and Abdalla for a 1% or better accuracy in calculating KI are followed. First, the singular element size should be less than 10% of the "Least Dimension". For the compact tension specimen this is the distance from the crack tip to the machined v-notch, 0.625 inches. The singular elements near the crack tip are 0.0625

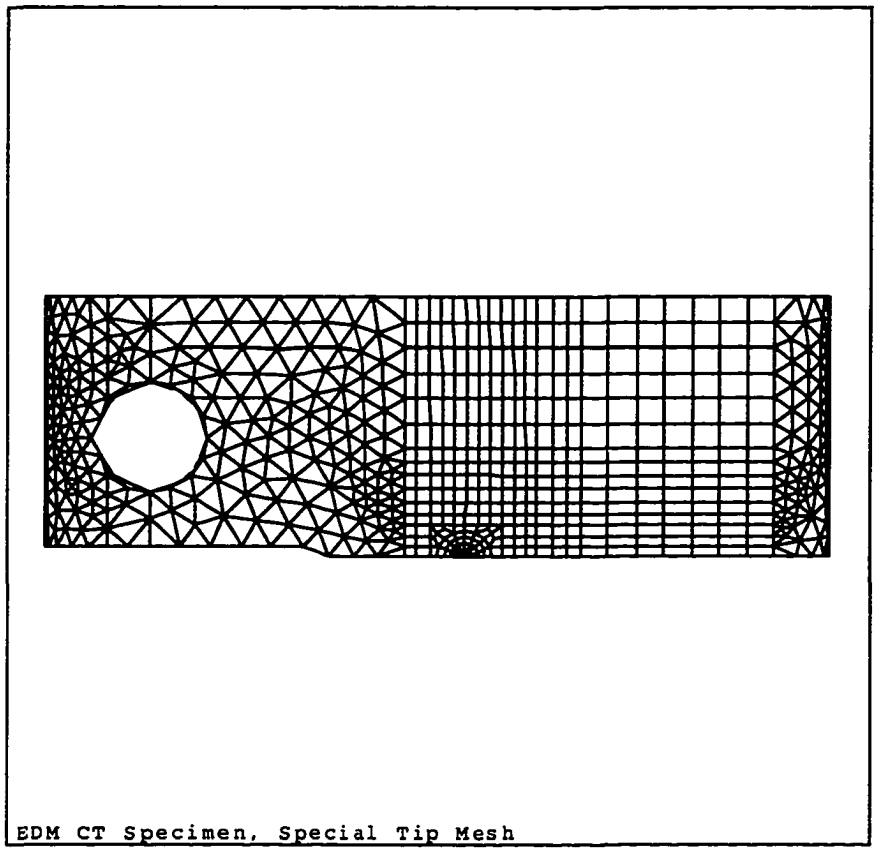

Figure 10. Compact tension FEM mesh, quarter symmetry used.

inches long. Second, there should be at least 16 nodes per 180 degrees of arc around the crack tip. Finally, the next layer of elements should have a length of 50% of the singular crack length. Figure 13 is a local view of the tip mesh and shows the 1% mesh criteria is satisfied. The ANSYS input deck for this model is listed in Appendix C.

The symmetry model is loaded with 500 pounds applied at the pin hole which is equivalent to 1000 pounds on the total specimen. Figures 14 and 15 show contour plots of the ε_{yy} strain resulting from this load (ε_{yy} is the strain acting on the experimental gage axis). The contours concentrate at the crack tip and to a lesser extent around the pin hole where the

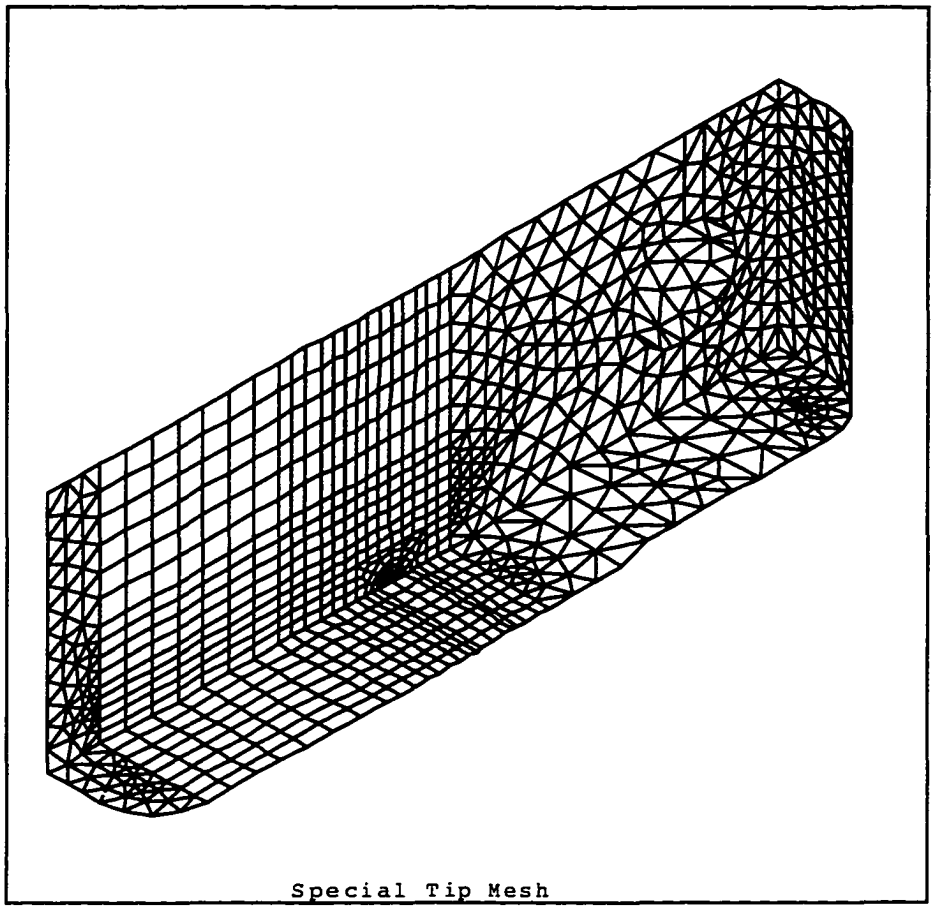

Figure 11. Iso view of compact tension specimen FEM mesh.

load is applied. Figure 16 is a cut section of the model which shows the variation in ε_{yy} with depth. The plot shows that the strain increases from the free surface to the center of the specimen. Figures 17 and 18 are contour plots of ε_{zz} and σ_{zz}, respectively, on a cut section of the model showing the region near the crack tip. From the variation in ε_{zz} it can be seen that the center of the specimen does not satisfy plane strain conditions since $\varepsilon_{zz} \neq 0$ at the center. The variation in σ_{zz} with depth shows that the free surface is in plane stress since $\sigma_{zz} = 0$ on the surface.

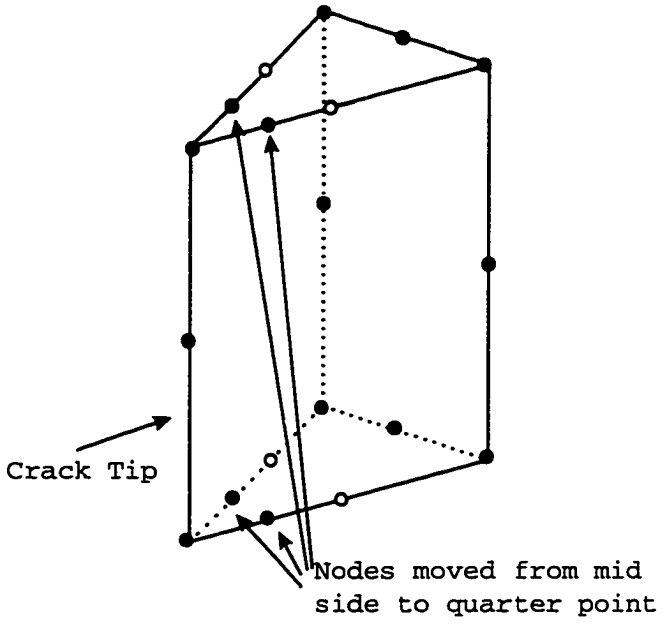

Figure 12. Crack tip singular finite element.

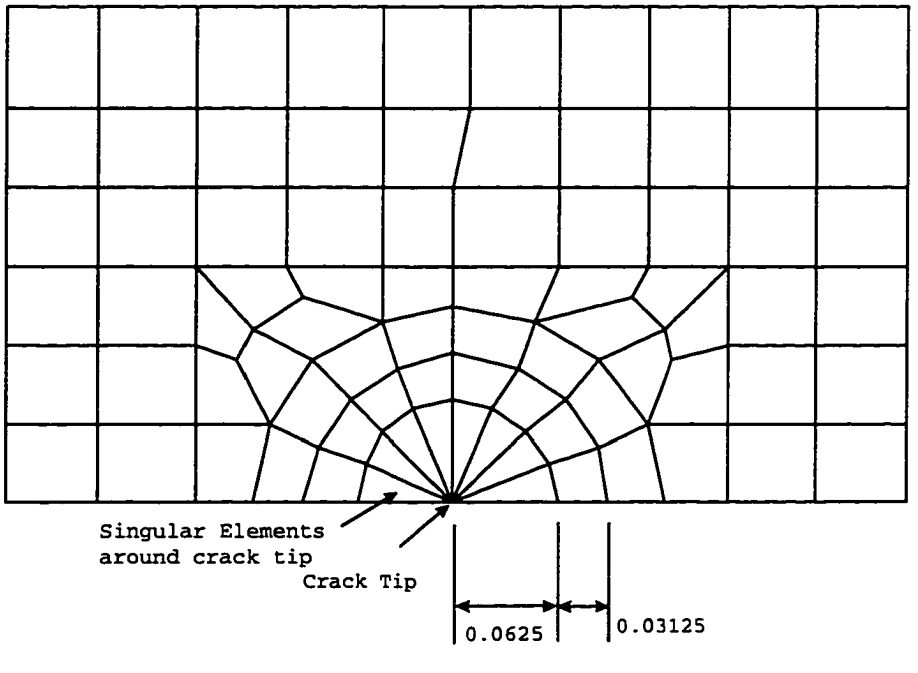

Figure 13. Close up view of tip mesh for the compact tension specimen.

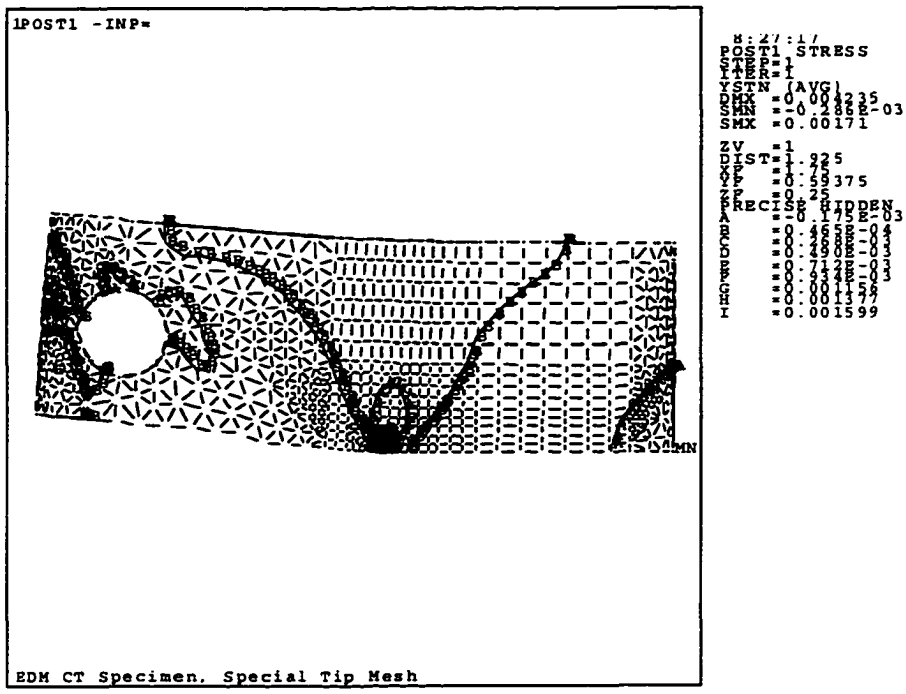

Figure 14. Contour plot of ε_{yy} strain.

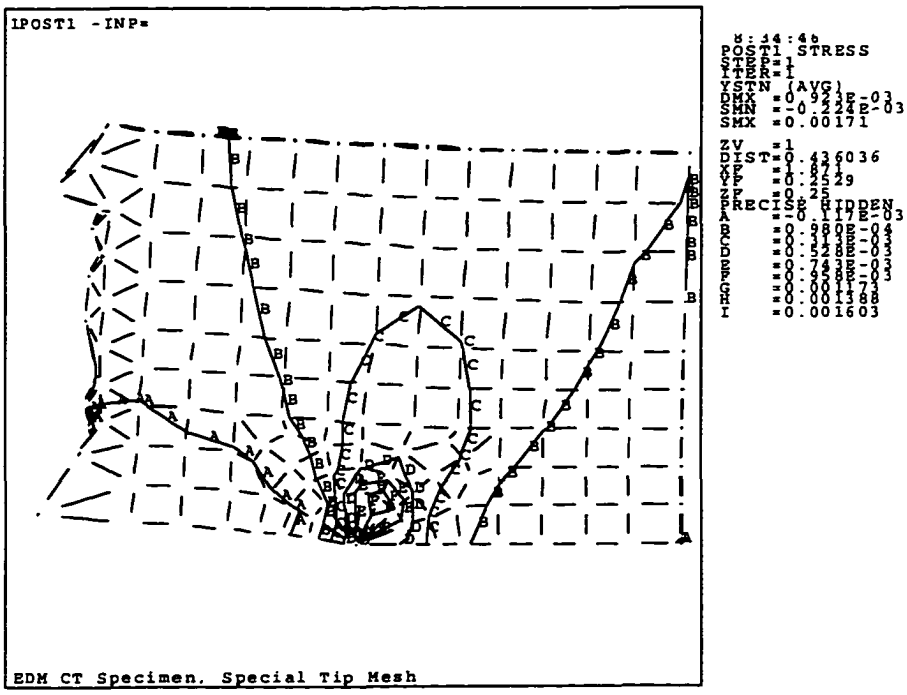

Figure 15. Close up view of ε_{yy} strain contours near the crack tip.

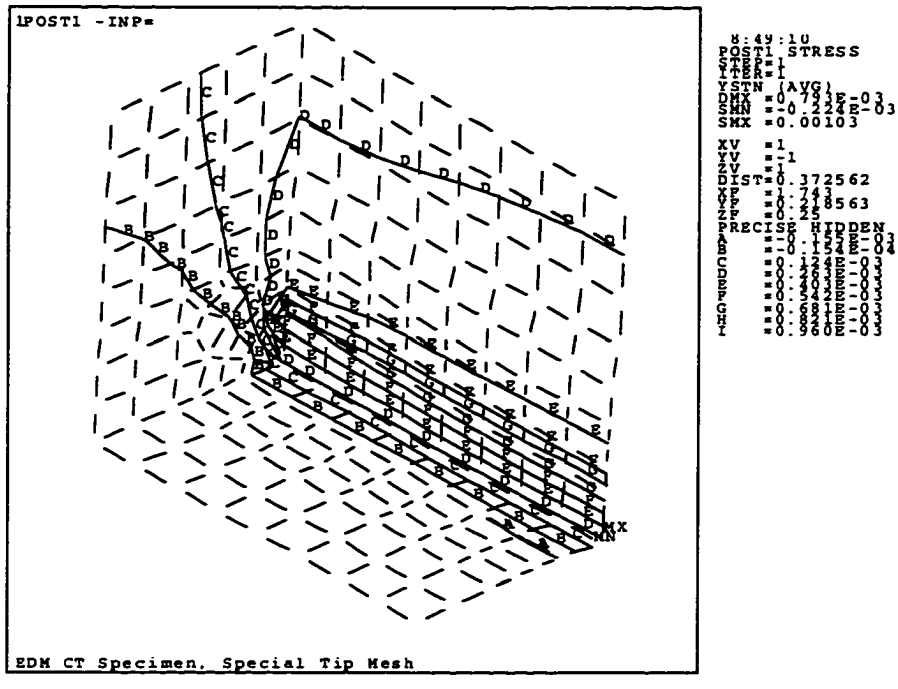

Figure 16. ε_{yy} strain at section cut from free surface on the left to the center symmetry plane on the right.

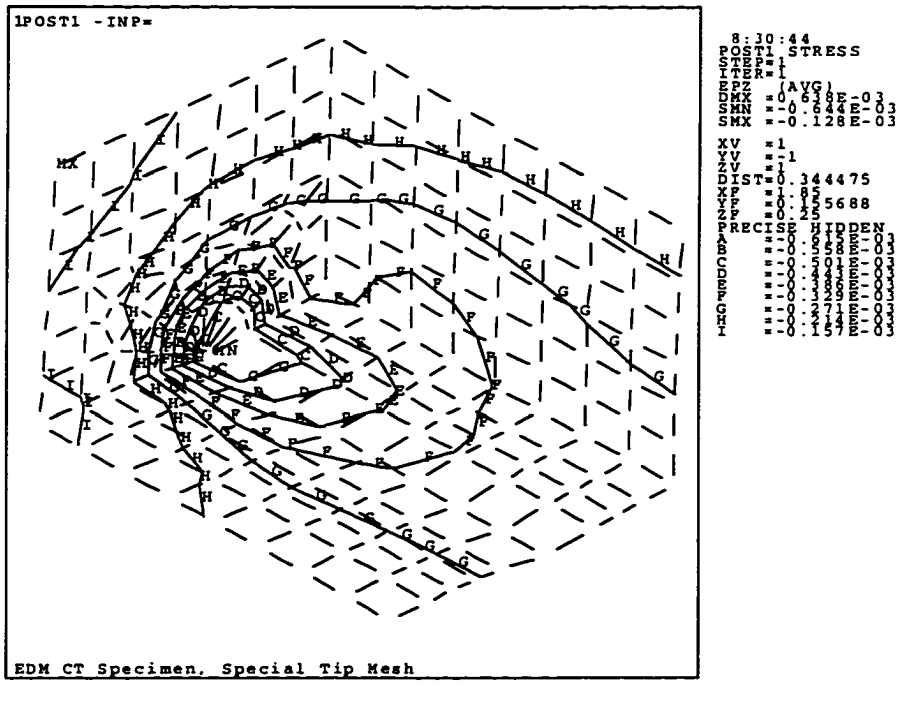

Figure 17. ε_{zz} strain showing the variation with thickness. Note that plane strain is not fully developed.

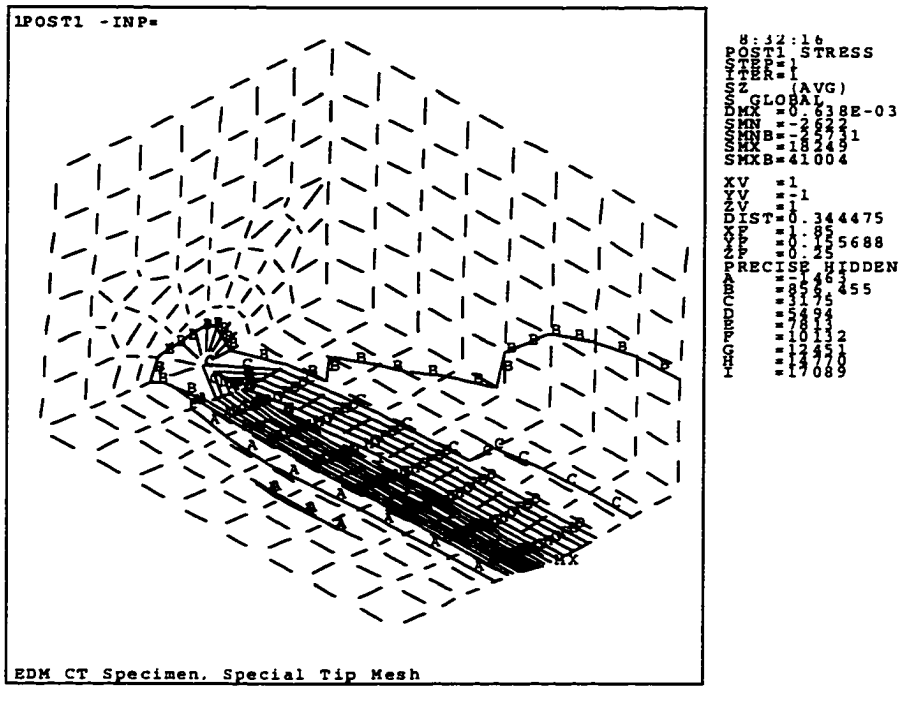

Figure 18. Close up view of σ_{zz} stress showing the variation with thickness and that the free surface is plane stress.

To calculate the KI stress intensity factor the displacement matching method was employed [33,34]. Expressed in the crack tip polar coordinates, shown in Figure 19, the displacements very near the crack tip are:

$$u = \frac{KI}{4\mu}\sqrt{\frac{r}{2\pi}}\left((2k-1)\cos\left(\frac{\theta}{2}\right) - \cos\left(\frac{3\theta}{2}\right)\right) - \frac{KII}{4\mu}\sqrt{\frac{r}{2\pi}}\left((2k+3)\sin\left(\frac{\theta}{2}\right) + \sin\left(\frac{3\theta}{2}\right)\right) + O(r) \tag{44}$$

$$v = \frac{KI}{4\mu}\sqrt{\frac{r}{2\pi}}\left((2k+1)\sin\left(\frac{\theta}{2}\right) - \sin\left(\frac{3\theta}{2}\right)\right) - \frac{KII}{4\mu}\sqrt{\frac{r}{2\pi}}\left((2k+3)\cos\left(\frac{\theta}{2}\right) + \cos\left(\frac{3\theta}{2}\right)\right) + O(r) \tag{45}$$

$$w = \frac{2KIII}{\mu}\sqrt{\frac{r}{2\pi}}\left(\sin\left(\frac{\theta}{2}\right)\right) + O(r) \tag{46}$$

where,

$$k = 3 - 4\nu \qquad \text{for plane strain} \tag{47}$$

$$k = \frac{3 - \nu}{1 + \nu} \qquad \text{for plane stress} \tag{48}$$

Note that Equations 47 and 48 define a different k than Equation 5. Equations 44, 45, and 46 are decoupled into separate equations for each stress intensity factor on the crack face, $\theta = \pm 180$ degrees, and as $r \rightarrow 0$ the higher order terms, $O(r)$, can be neglected. The equations reduce to:

$$u = \mp \frac{KII}{2\mu}\sqrt{\frac{r}{2\pi}}(1 + k) \tag{49}$$

$$v = \pm \frac{KI}{2\mu}\sqrt{\frac{r}{2\pi}}(1 + k) \tag{50}$$

$$w = \pm \frac{2KIII}{\mu}\sqrt{\frac{r}{2\pi}} \tag{51}$$

the sign being dependent on whether the value is evaluated on the top face (+ 180 degrees) or the bottom face (- 180 degrees).

Evaluating Equations 49, 50, and 51 across the crack from one face to the other yields:

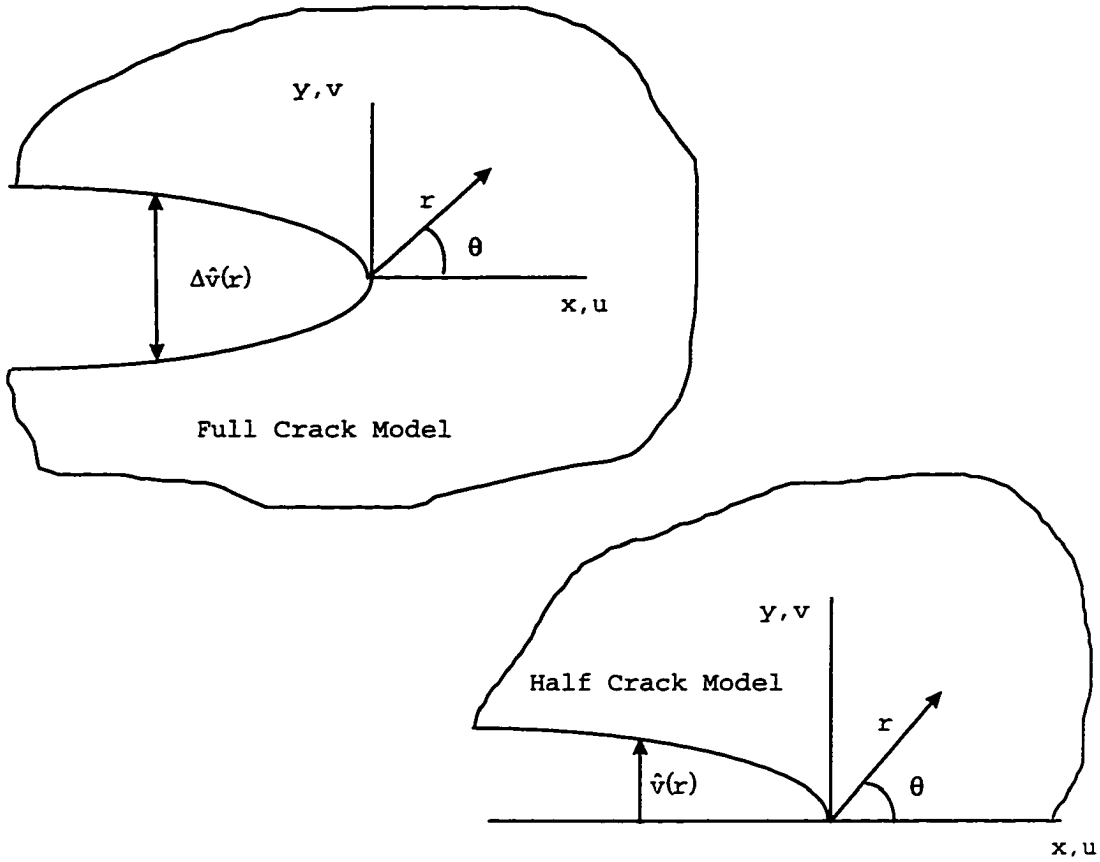

Figure 19. Crack tip coordinate system for finite element model stress intensity calculation.

$$\Delta u = -\frac{KII}{\mu}\sqrt{\frac{r}{2\pi}}(1 + k) \tag{52}$$

$$\Delta v = \frac{KI}{\mu}\sqrt{\frac{r}{2\pi}}(1 + k) \tag{53}$$

$$w = \frac{4KIII}{\mu}\sqrt{\frac{r}{2\pi}} \tag{54}$$

Now to evaluate the stress intensity factors the displacements are approximated with a linear fit of the nodal displacements near the crack tip, Equations 55-57. Either a full or half crack model can be used as shown on Figure 19.

$$\frac{\hat{u}}{\sqrt{r}} \text{ or } \frac{\Delta\hat{u}}{\sqrt{r}} = A + Br \tag{55}$$

$$\frac{\hat{v}}{\sqrt{r}} \text{ or } \frac{\Delta\hat{v}}{\sqrt{r}} = C + Dr \tag{56}$$

$$\frac{\hat{w}}{\sqrt{r}} \text{ or } \frac{\Delta\hat{w}}{\sqrt{r}} = E + Fr \tag{57}$$

Taking the limit as $r \rightarrow 0$:

$$\hat{u} \text{ or } \Delta\hat{u} = A \tag{58}$$

$$\hat{v} \text{ or } \Delta\hat{v} = C \tag{59}$$

$$\hat{w} \text{ or } \Delta\hat{w} = E \tag{60}$$

By substituting Equations 58 through 60 into 49 through 54 the stress intensity factors are determined for the half-crack or full-crack model.

$$KI = \frac{2\mu C\sqrt{2\pi}}{(1 + k)} \text{ or } \frac{\mu C\sqrt{2\pi}}{(1 + k)} \tag{61}$$

$$KII = \frac{2\mu A\sqrt{2\pi}}{(1 + k)} \text{ or } \frac{\mu A\sqrt{2\pi}}{(1 + k)} \tag{62}$$

$$KIII = \frac{\mu E\sqrt{2\pi}}{2} \text{ or } \mu E\sqrt{2\pi} \qquad (63)$$

Using the finite element model results and applying Equation 62 for a half-crack model, the KI stress intensity factors are computed at each node along the crack tip. Table 5 lists the results. The plane stress solution given in the table is valid only at the free surface and should not be used below the surface. The plane strain solution is not valid on the free surface but it does become nearly constant as the symmetry plane is approached. Since the center did not achieve complete plane strain the solution there is not entirely valid. The center plane strain solution is 8.5% larger than the theoretical solution given by Tada, Equation 41.

Table 5. KI stress intensity solution along crack tip in finite element model of Compact Tension specimen.

Depth From Surface, (in)	KI, psi (in)^.5 Plane Strain	KI, psi (in)^.5 Plane Stress
0.0000	5560	4954
0.0625	6194	5519
0.1250	6452	5749
0.1875	6649	5925
0.2500	6780	6042
0.3125	6870	6122
0.3750	6930	6175
0.4375	6964	6205
0.5000	6975	6215

Table 6. Finite element model strains at strain gage positions, relative to the crack tip, on the Compact Tension specimen.

X, inches	Y, Inches	α, radians	ε_{yy}, μ strain
0.010	0.2485	1.5708	320.3
0.045	0.2483	1.5708	338.1
0.080	0.2480	1.5708	337.1
0.115	0.2478	1.5708	317.2
0.150	0.2475	1.5708	274.4
0.185	0.2473	1.5708	228.4
0.220	0.2470	1.5708	179.2
0.255	0.2468	1.5708	133.6
0.290	0.2465	1.5708	90.6
0.325	0.2463	1.5708	49.8

Strains on the free surface of the finite element model were output at the locations of the strain gages used in the experiment conducted on the compact tension specimen. Table 6 lists these strains and the gage centriods relative to the crack coordinate system shown in Figure 1. The strains and locations are then used as input to the MLLS routine for KI only. The initial location of the crack tip and crack orientation are offset slightly and the routine iterates to find the tip location, orientation, and the KI stress intensity factor. The results are shown in Table 7.

The range of offsets that converge to the real crack tip is not large. The results are not consistent beyond the range shown in Table 7. This means that the experimenter must have good initial knowledge of the crack position and orientation. Within this range the crack tip location and orientation are found to an acceptably small deviation from the true position.

Table 7. Multiple linear least squares for KI only, results for numerical data.

Input X_{offset}, (inch)	Input Y_{offset}, (inch)	Input β_{offset}, (rad)	Output X_{offset}, (inch)	Output Y_{offset}, (inch)	Output β_{offset}, (rad)	KI psi in^.5
0.000	0.000	0.000	0.002	0.002	0.002	5315
0.030	0.030	0.015	0.000	0.000	0.016	5500
0.030	0.030	-0.015	0.000	0.000	0.016	5500
0.030	-0.030	0.015	0.000	0.000	0.016	5500
0.030	-0.030	-0.015	-0.002	0.000	-0.022	5579
-0.030	0.030	0.015	0.000	0.000	0.016	5500
-0.030	0.030	-0.015	-0.002	0.000	-0.022	5579
-0.030	-0.030	0.015	0.000	0.000	0.016	5500
-0.030	-0.030	-0.015	-0.002	0.000	-0.022	5579

The stress intensity factor calculated is 10% larger than the plane stress solution based on matching crack displacement, 4954 psi $\sqrt{inch}$ from Table 6, and is 15% less than the solution from Tada, Equation 41. With the crack tip location and orientation fixed at the initial location the KI is 5476 psi $\sqrt{inch}$ which matches the values in Table 7 to within 3%.

Experimental Procedure

The specimen was loaded in tension using a 20 Kip MTS machine and compact tension specimen grips operating at 10% range for 2000 pound maximum loading. The peak loading was selected for a maximum K_I of 12.8 Ksi $\sqrt{inch}$ which is below the material's K_{Ic} of 30 Ksi $\sqrt{inch}$. The strain gages were connected to a Measurements Group, Inc. strain indicator through a Measurements Group, Inc. switch and balance unit. The data are shown in Table 8.

Table 8. Strain and load data from Compact Tension Specimen experimental test.

	μ ε	μ ε	μ ε	μ ε	μ ε	μ ε	μ ε	μ ε
Gage 1	0	96	164	259	342	430	512	2
Gage 2	0	100	174	274	367	463	552	-2
Gage 3	0	98	170	267	354	445	537	-2
Gage 4	0	91	152	236	319	397	476	2
Gage 5	0	75	131	205	272	344	411	-3
Gage 6	0	69	113	170	223	275	331	2
Gage 7	0	54	88	124	170	210	252	1
Gage 8	0	44	70	99	129	161	197	2
Gage 9	0	32	48	59	81	99	119	-1
Gage 10	0	22	35	44	60	74	89	2
Load, pounds	0	250	450	750	1000	1250	1500	0

Data Analysis and Results

The data from Tables 6 and 8, for 1000 pounds load, are plotted in Figure 20. The slight gage orientation offset from the y axis, .007 radians or 0.4 degrees, was neglected for this comparative plot. The experimental data is in good agreement with the numerical data, better than 5% on average. The strain data for the 1000 pound load case was used as input for the MLLS routine for KI. The results are shown in Table 9. When the crack tip location and orientation are held fixed at the initial location the KI is 4558 psi $\sqrt{\text{inch}}$ which lower bounds the values in Table 9.

The experimental data does not converge as well as the numerical data when the MLLS routine is applied. The range of offsets over which the solution converges to a reasonable answer is more limited and the results are farther from the

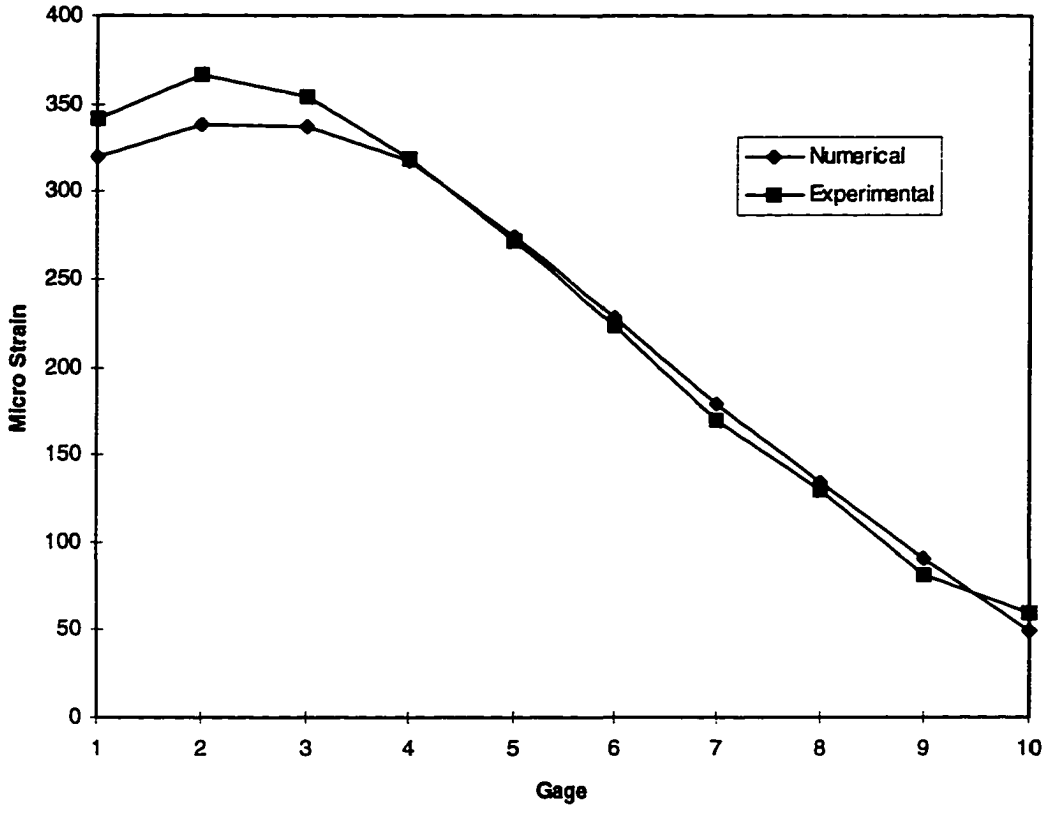

Figure 20. Strain at the gage locations for the compact tension specimen.

actual location. Also, the stress intensity factor solution ranges up to twice the fixed crack tip value.

With known crack location the MLLS method, using a three term expansion for the strain field, provides an accurate solution using experimental or numerical data from a single 10 element strip gage. With no prior knowledge of the crack tip location and orientation the MLLS method requires a rather close initial guess to converge to a reasonable answer.

Table 9. Multiple linear least squares for KI only, results for experimental data.

Input X_{offset}, (inch)	Input Y_{offset}, (inch)	Input β_{offset}, (rad)	Output X_{offset}, (inch)	Output Y_{offset}, (inch)	Output β_{offset}, (rad)	KI psi in^.5
0.000	0.000	0.000	-0.020	0.018	0.015	6280
0.020	0.020	0.015	-0.015	0.030	0.020	5822
0.020	0.020	-0.015	-0.010	0.035	-0.031	5288
0.020	-0.020	0.015	-0.015	0.030	0.020	5822
0.020	-0.020	-0.015	-0.040	0.010	-0.001	8775
-0.020	0.020	0.015	-0.015	0.030	0.020	5822
-0.020	0.020	-0.015	-0.015	0.030	0.020	5822
-0.020	-0.020	0.015	-0.045	0.005	0.018	9599
-0.020	-0.020	-0.015	-0.045	0.005	0.018	9599

Mixed Mode Plate Specimen

Specimen Description

The mixed mode plate test specimen is a 0.25 inch thick 6061 T6 aluminum plate machined as shown in Figure 21. The two slots are machined by the Electro Discharge Machine (EDM) process with a 0.010 inch diameter wire. This specimen is modeled after a photoelastic model used by Sanford and Dally [8]. This specimen will be shown to produce a ratio of KII/KI that varies from 0 to 2.2 depending upon which matched set (1 through 6) of holes the in-plane tensile load is applied.

Located on one face of the specimen, near the left crack tip, are two 10 element strip strain gages manufactured by Measurements Group, Inc. The gage type is EA-13-020PF-120, so the length for each element is 0.020 inches. Using a Cartesian coordinate system with the origin at the plate center as shown

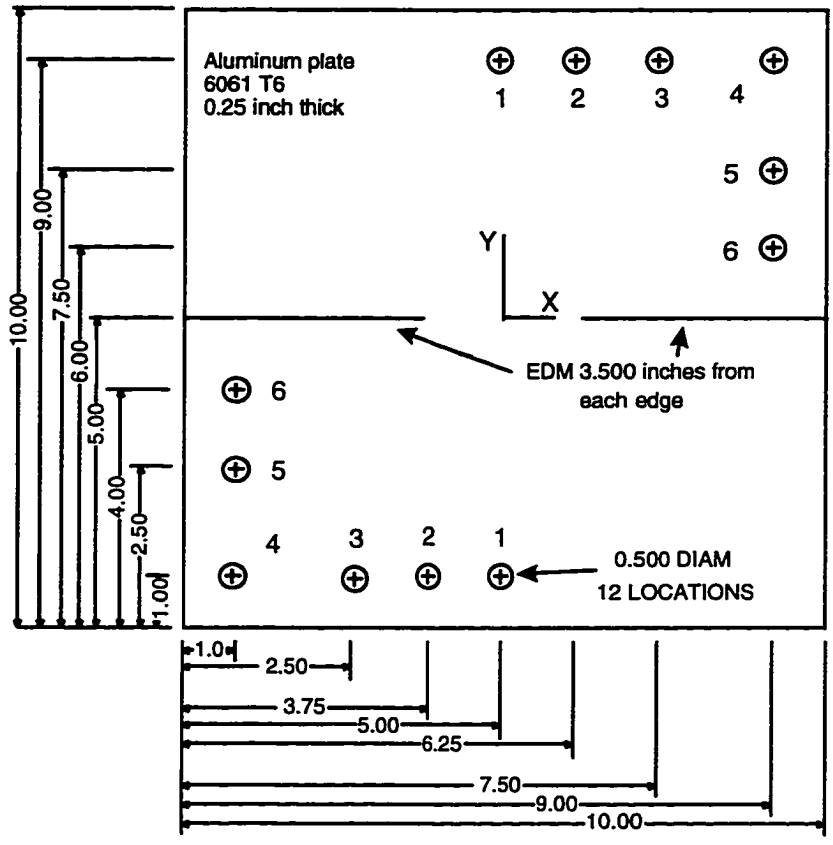

Figure 21. Mixed mode plate specimen dimensions.

in Figure 21, the locations of the 10 element gage centriods are listed in Table 10. Note that the crack tip is located at X = -1.477 inches. Positive Y values are for the "top" gage set and negative Y values for the "bottom" set. The gage orientation angle, α, has the same orientation as that shown in Figure 1. The gage locations satisfy all of the restrictions identified in the previous section.

Theoretical Solution

A closed form solution for the finite pin loaded plate in Figure 21 is not available. Solutions for an infinite plate with remote loads are found in Tada, et al [30] and Rooke and

Table 10. Mixed mode plate strain gage locations.

Gage #	X (inches)	Y (inches)	α (radians)
Crack Tip	-1.477	0.00000	
Top 1	-1.617	0.10145	1.5640
Top 2	-1.582	0.10121	1.5640
Top 3	-1.547	0.10098	1.5640
Top 4	-1.512	0.10074	1.5640
Top 5	-1.477	0.10050	1.5640
Top 6	-1.442	0.10026	1.5640
Top 7	-1.407	0.10003	1.5640
Top 8	-1.372	0.09979	1.5640
Top 9	-1.337	0.09955	1.5640
Top 10	-1.302	0.09931	1.5640
Bottom 1	-1.652	-0.10485	1.5834
Bottom 2	-1.617	-0.10441	1.5834
Bottom 3	-1.582	-0.10397	1.5834
Bottom 4	-1.547	-0.10353	1.5834
Bottom 5	-1.512	-0.10309	1.5834
Bottom 6	-1.477	-0.10265	1.5834
Bottom 7	-1.442	-0.10221	1.5834
Bottom 8	-1.407	-0.10177	1.5834
Bottom 9	-1.372	-0.10133	1.5834
Bottom 10	-1.337	-0.10089	1.5834

Cartwright [31]. The solution from Tada is more compact and is used here. Since this specimen is pin loaded only the in plane tension, P, is carried for the solution. Figure 22 illustrates the crack locations and the loading. The KI and KII stress intensity factors are expressed as functions of the applied in-plane load, P, and the angle, γ, that the load acts on relative to the cracks:

$$\begin{Bmatrix} KI \\ KII \end{Bmatrix} = \frac{1}{\sqrt{\pi a}} \begin{Bmatrix} P \sin \gamma \\ P \cos \gamma \end{Bmatrix} \tag{64}$$

Figure 23 summarizes the KI and KII predictions for the theoretical solution as a function of the angle of the applied

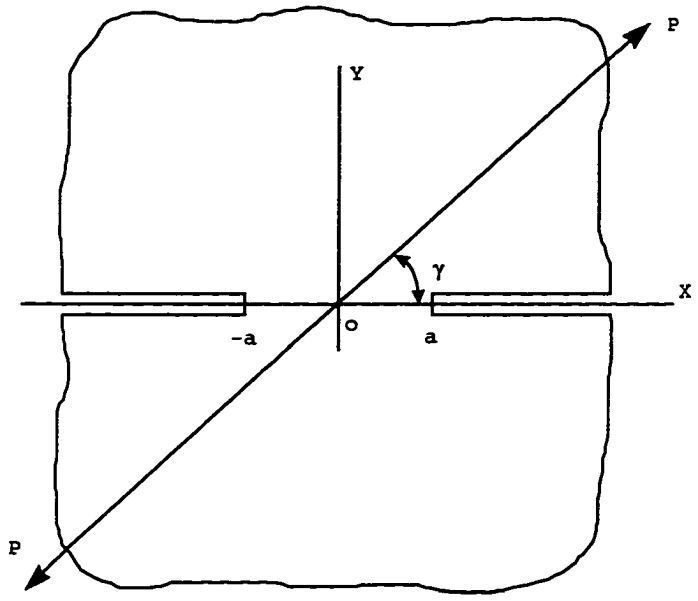

Figure 22. Description of load relative to crack tip location for theoretical solution of mixed mode plate specimen.

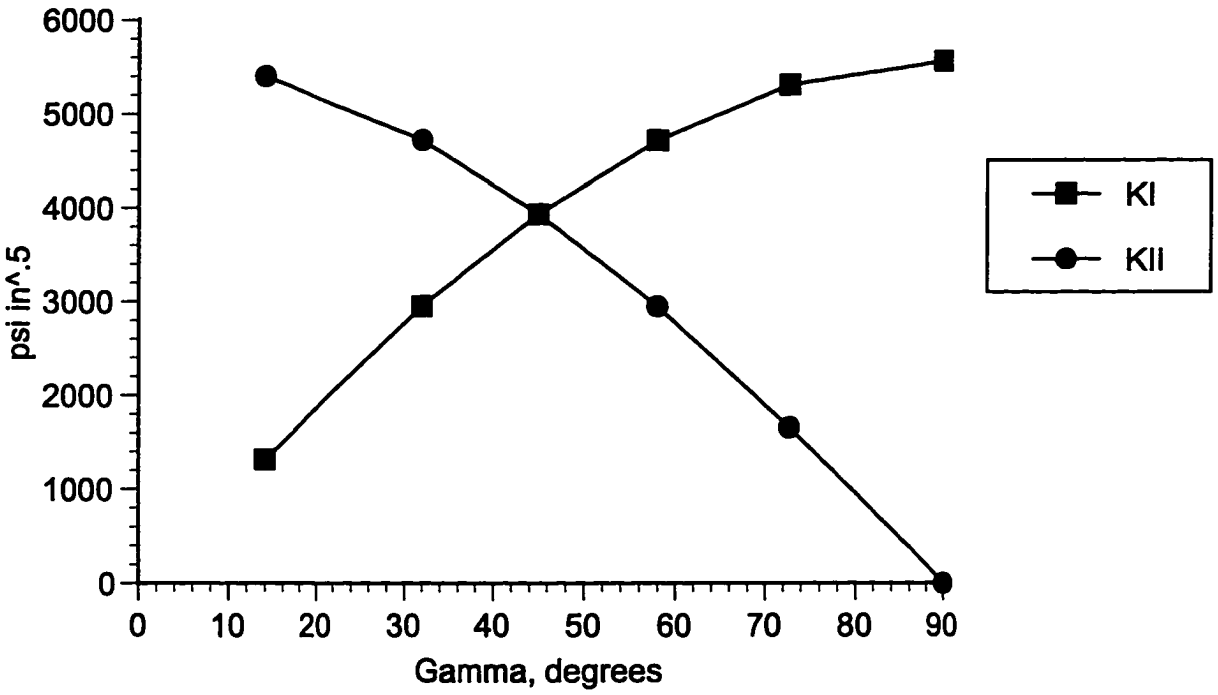

Figure 23. KI and KII as a function of the angle of the applied load.

load. The ratio of KII to KI, as a function of the angle of the applied load, is plotted in Figure 24. There are two issues regarding the use of this solution for the specimen in Figure 21. The first is that the specimen is a finite instead of an infinite plane, and the second is that the specimen is pin loaded in the vicinity of the crack tips, not infinitely remotely loaded. A numerical solution was developed to account for these two problems.

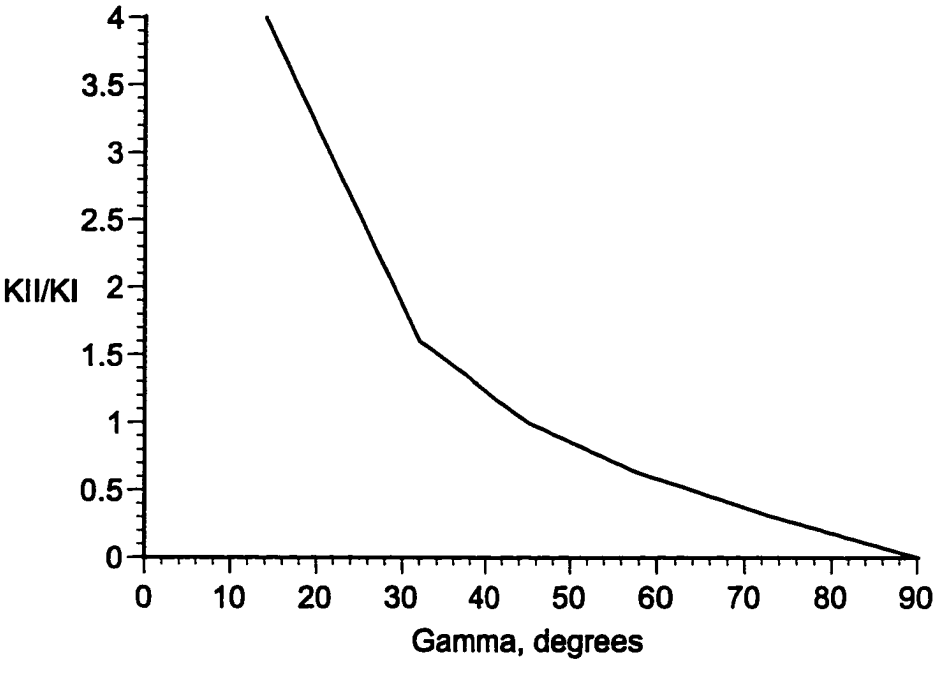

Figure 24. The ratio of KII to KI as a function of the angle of the applied load.

Numerical Solution

The finite element model generated has 26458 nodes and 12054 isoparametric 6 node plane stress elements. A truncated listing for the load case 1 of the model appears in Appendix D. Load cases 2 through 6 are similar; only the locations of the boundary conditions and applied load are changed. The

nodes and elements are generated with an automeshing routine and, for brevity, lists of these are not included. The criteria established in the previous section for mesh density and singular tip element selection are followed, with two exceptions. First, since this plate is relatively thin, 6 node plane stress elements with thickness input are used in a 2D mesh instead of the 3D solid elements. Second, since the problem is solved in 2D, a higher mesh density than the minimum recommended can be used without exceeding the computational resources. An overall view of the model is shown in Figure 25 and a local view of the left crack tip in Figure 26. The numerical data are taken at the left crack tip so the mesh density there is increased.

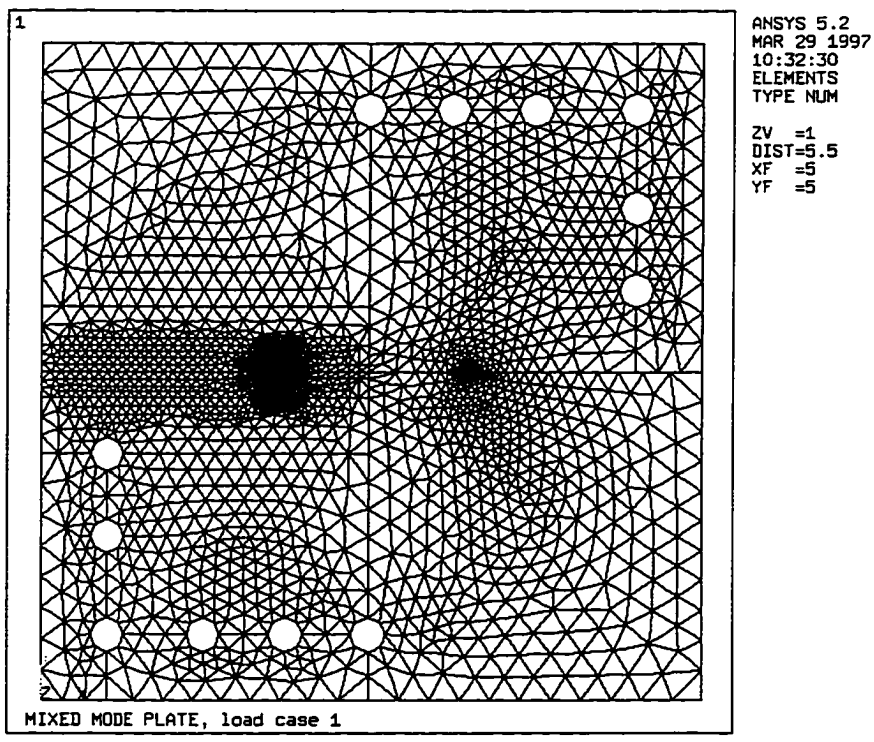

Figure 25. Mixed mode plate FEM mesh.

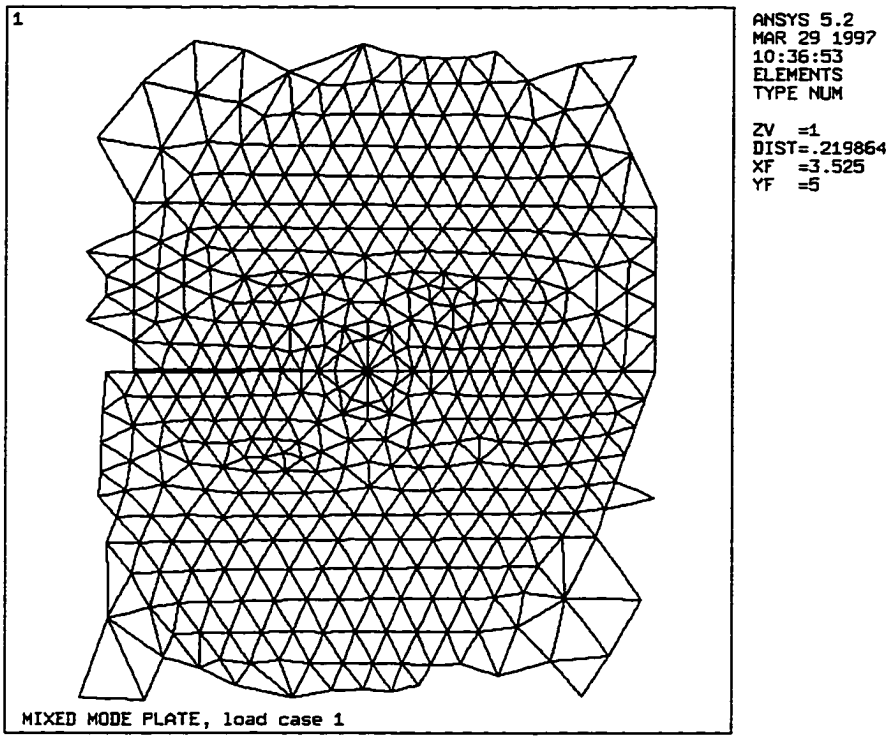

Figure 26. Close up of left hand crack tip in mixed mode plate FEM mesh.

Six load cases are run, one for each set of diagonally opposed holes shown in Figure 21. The load used is 3000 pounds. As in the previous section, strains are output from the model at the strip gage locations and are shown in Table 11. Then, using Equations 55 through 63, in a similar manner as the compact tension specimen, the KI and KII stress intensity factors are computed using the displacements near the crack tip. Using the strains in Table 11 and setting the crack tip location and orientation fixed and known the KI and KII stress intensity factors are then computed using the MIXMODE routine listed in Appendix B. The results for these computations are shown in Figures 27 and 28. The two solution methods agree very well, the largest deviation being only 1.3%

Table 11. Strains at gage locations for mixed mode plate specimen finite element model.

Gage #	Case 1 ε_{yy}, με	Case 2 ε_{yy}, με	Case 3 ε_{yy}, με	Case 4 ε_{yy}, με	Case 5 ε_{yy}, με	Case 6 ε_{yy}, με
Top 1	42.3	48.0	49.3	48.1	50.7	45.7
Top 2	82.4	78.6	68.2	51.6	38.6	12.6
Top 3	177.6	160.6	132.7	89.6	50.0	-16.4
Top 4	357.7	332.6	289.6	213.0	141.1	14.4
Top 5	576.9	564.3	526.3	430.9	343.2	164.6
Top 6	679.9	695.6	682.7	600.0	528.3	347.5
Top 7	640.1	670.8	673.3	610.0	559.5	406.1
Top 8	559.6	589.6	592.5	539.0	499.0	369.9
Top 9	488.9	511.5	507.3	455.8	417.1	303.4
Top 10	437.2	451.2	438.4	385.1	344.5	239.1
Bottom 1	28.1	-2.3	-59.5	-130.2	-198.4	-286.6
Bottom 2	44.8	20.0	-31.7	-98.5	-162.3	-248.2
Bottom 3	86.4	72.7	31.3	-29.9	-87.1	-173.3
Bottom 4	181.6	185.3	158.6	101.0	49.4	-47.7
Bottom 5	357.6	378.3	362.8	296.4	238.7	105.9
Bottom 6	571.5	589.4	562.3	462.2	372.6	174.7
Bottom 7	669.9	662.2	603.6	464.7	336.3	88.4
Bottom 8	636.8	606.6	524.7	396.5	224.1	-30.2
Bottom 9	558.6	518.6	428.8	277.0	134.5	-100.3
Bottom 10	487.7	446.4	357.2	215.5	83.4	-127.0

for the KII's in case 5. The solutions show that the finite plate and pin loading cause a much different result than the infinite plate with remote point loading used for the theoretical calculation and shown in Figures 23 and 24. The actual test specimen does not reach a ratio of KII to KI as high as the theory would predict.

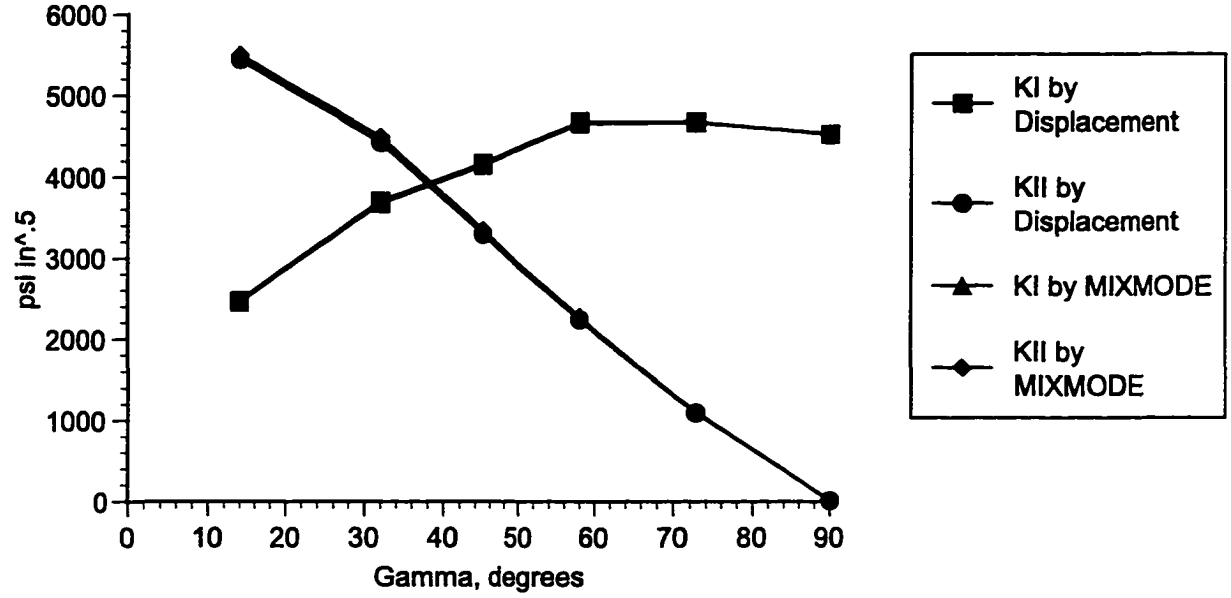

Figure 27. KI and KII for the numerical model as a function of the angle of the applied load.

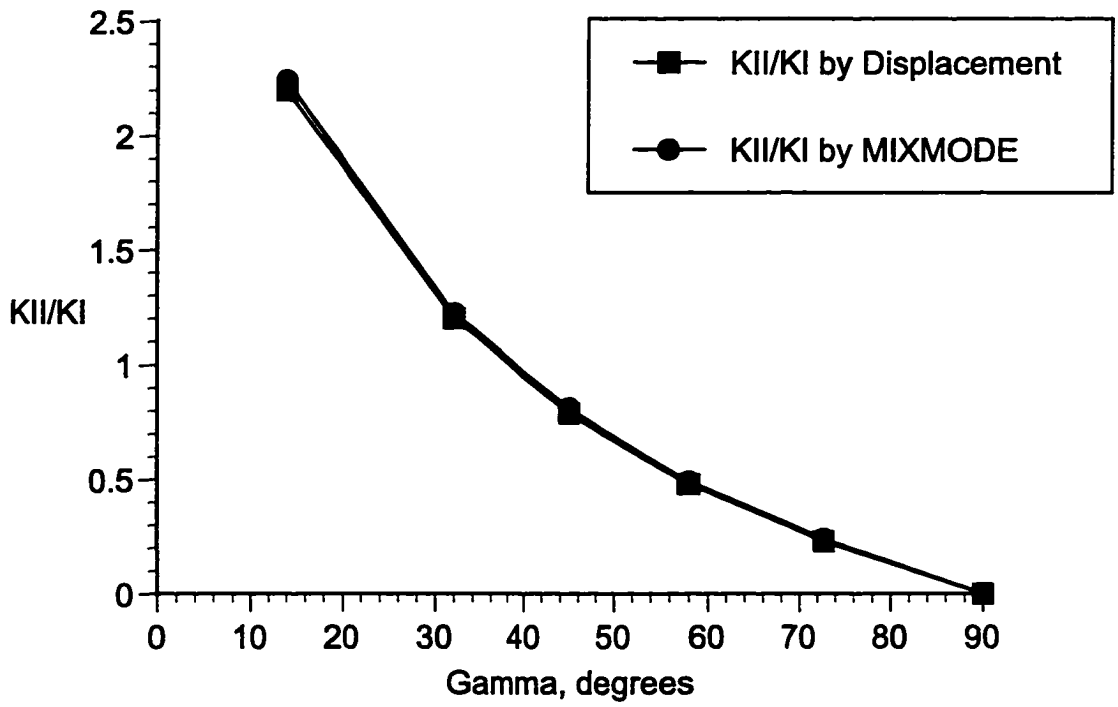

Figure 28. The ratio of KII to KI for the numerical model as a function of the applied load.

For all six load cases contour plots of the ε_{yy} strain are shown in Figures 29 through 34. The contours show the change in the crack tip local strain field as the angle of the applied load is changed.
For each load case, results of the MIXMODE routine for mixed modes with unknown crack initial position and orientation are plotted in Figures 35 and 36. The range of initial offsets at which the routine started, relative to the crack tip, are:

- $-0.1 \leq x_{off} \leq 0.1$ inches
- $-0.05 \leq y_{off} \leq 0.05$ inches
- $-0.05 \leq \beta_{off} \leq 0.05$ radians

The output ranges over:

- $-0.002 \leq x_{off} \leq 0.002$ inches
- $-0.005 \leq y_{off} \leq 0.005$ inches
- $-0.24 \leq \beta_{off} \leq 0.29$ radians

This indicates that the routine works well at locating the crack tip, but that the orientation angle is found over a broader range. The vertical bars in Figures 35 and 36 represent the limits of the range over which the solution converged for each case; the data points are the converged solutions with the initial offsets set to zero.

Experimental Procedure

The specimen is loaded in tension using the 20 Kip MTS machine and grips operating at 20% range for 4000 pound maximum loading. The peak loading is selected for a maximum K_I of 7.4 Ksi $\sqrt{inch}$, which is below the materials K_{Ic} of 30

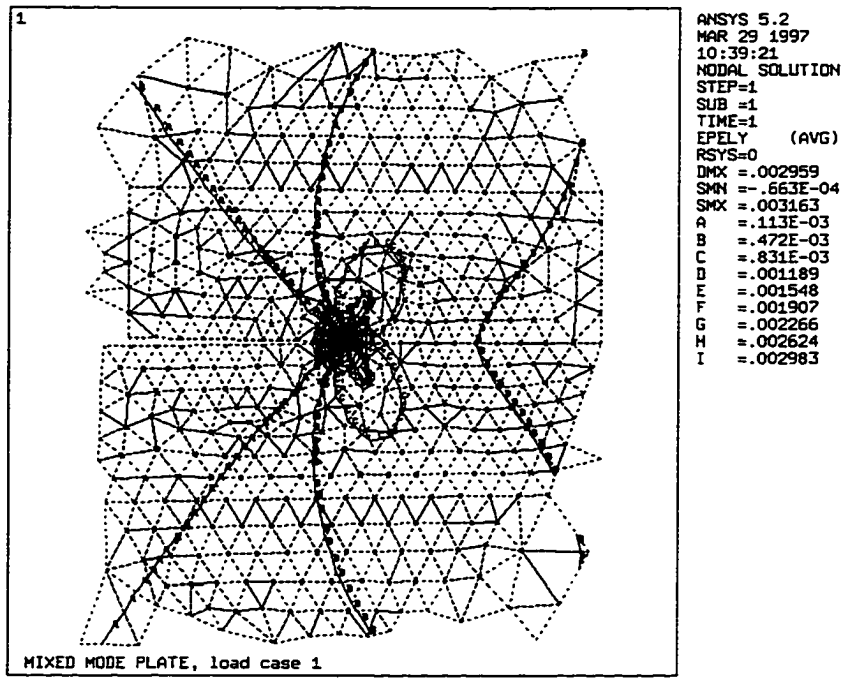

Figure 29. ε_{yy} strain for case 1 loading of mixed mode plate.

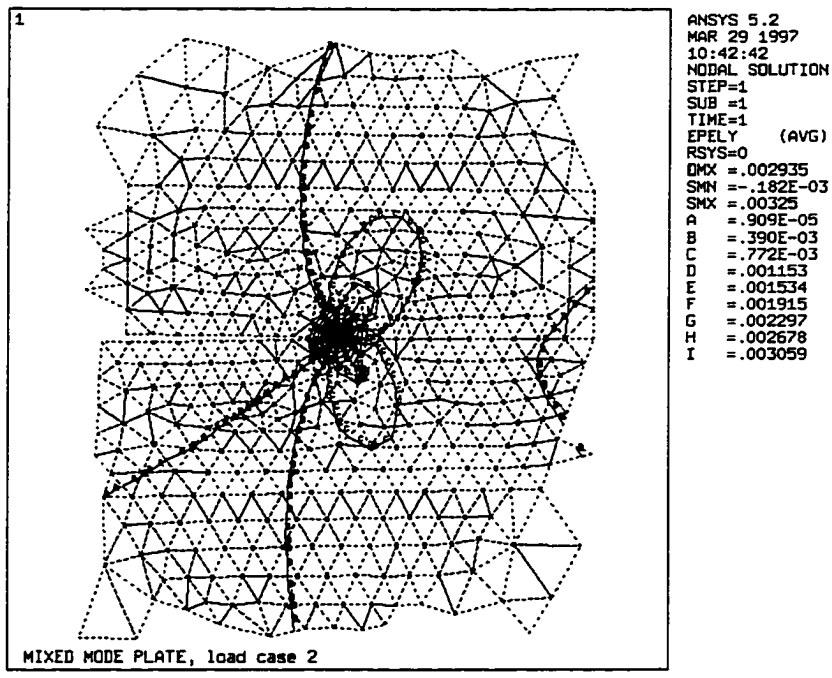

Figure 30. ε_{yy} strain for case 2 loading of mixed mode plate.

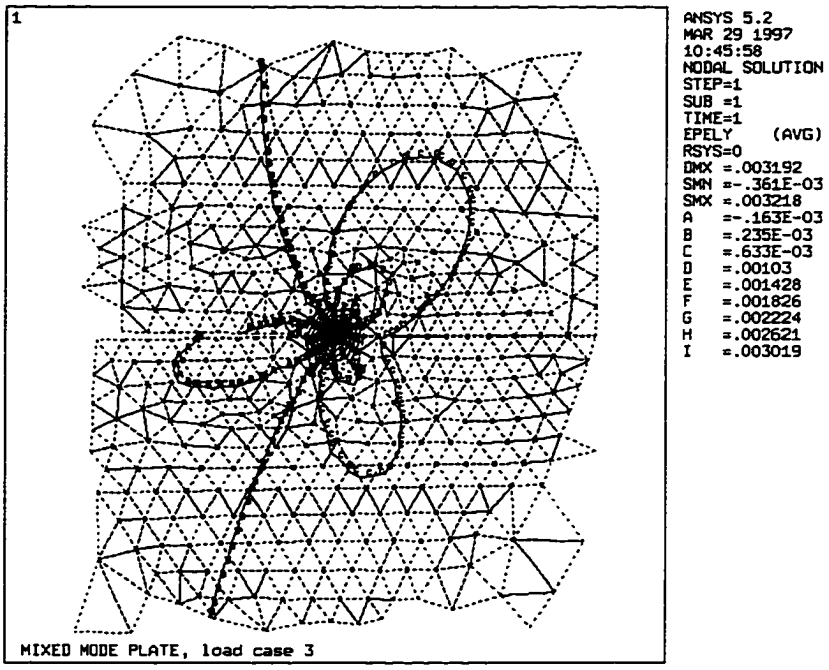

Figure 31. ε_{yy} strain for case 3 loading of mixed mode plate.

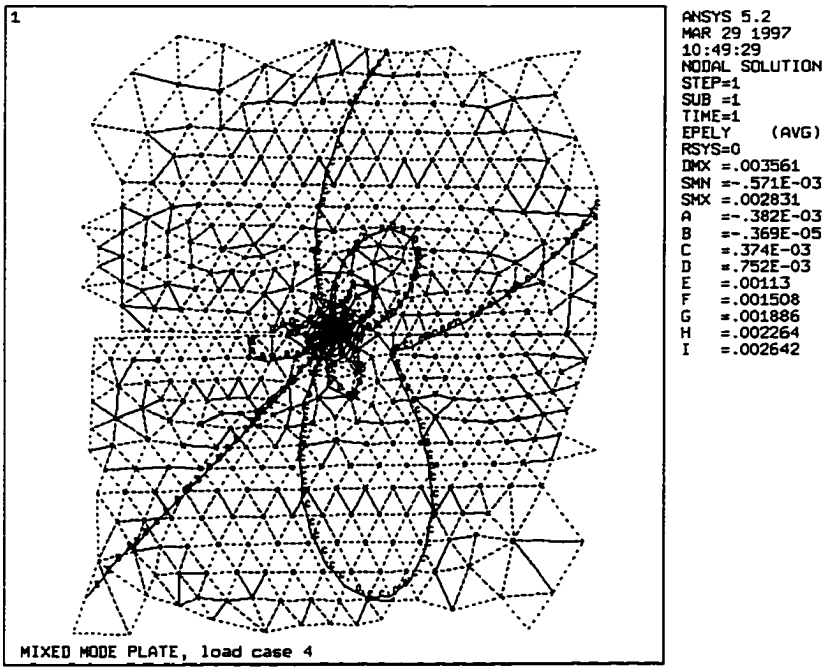

Figure 32. ε_{yy} strain for case 4 loading of mixed mode plate.

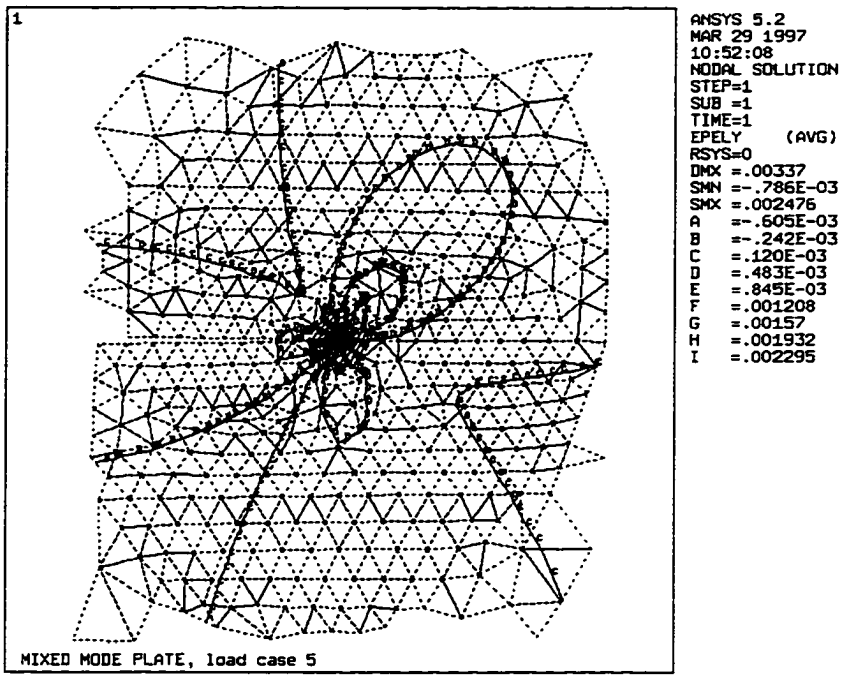

Figure 33. ε_{yy} strain for case 5 loading of mixed mode plate.

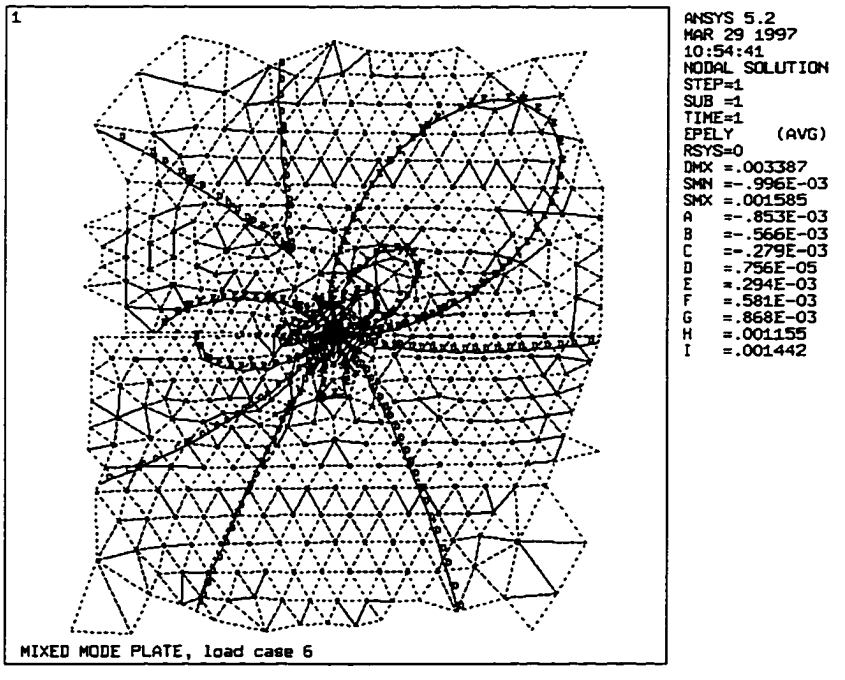

Figure 34. ε_{yy} strain for case 6 loading of mixed mode plate.

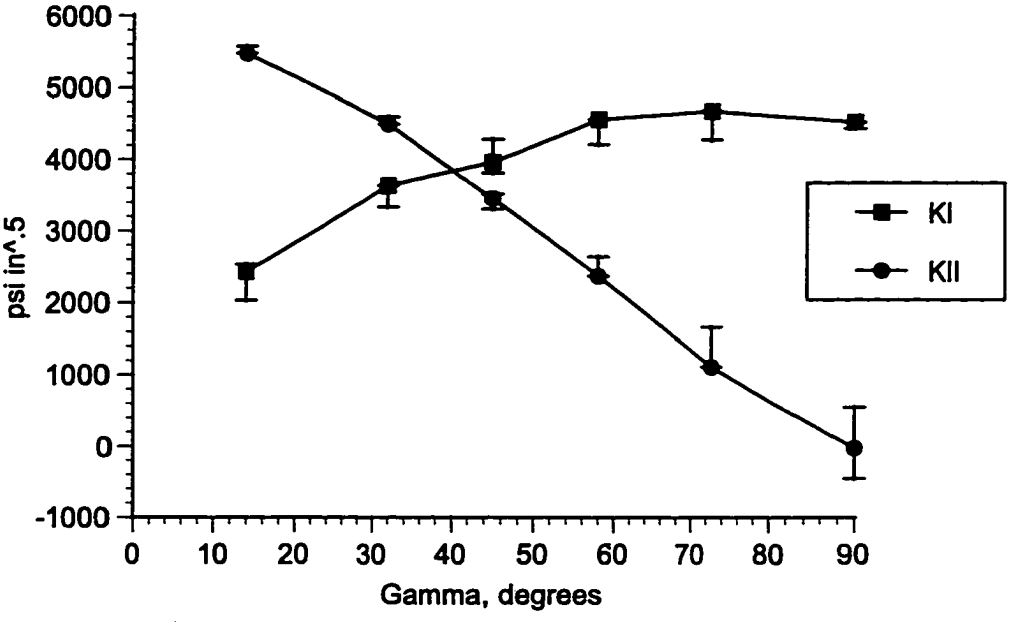

Figure 35. KI and KII calculated using MIXMODE routine and a range of crack location and orientation initial offsets from the true crack position.

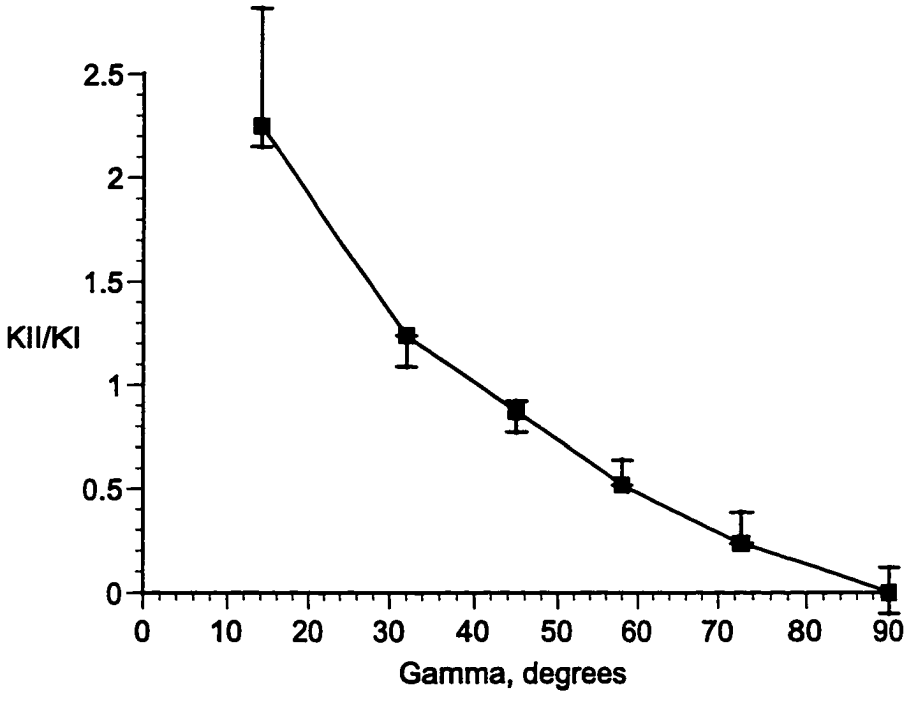

Figure 36. The ratio of KII to KI calculated using MIXMODE and a range of crack location and orientation initial offsets from the true crack position.

Ksi $\sqrt{inch}$. The strain data is collected using two Measurements Group, Inc. strain indicators through two Measurements Group, Inc. switch and balance units. Six load cases are run, each using one set of the diagonally opposed sets of holes shown in Figure 21. The strain data collected at the gage locations for 3000 pounds load is listed in Table 12. Gage Top 7 failed and is not included in the table.

Data Analysis and Results

The strain readings from Table 12 are processed using the MIXMODE routine for mixed modes and a known, fixed, crack location and orientation. The resulting stress intensity values are plotted in Figures 37 and 38 as a function of the angle of the applied load. For all of the load cases results of the MIXMODE routine for mixed modes with unknown crack initial position and orientation are plotted in Figures 39 and 40. The range of initial offsets at which the routine started, relative to the crack tip, are:

$-0.05 \leq x_{off} \leq 0.05$ inches

$-0.03 \leq y_{off} \leq 0.03$ inches

$-0.03 \leq \beta_{off} \leq 0.03$ radians

The output ranges over:

$-0.007 \leq x_{off} \leq 0.002$ inches

$-0.008 \leq y_{off} \leq 0.006$ inches

$-0.3 \leq \beta_{off} \leq 0.29$ radians

which indicates that the routine works well at locating the crack tip, but that the orientation angle has a larger

Table 12. Strains at gage locations for mixed mode plate specimen, experimental test, 3000 pounds load per case.

Gage #	Case 1 ε_{yy}, με	Case 2 ε_{yy}, με	Case 3 ε_{yy}, με	Case 4 ε_{yy}, με	Case 5 ε_{yy}, με	Case 6 ε_{yy}, με
Top 1	48	48	50	53	60	50
Top 2	86	73	64	54	50	17
Top 3	198	161	130	95	70	-20
Top 4	408	341	290	223	173	2
Top 5	643	570	521	446	392	154
Top 6	744	690	667	615	581	339
Top 8	611	575	568	539	533	351
Top 9	532	491	476	443	435	271
Top 10	485	438	414	374	364	207
Bottom 1	-21	-11	-52	-113	-158	-233
Bottom 2	29	2	-42	-98	-137	-213
Bottom 3	66	42	6	-50	-83	-167
Bottom 4	161	141	116	66	39	-68
Bottom 5	355	333	317	264	238	78
Bottom 6	593	545	512	429	384	131
Bottom 7	716	627	555	422	345	15
Bottom 8	695	582	482	325	231	-114
Bottom 9	622	504	398	242	150	-171
Bottom 10	551	437	336	190	108	-181

error associated with it. Note that the initial range is more limited than that used for the numerical data. This is necessary for convergence to a reasonable answer. The vertical bars in Figures 39 and 40 represent the limits of the range over which the solution converges for each case; the data points are the converged solutions with the initial offsets set to zero. The solution agrees well with the

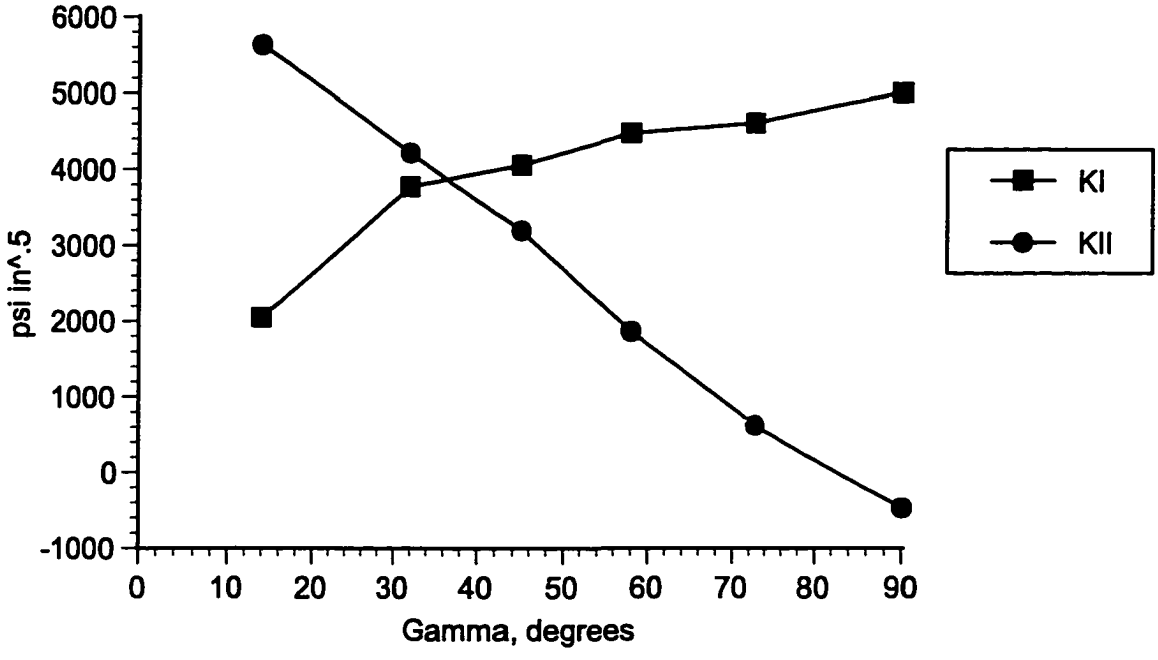

Figure 37. KI and KII for the experimental data as a function of the angle of the applied load.

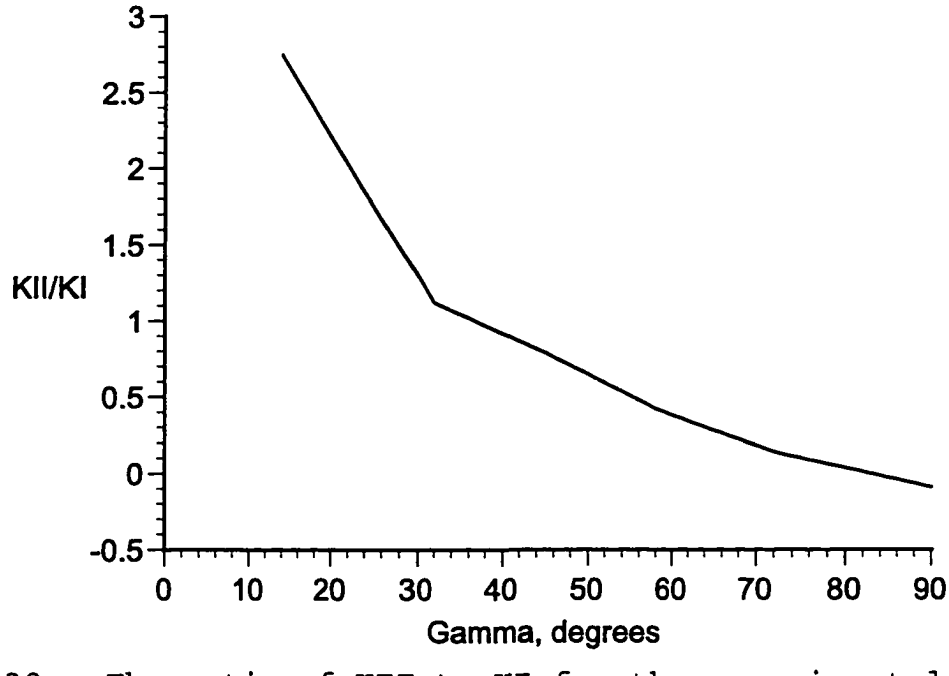

Figure 38. The ratio of KII to KI for the experimental data as a function of the angle of the applied load.

numerical solution presented in Figures 34 and 35 but the spread in the range of solutions is wider. Figure 41 is a final comparison of the experimental and numerical solutions for KI and KII with the range bars omitted. The experimental KI results agree well with the numerical KI results, the KII results are slightly spread.

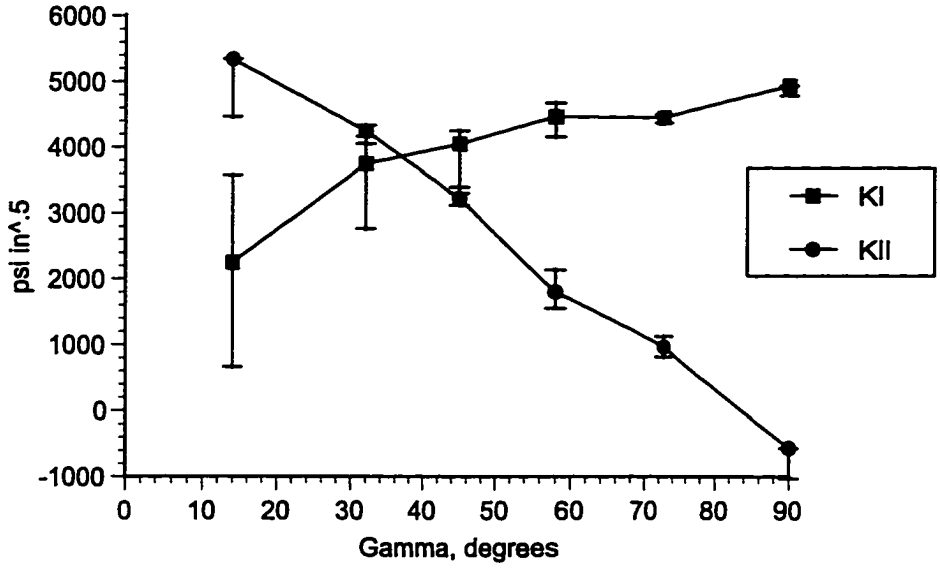

Figure 39. KI and KII calculated using MIXMODE and a range of crack location and orientation initial offsets from the true crack position, using experimental data.

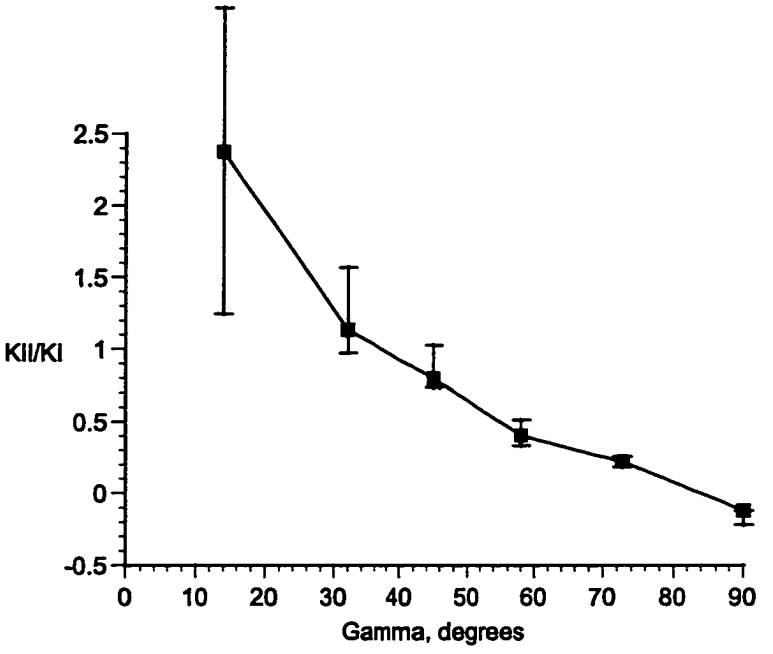

Figure 40. The ratio of KII to KI calculated using MIXMODE and a range of crack location and orientation initial offsets from the true crack position, using experimental data.

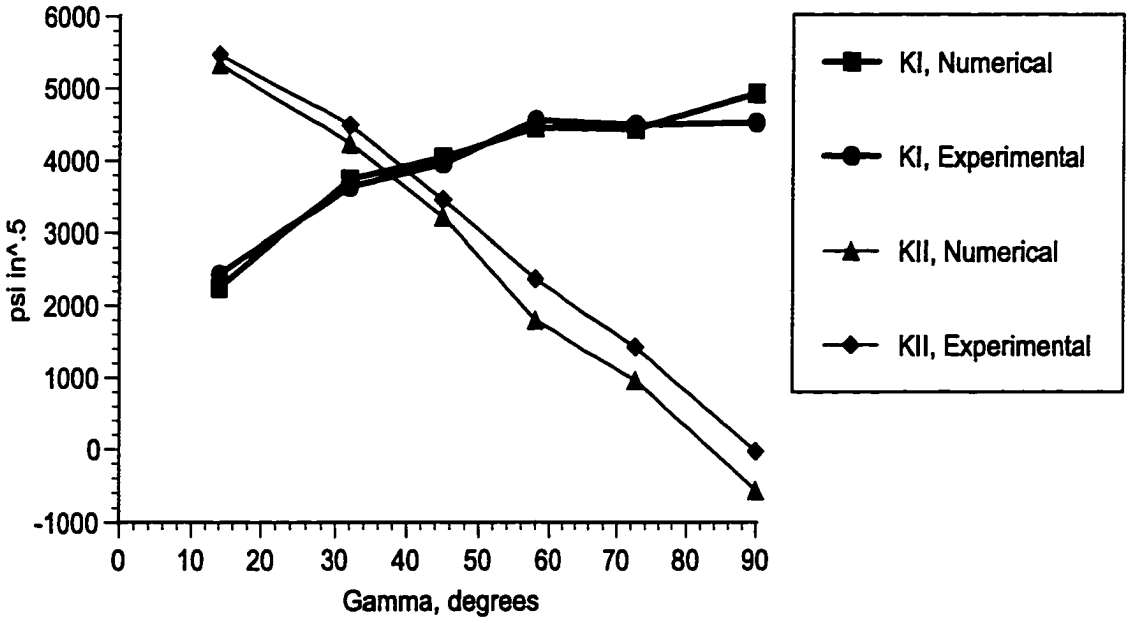

Figure 41. KI and KII calculated using MIXMODE for the experimental and numerical data.

CHAPTER 6. CONCLUSIONS AND DISCUSSIONS

The method developed to determine KI and KII works well for known crack locations and orientations. The mixed mode plate specimen with two strip gages located near the crack tip and parallel to it provides excellent agreement with the finite element numerical solution. The MIXMODE routine using the numerical data is within 1.3 % of the displacement matching method. The experimental data processed with MIXMODE is within 8 % for the KI values. The experimental KII values are within 2 % at the low load angle, where KII is the dominate stress intensity factor, but there is an offset at the high load angle. At the high load angle the KI term is dominate. The 600 psi $\sqrt{inch}$ difference between the KII solutions at the 90 degree load angle is only 12 % of the KI solution.

For unknown crack locations and orientations good initial knowledge of the vicinity of the crack tip is required. Using two strip gages, as on the mixed mode plate, provides better tip locating ability and stress intensity factor solution than the one strip gage on the compact tension specimen. The crack orientation is found with less precision than the tip location is.

The mixed mode plate characterized in Chapter 5 provides a convenient tool for experimenting with other techniques to determine mixed mode stress intensity factors. A KII to KI ratio range of 0 to 2.2 is now available in a single specimen. The specimens used by previous experimenters [7, 8, 10, 13, 14, 18, 19, 23,28] are fixed to a singe KII to KI ratio, a new specimen must be machined to investigate a different KII to KI ratio.

The higher order terms, those beyond $\sqrt{r}$, in Equation 12 are shown to be unnecessary for accurately determining the

stress intensity factors from strain gage data. This reduces the number of variables that need to be used with a limited number of strain gages. The benefits of a least squares fit are enhanced. Empirically, this is pleasing since it is expected that the strain field away from the crack tip will not have a high order dependence on distance from the crack tip.

There are several areas of additional research that this topic brings to mind. These are:

1. Expand the MIXMODE routine to include the KIII term.
2. Create a test specimen with all three stress intensity factors active, KI, KII, and KIII.
3. Expand the relationships to include non isotropic materials.
4. Derive the surface strain fields for other types of cracks, such as corner cracks and elliptical face cracks.
5. Use this method to monitor a crack in a structure as it is loaded in service.
6. Optimize the placement of gages around an existing flaw for monitoring growth during cyclic loading.

The accuracy of the KI and KII solutions for different applications requires some discussion. For the creation of crack growth curves the stress intensity factor and crack growth must both be measured very closely. For this application the method proposed here would need to use known crack tip location and orientation.

For many engineering applications the knowledge of KI, KII, and tip location do not require such precision. A reasonable estimate is often sufficient to solve the problem

at hand. A fine example of this is cracking found in the Space Shuttle Main Engine (SSME) High Pressure Fuel TurboPump (HPFTP) turbine blade attachments. On July 24, 1991, SSME engine 0215 experienced a failure of the second stage turbine of the HPFTP [45]. The failure was attributed to the growth of an internal defect to critical size, which liberated a second stage airfoil just above the attachment [46]. The problem was twofold; first the defect was undetected by inspections during manufacturing and, second, fracture mechanics would not predict the crack growth to failure.

The first problem is beyond the scope of this paper. References 45 and 46 provide a detailed discussion. For the second problem the published da/dN (crack length change, da, per loading cycle, dN) vs. ΔK (change in stress intensity factor per load cycle) is compared with the calculated ΔK for the flaw and the measured da/dN from crack growth arrest marks. Additional data points for this comparison of the da/dN vs. ΔK are available from earlier blade attachment cracking experience [47]. Figure 42 shows the da/dN vs. ΔK curve originally published for the blade material with several of the actual blade cracks plotted on the same graph [48].

The actual growth rate experienced in service was 3 to 4 orders of magnitude greater than the published material property curve. Even a rough order of magnitude estimate of ΔK will highlight this difference. A factor of 2 in variation of the ΔK does not affect the conclusion that the laboratory data does not account for the environment experienced by the blades. Subsequent corrections to the test environments resulted in a curve that passes through the data points the blade analysis provided.

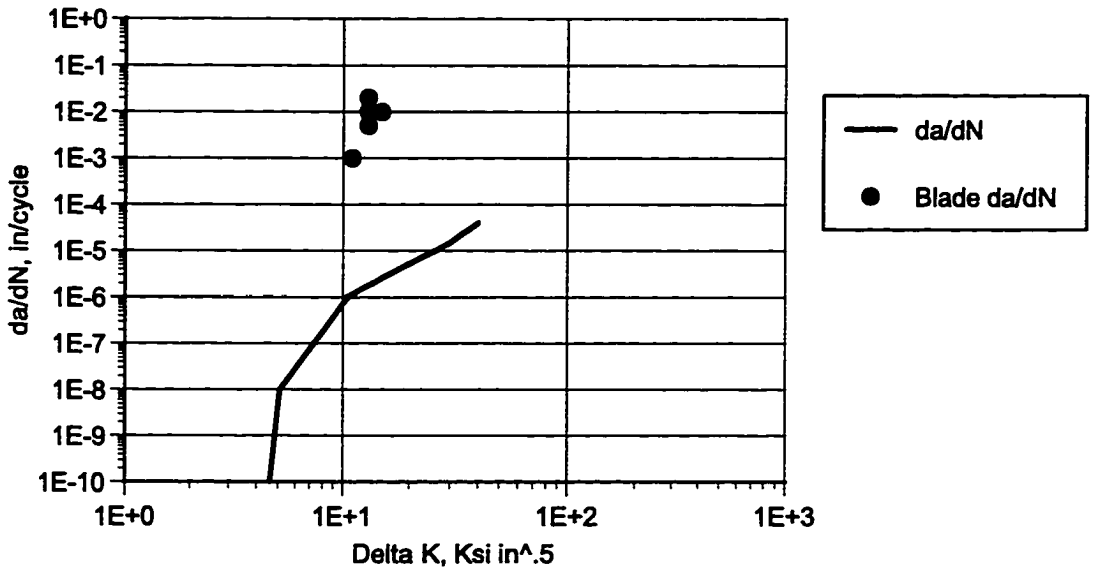

Figure 42. Laboratory da/dN curve for blade material with actual blade crack da/dN superimposed.

The conclusion is that an investigation into cracking would benefit from the MIXMODE routine if the component could be instrumented with strain gages while being subjected to service loads. The reasonableness of the material property curves and fracture analysis could be readily assessed.

APPENDIX A. MLLS FORTRAN CODE LISTING

```
c     Search Routine using the FOURTH ROOT OF NWR 5/21/95
C     This version incorporates weighted residuals 2-27-95
c     This program controls the input and output data and sets up the
iterations
c     for a minimization of a multiple linear least squares search for the
c     best fit of coefficients to an equation describing the strain field
c     around a crack tip
c
c
c     The first COMMON block contains the variables used for 27 solutions
c     of the MLLS problem, these are used by the main program, and the
c     subroutine FIT.  The crack tip offsets are stored here.
c
      COMMON/CMAIN/CRACKX,CRACKY,CRACKB,CRACKAO,CRACKBO,CRACKA1
     &   ,CRAW14,XCL,YCL,BETAL,DX,DY,DB,DXYMAX,DBMAX,DXYMIN
     &   ,DBMIN,XMAX,XMIN,YMAX,YMIN,BMAX,BMIN,COUNT
      REAL CRACKX(27),CRACKY(27),CRACKB(27),CRACKAO(27),CRACKBO(27)
     &   ,CRACKA1(27),XCL,YCL,BETAL,DX,DY,DB,DXYMAX,CRAW14(27)
     &   ,DBMAX,DXYMIN,DBMIN,XMAX,XMIN,YMAX,YMIN,BMAX,BMIN
      INTEGER COUNT
c
c     CRACKX(27) - array of 27 crack tip global x locations
c     CRACKY(27) - array of 27 crack tip global y locations
c     CRACKB(27) - array of 27 crack tip global beta angles
c     CRACKAO(27) - array of 27 parameter A0
c     CRACKBO(27) - array of 27 parameter B0
c     CRACKA1(27) - array of 27 parameter A1
c     CRAW14(27) - array of 27 sum of Fourth Root weighted residuals
c     XCL - crack tip x master location for a particular set of 27
c     YCL - crack tip y master location for a particular set of 27
c     BETAL - crack tip beta master angle for a particular set of 27
c     DX - current tip +/- x variation, this set of 27
c     DY - current tip +/- y variation, this set of 27
c     DB - current tip +/- beta variation, this set of 27
c     DXYMAX - maximum tip +/- x,y variation,user input
c     DBMAX - maximum tip +/- beta orientation,user input
c     DXYMIN - minimum tip +/- x,y variation,user input
c     DBMIN - minimum tip +/- beta orientation,user input
c     XMAX - maximum + x location allowed, user input
c     XMIN - maximum - x location allowed, user input
c     YMAX - maximum + y location allowed, user input
c     YMIN - maximum - y location allowed, user input
c     BMAX - maximum + beta orientation allowed, user input
c     BMIN - maximum + beta orientation allowed, user input
c     COUNT - index used within the set of 27
c
c     The COMMON block CFIT contains the strain data as measured on the
c     hardware or FEM model in global coordinates and the current solution
c     from MLLS as the 27 cases are stepped through
c
      COMMON/CFIT/XG,YG,ANB,STRN,MU,K,BETA,N,XC,YC,AO,BO,A1
     &   ,WGH14,STRNSUM
      REAL XG(80),YG(80),ANB(80),STRN(80),MU,K,BETA,XC,YC
      REAL AO,BO,A1,WGH14,STRNSUM
      INTEGER N
c
c     XG(80) - gage x locations, user input
```

```
c     YG(80) - gage y locations, user input
c     ANB(80) - gage angles in global system, user input
c     STRN(80) - gage strain, user input
c     MU - shear modulus, user input
c     K - plane stress constant, user input
c     BETA - guess of crack tip orientation, user input
c     N - number of data points
c     XC - guess of crack tip x location, user input
c     YC - guess of crack tip y location, user input
c     AO - parameter A0 from current iteration of fit
c     BO - parameter B0 from current iteration of fit
c     A1 - parameter A1 from current iteration of fit
c     WGH14 - sum of Cube Root of weighted differences
c     STRNSUM - sum of absolute value of input strains
c

c     The COMMON block CMMLS contains the output from the MLLS routine for
c     the current case as the 27 cases are stepped through.  These
variables
c     are then placed in the 27 deep vectors in COMMON block CMAIN.
c
      COMMON/CMLLS/Y,X1,X2,SUMY2,SY2,SR2,FT1,FT2,BOGO,GO,R,THETA,ALPHA
      REAL Y(80),X1(80),X2(80),SUMY2,SY2,SR2,FT1,FT2
      REAL BOGO
      REAL GO,R(80),THETA(80),ALPHA(80)
c
c     Y(80) - response variate
c     X1(80) - first predictor variate
c     X2(80) - second predictor variate
c     N - number of data points
c     SUMY2 - sum of the Y's, Squared
c     SY2 - residual sum mean squares after mean
c     SR2 - regression mean sum of squares
c     FT1 - first test statistic
c     FT2 - second test statistic
c     BOGO - m from Y=AOX1+A1X2+m
c     GO - function G0
c     R(80) - gage radial distance from crack tip
c     THETA(80) - gage angle location from crack tip, crack coord. sys
c     ALPHA(80) - gage orientation angle in crack coord. sys
c
      REAL K1
      INTEGER I,IN,IO,L,M,P,MINIMUM,MAX
      CHARACTER*16 FILIN,FILOUT
      DATA IN,IO/21,22/
c
c     K1 - stress intensity factor
c     I - general use index
c     IN - input file unit number
c     IO - output file unit number
c     L,M,P - general use index
c     MINIMUM - number of 1 - 27 with with minumum residual parameter
c     MAX - iteration counter, program stoped at 100
c     FILIN - name of input data file
c     FILOUT - name of output data file
C
C Read in the data file names
C
      WRITE (*,100)
```

```
100   FORMAT (' INPUT FILE NAME:')
      READ (*,101) FILIN
101   FORMAT (A16)
      WRITE (*,102)
102   FORMAT (' OUTPUT FILE NAME:')
      READ (*,101) FILOUT
      OPEN (IN,FILE=FILIN)
      OPEN (IO,FILE=FILOUT)
C
C Read the data files into variables
C
      READ (IN,103) N
103   FORMAT (I3)
      READ (IN,104) (STRN(I),XG(I),YG(I),ANB(I),I=1,N)
104   FORMAT (1x,F10.6,1X,F10.6,1X,F10.6,1X,F10.6)
      WRITE (*,105) (STRN(I),XG(I),YG(I),ANB(I),I=1,N)
      WRITE (IO,105) (STRN(I),XG(I),YG(I),ANB(I),I=1,N)
105   FORMAT (1X,G12.6,1X,G12.6,1X,G12.6,1X,G12.6)
      READ (IN,106) XC,YC,BETA
106   FORMAT (1x,F10.6,1X,F10.6,1X,F10.6)
108   FORMAT (1x,G12.6,1X,G12.6,1X,G12.6)
      WRITE (*,108) XC,YC,BETA
      WRITE (IO,108) XC,YC,BETA
      READ (IN,107) MU,K
107   FORMAT (1x,F10.6,1X,F10.6)
109   FORMAT (1x,G12.6,1X,G12.6)
      WRITE (*,109) MU,K
      WRITE (IO,109) MU,K
      READ (IN,107) DXYMAX,DXYMIN
      WRITE (*,109) DXYMAX,DXYMIN
      WRITE (IO,109) DXYMAX,DXYMIN
      READ (IN,107) DBMAX,DBMIN
      WRITE (*,109) DBMAX,DBMIN
      WRITE (IO,109) DBMAX,DBMIN
      READ (IN,107) XMAX,XMIN
      WRITE (*,109) XMAX,XMIN
      WRITE (IO,109) XMAX,XMIN
      READ (IN,107) YMAX,YMIN
      WRITE (*,109) YMAX,YMIN
      WRITE (IO,109) YMAX,YMIN
      READ (IN,107) BMAX,BMIN
      WRITE (*,109) BMAX,BMIN
      WRITE (IO,109) BMAX,BMIN
C
C
C     SET UP FOR FIRST ITERATION
C
      XCL=XC
      YCL=YC
      BETAL=BETA
      DX=DXYMAX
      DY=DXYMAX
      DB=DBMAX
      MAX=0
C
C     COMPUTE 27 MLLS SOLUTIONS
C
220   MAX=MAX+1
      WRITE (*,3000) MAX
```

```
      WRITE (*,209) XCL
      WRITE (*,210) YCL
      WRITE (*,211) BETAL
3000  FORMAT (1X,I4)
      IF (MAX.GT.100) THEN
        GOTO 999
      ENDIF
      DO 200 L=1,3
        DO 201 M=1,3
        DO 202 P=1,3
          COUNT=(L-1)*9+(M-1)*3+P
          CRACKX(COUNT)=XCL-DX+(L-1)*DX
          CRACKY(COUNT)=YCL-DY+(M-1)*DY
          CRACKB(COUNT)=BETAL-DB+(P-1)*DB
202         CONTINUE
201       CONTINUE
200     CONTINUE
      DO 300 COUNT=1,27
        CALL FIT
        CRACKAO(COUNT)=AO
        CRACKBO(COUNT)=BO
        CRACKA1(COUNT)=A1
        CRAW14(COUNT)=WGH14
300     CONTINUE
C
C     FIND THE SMALLEST SUM OF FOURTH ROOT OF WEIGHTED DFFERENCES IN THE
SET OF 27
C
      MINIMUM=1
      DO 400 COUNT=2,27
        IF(CRAW14(MINIMUM).GT.CRAW14(COUNT))THEN
        MINIMUM=COUNT
        ENDIF
400     CONTINUE
C
C    CHECK TO SEE IF MINIMUM IS AT INITIAL POINT
C
      IF(MINIMUM.EQ.14) THEN
        IF((DX.LE.DXYMIN).AND.(DY.LE.DXYMIN).AND.(DB.LE.DBMIN))THEN
        GOTO 1000
      ELSE
        DX=DX/2
        DY=DY/2
        DB=DB/2
      ENDIF
      GOTO 220
      ELSE
        XCL=CRACKX(MINIMUM)
        YCL=CRACKY(MINIMUM)
        BETAL=CRACKB(MINIMUM)
      ENDIF
      IF(((XCL.GE.XMIN).AND.(XCL.LE.XMAX))
     &    .AND.((YCL.GE.YMIN).AND.(YCL.LE.YMAX))
     &    .AND.((BETAL.GE.BMIN).AND.(BETAL.LE.BMAX))) THEN
         GOTO 220
        ELSE
         GOTO 998
        ENDIF
C
```

```
C     998 IS AN ERROR ENDING
C
998   WRITE (*,1998)
      WRITE (IO,1998)
1998  FORMAT (' XCL, YCL, AND/OR BETAL OUT OF RANGE')
      GOTO 1000
C
C     999 IS AN ERROR ENDING
C
999   WRITE (*,1999)
      WRITE (IO,1999)
1999  FORMAT (' STOPPED BY OVER 100 ITERATIONS')
      GOTO 1000
C
C     1000 IS A NORMAL ENDING
C
1000   WRITE (*,2000)
      WRITE (IO,2000)
2000  FORMAT (' NORMAL EXIT')
      WRITE (IO,206) CRACKAO(MINIMUM)
      WRITE (*,206) CRACKAO(MINIMUM)
206   FORMAT (1X,' AO= ',E16.6)
      WRITE (IO,207) CRACKBO(MINIMUM)
      WRITE (*,207) CRACKBO(MINIMUM)
207   FORMAT (1X,' BO= ',E16.6)
      WRITE (IO,208) CRACKA1(MINIMUM)
      WRITE (*,208) CRACKA1(MINIMUM)
208   FORMAT (1X,' A1= ',E16.6)
      WRITE (IO,209) CRACKX(MINIMUM)
      WRITE (*,209) CRACKX(MINIMUM)
209   FORMAT (1X,' XCL= ',E16.6)
      WRITE (IO,210) CRACKY(MINIMUM)
      WRITE (*,210) CRACKY(MINIMUM)
210   FORMAT (1X,' YCL= ',E16.6)
      WRITE (IO,251) CRAW14(MINIMUM)
      WRITE (*,251) CRAW14(MINIMUM)
251   FORMAT (1X,' WRN14= ',E16.6)
      WRITE (IO,211) CRACKB(MINIMUM)
      WRITE (*,211) CRACKB(MINIMUM)
211   FORMAT (1X,' BETAL= ',E16.6,' radians')
      K1=SQRT(2*3.1415927)*CRACKAO(MINIMUM)
      WRITE (IO,212) K1
      WRITE (*,212) K1
212   FORMAT (1X,' K1= ',E16.6)
      BETAL=(180/3.1415927)*CRACKB(MINIMUM)
      WRITE (IO,213) BETAL
      WRITE (*,213) BETAL
213   FORMAT (1X,' BETAL= ',E16.6,' degrees')
      CLOSE (IN)
      CLOSE (IO)
      WRITE (*,1300)
      READ (*,1301) IN
1300  FORMAT (1X,'TYPE RETURN TO CONTINUE ')
1301  FORMAT (1X,I1)
      STOP
      END
```

```
      SUBROUTINE FIT

c     This routine prepares data and calls MLLS
c     This routine is updated and valid 5/21/95.  It includes ONLY
c     fourth root of normalized weighted residuals.
c     This version is for 27 solutions.
c
c
C     Declare REAL Function and internal vectors and matrices
c
c     The first COMMON block contains the variables used for 27 solutions
c     of the MLLS problem, these are used by the main program, and the
c     subroutine FIT.  The crack tip offsets are storred here.
c
c     The first COMMON block contains the variables used for 27 solutions
c     of the MLLS problem, these are used by the main program, and the
c     subroutine FIT.  The crack tip offsets are storred here.
c
      COMMON/CMAIN/CRACKX,CRACKY,CRACKB,CRACKAO,CRACKBO,CRACKA1
     &   ,CRAW14,XCL,YCL,BETAL,DX,DY,DB,DXYMAX,DBMAX,DXYMIN
     &   ,DBMIN,XMAX,XMIN,YMAX,YMIN,BMAX,BMIN,COUNT
      REAL CRACKX(27),CRACKY(27),CRACKB(27),CRACKAO(27),CRACKBO(27)
     &   ,CRACKA1(27),XCL,YCL,BETAL,DX,DY,DB,DXYMAX,CRAW14(27)
     &   ,DBMAX,DXYMIN,DBMIN,XMAX,XMIN,YMAX,YMIN,BMAX,BMIN
      INTEGER COUNT
c
c
      COMMON/CFIT/XG,YG,ANB,STRN,MU,K,BETA,N,XC,YC,AO,BO,A1
     &   ,WGH14,STRNSUM
      REAL XG(80),YG(80),ANB(80),STRN(80),MU,K,BETA,XC,YC
      REAL AO,BO,A1,WGH14,STRNSUM
      INTEGER N
c
c     The COMMON block CMMLS contains the output from the MLLS routine for
c     the current case as the 27 cases are stepped through.  These
variables
c     are then placed in the 27 deep vectors in COMMON block CMAIN.
c
      COMMON/CMLLS/Y,X1,X2,SUMY2,SY2,SR2,FT1,FT2,BOGO,GO,R,THETA,ALPHA
      REAL Y(80),X1(80),X2(80),SUMY2,SY2,SR2,FT1,FT2
      REAL BOGO
      REAL GO,R(80),THETA(80),ALPHA(80)
      INTEGER I,J
C
C     Initialize parameter and output variables
c
      STRNSUM=0.0
      DO 10 I=1,N
        R(I)=SQRT((XG(I)-CRACKX(COUNT))**2+(YG(I)-CRACKY(COUNT))**2)
        THETA(I)=ATAN2((-(XG(I)-CRACKX(COUNT))*SIN(CRACKB(COUNT))
     &      +(YG(I)-CRACKY(COUNT))*COS(CRACKB(COUNT))),
     &      ((XG(I)-CRACKX(COUNT))*COS(CRACKB(COUNT))
     &      +(YG(I)-CRACKY(COUNT))*SIN(CRACKB(COUNT))))
        ALPHA(I)=ANB(I)-CRACKB(COUNT)
        Y(I)=2*MU*STRN(I)
        X1(I)=(1./SQRT(R(I)))*(K*COS(THETA(I)/2)
     &      -0.5*SIN(THETA(I))*SIN(1.5*THETA(I))*COS(2*ALPHA(I))
     &      +0.5*SIN(THETA(I))*COS(1.5*THETA(I))*SIN(2*ALPHA(I)))
        X2(I)=SQRT(R(I))*COS(THETA(I)/2)*(K+
```

```
     &      SIN(THETA(I)/2)*SIN(THETA(I)/2)*COS(2*ALPHA(I))
     &      -0.5*SIN(THETA(I))*SIN(2*ALPHA(I)))
          STRNSUM=STRNSUM+ABS(STRN(I))
10        CONTINUE
       CALL MLLS
       GO=K+COS(2*ALPHA(1))
       BO=BOGO/GO
       WGH14=0.0
       DO 110 I=1,N
          WGH14=WGH14+SQRT(SQRT(ABS((2*MU*STRN(I)-AO*X1(I)-A1*X2(I)
     &  -BO*GO)*STRN(I)/(MU*STRNSUM))))
110    CONTINUE
100    FORMAT (1X,I2,1X,G12.6,1X,G12.6)
        WRITE (*,100) N,AO,WGH14
C
       RETURN
       END


SUBROUTINE MLLS
c      Least Square subroutine for search program
c
C      Declare REAL Function and internal vectors and matrices
c
c      The COMMON block CFIT contains the strain data as measured on the
c      hardware or FEM model in global coordinates and the current solution
c      from MLLS as the 27 cases are stepped through
c
       COMMON/CFIT/XG,YG,ANB,STRN,MU,K,BETA,N,XC,YC,AO,BO,A1
     &  ,WGH14,STRNSUM
       REAL XG(80),YG(80),ANB(80),STRN(80),MU,K,BETA,XC,YC
       REAL AO,BO,A1,WGH14,STRNSUM
       INTEGER N
c
c      The COMMON block CMMLS contains the output from the MLLS routine for
c      the current case as the 27 cases are stepped through.  These
variables
c      are then placed in the 27 deep vectors in COMMON block CMAIN.
c
       COMMON/CMLLS/Y,X1,X2,SUMY2,SY2,SR2,FT1,FT2,BOGO,GO,R,THETA,ALPHA
       REAL Y(80),X1(80),X2(80),SUMY2,SY2,SR2,FT1,FT2
       REAL BOGO
       REAL GO,R(80),THETA(80),ALPHA(80)
       REAL X(80,3),B(3),X1AVE,X2AVE,Y2SUM,XTX(3,3)
       REAL XTXINV(3,3),XTY(3),BTXTY
       INTEGER I,J,L
C
C      X(80,3) - centered set of data
C      B(3) - vector of estimation parameters
C      X1AVE - average of X1 values
C      X2AVE - average of X2 values
C      Y2SUM - sum of Y^2
C      XTX(3,3) - X transpose times X
C      XTXINV(3,3) - XTX inverse
C      XTY(3) - X transpose times Y
C      BTXTY - B transpose times XTY
C      I,J,L - general use index
C
```

```
C     Initialize parameter and output variables
c
100   FORMAT (1X,I2,1X,G12.6,1X,G12.6,1X,G12.6)
101   FORMAT (1X,G12.6,1X,G12.6,1X,G12.6,1X,G12.6,1X,G12.6,1X,G12.6)
      X1AVE=0.0
      X2AVE=0.0
      Y2SUM=0.0
      SUMY2=0.0
      DO 10 I=1,N
      X1AVE=X1AVE+X1(I)
      X2AVE=X2AVE+X2(I)
      Y2SUM=Y2SUM+Y(I)*Y(I)
      SUMY2=SUMY2+Y(I)
10    CONTINUE
C
      X1AVE=X1AVE/N
      X2AVE=X2AVE/N
      SUMY2=SUMY2**2.
C
C  create centered data in x matrix and initialize other arrays
C
      DO 20 I=1,N
         X(I,1)=1.0
         X(I,2)=X1(I)-X1AVE
         X(I,3)=X2(I)-X2AVE
20       CONTINUE
      DO 25 I=1,3
         XTY(I)=0.0
         B(I)=0.0
         DO 26 J=1,3
            XTX(I,J)=0.0
            XTXINV(I,J)=0.0
26          CONTINUE
25       CONTINUE
      DO 30 I=1,3
         DO 40 J=1,3
            DO 50 L=1,N
               XTX(I,J)=XTX(I,J)+X(L,I)*X(L,J)
50           CONTINUE
40          CONTINUE
30       CONTINUE
      CALL INV2(XTX,XTXINV,3,3)
      DO 60 I=1,3
         DO 70 J=1,N
            XTY(I)=XTY(I)+X(J,I)*Y(J)
70          CONTINUE
60       CONTINUE
      DO 80 I=1,3
         DO 90 J=1,3
            B(I)=B(I)+XTXINV(I,J)*XTY(J)
90          CONTINUE
80       CONTINUE
      BOGO=B(1)-B(2)*X1AVE-B(3)*X2AVE
      AO=B(2)
      A1=B(3)
      SY2=(Y2SUM-SUMY2/N)/(N-1)
      FT1=SUMY2/(N*SY2)
      BTXTY=B(1)*XTY(1)+B(2)*XTY(2)+B(3)*XTY(3)
      SR2=(BTXTY-(SUMY2)/N)/2
```

```
      S2=(Y2SUM-BTXTY)/(N-3)
      RETURN
      END



      SUBROUTINE INV2 (A,Z,N,KR)
      REAL  A(KR,KR),Z(KR,KR)
      REAL SMAX,S,XOFF,X
      INTEGER N,KR,I,J,NIT,NOT,NERROR,IT,NM1,L
      INTEGER LA,K,JMAX,LS,M,M1,LMAX,IOFF,JOFF,JC
      REAL W(150),U(150),IV(150)
     +      ,IRE(150),BIN(150)
      DATA  NIT,NOT/5,25/
C
C  MATRIX INVERSION  (A**-1 = Z).  RANK ANNIHILATION METHOD.
C  THE INVERSION CHECK Z*A IS CALCULATED AND PRINTED.
C  THE MAXIMUM SIZE IS
C    N=150
C  CODED BY CARL BODLEY.  FEBRUARY  1967.
C
C    SUBROUTINE ARGUMENTS
C  A  = INPUT MATRIX TO BE INVERTED.  SIZE(N,N).
C  Z  = OUTPUT RESULT MATRIX.  SIZE (N,N).
C  N  = INPUT SIZE OF MATRICES A,Z.  MAX = 150.
C  KR = INPUT ROW DIMENSION OF A,Z IN CALLING PROGRAM.
C
 2000 FORMAT  (// 10X,10(7X,1H(,I2,1H)))
 2001 FORMAT  (// 10X,41HSUBROUTINE INV2 HAS CALCULATED DATA BELOW)
 2002 FORMAT  (///10X,37HTHE (A**-1)*(A) INVERSION CHECK GIVES
     *      ///10X,25HTHE DIAGONAL ELEMENTS ARE // (13X,10F11.8))
 2003 FORMAT  (// 10X,35HTHE MAXIMUM OFF-DIAGONAL ELEMENT IS
     *                          E11.3, 2X, 4HAT ( I3, 1H, I3, 1H) )
C
c     OPEN (UNIT=25,FILE="INV2.DAT",STATUS="NEW")
                                    NERROR=1
      IF (N.GT.150)GO TO 999
C
                                    NERROR=2
C
C     GENERATE INITIAL ROW INDICES.
      IT=1
      GO TO 90
91    IT=2
90    DO 5 I=1,N
      IRE(I)=I
5     IV(I)=I
C
C     CONDITION A FOR MAXIMUM DIAGONAL ELEMENTS.
      NM1=N-1
      DO 6 L=1,NM1
      SMAX=0.0
      DO 8 J=L,N
      LA=IRE(J)
      I=L
      K=LA
      IF (IT.EQ.2) I=LA
      IF (IT.EQ.2) K=L
      IF (ABS(A(K,I)).LE.SMAX) GO TO 8
```

```
      JMAX=J
      SMAX=ABS(A(K,I))
8     CONTINUE
      LS=IRE(L)
      IRE(L)=IRE(JMAX)
6     IRE(JMAX)=LS
      DO 7 L=1,N
      LA=IRE(L)
      BIN(L)=A(LA,L)
      IF(IT.EQ.2) BIN(L)=A(L,LA)
7     IF (BIN(L).EQ.0.0) BIN(L)=1.0
C
C     GENERATE INITIAL Z AND ABAR.
      DO 10 L=1,N
      LA=IRE(L)
      I=L
      K=LA
      IF (IT.EQ.2) I=LA
      IF (IT.EQ.2) K=L
      DO 15 J=1,N
      M=J
      M1=LA
      IF(IT.EQ.2) M=LA
      IF (IT.EQ.2) M1=J
15    Z(M,M1)=0.0
      Z(I,K)=1.0/BIN(L)
10    A(K,I)=A(K,I)-BIN(L)
C
C     INVERSION LOOP, USES ROW OF ABAR WITH MAXIMUM S.
      DO 35 L=1,N
      SMAX=0.0
      DO 23 J=L,N
      LA=IV(J)
      S=1.0
      DO 26 K=1,N
26    S=S+A(LA,K)*Z(K,LA)
      IF (ABS(S).LE.SMAX) GO TO 23
      LMAX=J
      SMAX=ABS(S)
23    CONTINUE
      IF (SMAX.GT.1.0E-99) GO TO 60
                                                  NERROR=3
      IF (IT.EQ.2) GO TO 999
      GO TO 65
60    LS=IV(L)
      IV(L)=IV(LMAX)
      IV(LMAX)=LS
      LA=IV(L)
      DO 25 I=1,N
      W(I)=0.0
      DO 25 J=1,N
25    W(I)=W(I)+A(LA,J)*Z(J,I)
      S=1.0+W(LA)
      DO 30 I=1,N
30    U(I)=Z(I,LA)
      DO 35 I=1,N
      DO 35 J=1,N
35    Z(I,J)=Z(I,J)-U(I)*W(J)/S
C
```

```
C     RESTORE A.
65    DO 40 L=1,N
      LA=IRE(L)
      I=L
      K=LA
      IF (IT.EQ.2) I=LA
      IF (IT.EQ.2) K=L
40    A(K,I)=A(K,I)+BIN(L)
      IF (SMAX.LE.1.0E-99) GO TO 91
C
C     COMPUTE INVERSION CHECK Z*A.
      XOFF=0.0
      DO 50 J=1,N
      DO 45 I=1,N
      X=0.
      DO 46 K=1,N
46    X=X+Z(I,K)*A(K,J)
      IF (I.NE.J) GO TO 47
      U(I)=X
      GO TO 45
47    IF (ABS(X).LT.XOFF) GO TO 45
      XOFF=X
      IOFF=I
      JOFF=J
45    CONTINUE
50    CONTINUE
C
C     PRINT INVERSION CHECK AND MAXIMUM OFF-DIAGONAL ELEMENT.
c     WRITE (NOT,2000) (JC, JC=1,10)
c     WRITE (NOT,2001)
c     WRITE (NOT,2002) (U(I), I=1,N)
c     WRITE (NOT,2003) XOFF , IOFF , JOFF
c     WRITE (NOT,2020) ((A(I,J), I=1,N), J=1,N)
c     WRITE (NOT,2020) ((Z(I,J), I=1,N), J=1,N)
2020  FORMAT(1X,E14.6)
      RETURN
98    Z(1,1)=1.0/A(1,1)
C
 999  WRITE (NOT,*) 'ERROR NUMBER',NERROR
c     CLOSE (25)
      END
```

APPENDIX B. MIXMODE FORTRAN CODE LISTING

```
c     Search Routine using the FOURTH ROOT OF NWR 5/21/95
C     This version incorporates weighted residuals 2-27-95
C     Modified 2/97 for mixed mode data reduction
c     This program controls the input and output data and sets up the
iterations
c     for a minimization of a multiple linear least squares search for the
c     best fit of coefficients to an equation describing the strain field
c     around a crack tip
c
c
c     The first COMMON block contains the variables used for 27 solutions
c     of the MLLS problem, these are used by the main program, and the
c     subroutine FIT.  The crack tip offsets are stored here.
c
      COMMON/CMAIN/CRACKX,CRACKY,CRACKB,CRACKAO,CRACKBO,CRACKA1,CRACKC0
     &   ,CRACKC1,CRAW14,XCL,YCL,BETAL,DX,DY,DB,DXYMAX,DBMAX,DXYMIN
     &   ,DBMIN,XMAX,XMIN,YMAX,YMIN,BMAX,BMIN,COUNT
      REAL CRACKX(27),CRACKY(27),CRACKB(27),CRACKAO(27),CRACKBO(27)
     &   ,CRACKA1(27),CRACKC0(27),CRACKC1(27)
     &   ,XCL,YCL,BETAL,DX,DY,DB,DXYMAX,CRAW14(27)
     &   ,DBMAX,DXYMIN,DBMIN,XMAX,XMIN,YMAX,YMIN,BMAX,BMIN
      INTEGER COUNT
c
c     CRACKX(27) - array of 27 crack tip global x locations
c     CRACKY(27) - array of 27 crack tip global y locations
c     CRACKB(27) - array of 27 crack tip global beta angles
c     CRACKAO(27) - array of 27 parameter A0
c     CRACKBO(27) - array of 27 parameter B0
c     CRACKA1(27) - array of 27 parameter A1
c     CRACKC0(27) - array of 27 parameter C0
c     CRACKC1(27) - array of 27 parameter C1
c     CRAW14(27) - array of 27 sum of Fourth Root weighted residuals
c     XCL - crack tip x master location for a particular set of 27
c     YCL - crack tip y master location for a particular set of 27
c     BETAL - crack tip beta master angle for a particular set of 27
c     DX - current tip +/- x variation, this set of 27
c     DY - current tip +/- y variation, this set of 27
c     DB - current tip +/- beta variation, this set of 27
c     DXYMAX - maximum tip +/- x,y variation,user input
c     DBMAX - maximum tip +/- beta orientation,user input
c     DXYMIN - minimum tip +/- x,y variation,user input
c     DBMIN - minimum tip +/- beta orientation,user input
c     XMAX - maximum + x location allowed, user input
c     XMIN - maximum - x location allowed, user input
c     YMAX - maximum + y location allowed, user input
c     YMIN - maximum - y location allowed, user input
c     BMAX - maximum + beta orientation allowed, user input
c     BMIN - maximum + beta orientation allowed, user input
c     COUNT - index used within the set of 27
c
c     The COMMON block CFIT contains the strain data as measured on the
c     hardware or FEM model in global coordinates and the current solution
c     from MLLS as the 27 cases are stepped through
c
      COMMON/CFIT/XG,YG,ANB,STRN,MU,K,BETA,N,XC,YC,AO,BO,A1
     &   ,C0,C1,WGH14,STRNSUM
```

```
      REAL XG(80),YG(80),ANB(80),STRN(80),MU,K,BETA,XC,YC
      REAL AO,BO,A1,C0,C1,WGH14,STRNSUM
      INTEGER N
c
c     XG(80) - gage x locations, user input
c     YG(80) - gage y locations, user input
c     ANB(80) - gage angles in global system, user input
c     STRN(80) - gage strain, user input
c     MU - shear modulus, user input
c     K - plane stress constant, user input
c     BETA - guess of crack tip orientation, user input
c     N - number of data points
c     XC - guess of crack tip x location, user input
c     YC - guess of crack tip y location, user input
c     AO - parameter A0 from current iteration of fit
c     BO - parameter B0 from current iteration of fit
c     A1 - parameter A1 from current iteration of fit
c     C0 - parameter C0 from current iteration of fit
c     C1 - parameter C1 from current iteration of fit
c     WGH14 - sum of Cube Root of weighted differences
c     STRNSUM - sum of absolute value of input strains
c

c     The COMMON block CMMLS contains the output from the MLLS routine for
c     the current case as the 27 cases are stepped through.  These
variables
c     are then placed in the 27 deep vectors in COMMON block CMAIN.
c
      COMMON/CMLLS/Y,X1,X2,X3,X4,SUMY2,SY2,SR2,FT1,FT2,BOGO,GO,R,THETA
     & ,ALPHA
      REAL Y(80),X1(80),X2(80),X3(80),X4(80),SUMY2,SY2,SR2,FT1,FT2
      REAL BOGO
      REAL GO,R(80),THETA(80),ALPHA(80)
c
c     Y(80) - response variate
c     X1(80) - first predictor variate
c     X2(80) - second predictor variate
c     X3(80) - third predictor variate
c     X4(80) - fourth predictor variate
c     N - number of data points
c     SUMY2 - sum of the Y's, Squared
c     SY2 - residual sum mean squares after mean
c     SR2 - regression mean sum of squares
c     FT1 - first test statistic
c     FT2 - second test statistic
c     BOGO - m from Y=AOX1+A1X2+m
c     GO - function G0
c     R(80) - gage radial distance from crack tip
c     THETA(80) - gage angle location from crack tip, crack coord. sys
c     ALPHA(80) - gage orientation angle in crack coord. sys
c
      REAL K1,K11
      INTEGER I,IN,IO,L,M,P,MINIMUM,MAX
      CHARACTER*16 FILIN,FILOUT
      DATA IN,IO/21,22/
c
c     K1 - mode 1 stress intensity factor
c     K11 - mode 11 stress intensity factor
c     I - general use index
```

```
c     IN - input file unit number
c     IO - output file unit number
c     L,M,P - general use index
c     MINIMUM - number of 1 - 27 with minimum residual parameter
c     MAX - iteration counter, program stopped at 100
c     FILIN - name of input data file
c     FILOUT - name of output data file
C
C Read in the data file names
C
      WRITE (*,100)
100   FORMAT (' INPUT FILE NAME:')
      READ (*,101) FILIN
101   FORMAT (A16)
      WRITE (*,102)
102   FORMAT (' OUTPUT FILE NAME:')
      READ (*,101) FILOUT
      OPEN (IN,FILE=FILIN)
      OPEN (IO,FILE=FILOUT)
C
C Read the data files into variables
C
      READ (IN,103) N
103   FORMAT (I3)
      READ (IN,104) (STRN(I),XG(I),YG(I),ANB(I),I=1,N)
104   FORMAT (1x,F10.6,1X,F10.6,1X,F10.6,1X,F10.6)
      WRITE (*,105) (STRN(I),XG(I),YG(I),ANB(I),I=1,N)
      WRITE (IO,105) (STRN(I),XG(I),YG(I),ANB(I),I=1,N)
105   FORMAT (1X,G12.6,1X,G12.6,1X,G12.6,1X,G12.6)
      READ (IN,106) XC,YC,BETA
106   FORMAT (1x,F10.6,1X,F10.6,1X,F10.6)
108   FORMAT (1x,G12.6,1X,G12.6,1X,G12.6)
      WRITE (*,108) XC,YC,BETA
      WRITE (IO,108) XC,YC,BETA
      READ (IN,107) MU,K
107   FORMAT (1x,F10.6,1X,F10.6)
109   FORMAT (1x,G12.6,1X,G12.6)
      WRITE (*,109) MU,K
      WRITE (IO,109) MU,K
      READ (IN,107) DXYMAX,DXYMIN
      WRITE (*,109) DXYMAX,DXYMIN
      WRITE (IO,109) DXYMAX,DXYMIN
      READ (IN,107) DBMAX,DBMIN
      WRITE (*,109) DBMAX,DBMIN
      WRITE (IO,109) DBMAX,DBMIN
      READ (IN,107) XMAX,XMIN
      WRITE (*,109) XMAX,XMIN
      WRITE (IO,109) XMAX,XMIN
      READ (IN,107) YMAX,YMIN
      WRITE (*,109) YMAX,YMIN
      WRITE (IO,109) YMAX,YMIN
      READ (IN,107) BMAX,BMIN
      WRITE (*,109) BMAX,BMIN
      WRITE (IO,109) BMAX,BMIN
C
C
C     SET UP FOR FIRST ITERATION
C
      XCL=XC
```

```
      YCL=YC
      BETAL=BETA
      DX=DXYMAX
      DY=DXYMAX
      DB=DBMAX
      MAX=0
C
C     COMPUTE 27 MLLS SOLUTIONS
C
220   MAX=MAX+1
      WRITE (*,3000) MAX
      WRITE (*,209) XCL
      WRITE (*,210) YCL
      WRITE (*,211) BETAL
3000  FORMAT (1X,I4)
      IF (MAX.GT.100) THEN
        GOTO 999
      ENDIF
      DO 200 L=1,3
        DO 201 M=1,3
        DO 202 P=1,3
          COUNT=(L-1)*9+(M-1)*3+P
          CRACKX(COUNT)=XCL-DX+(L-1)*DX
          CRACKY(COUNT)=YCL-DY+(M-1)*DY
          CRACKB(COUNT)=BETAL-DB+(P-1)*DB
202         CONTINUE
201       CONTINUE
200     CONTINUE
      DO 300 COUNT=1,27
        CALL FIT
        CRACKAO(COUNT)=AO
        CRACKBO(COUNT)=BO
        CRACKC0(COUNT)=C0
        CRACKA1(COUNT)=A1
        CRACKC1(COUNT)=C1
        CRAW14(COUNT)=WGH14
300     CONTINUE
C
C     FIND THE SMALLEST SUM OF FOURTH ROOT OF WEIGHTED DFFERENCES IN THE
SET OF 27
C
      MINIMUM=1
      DO 400 COUNT=2,27
        IF(CRAW14(MINIMUM).GT.CRAW14(COUNT))THEN
        MINIMUM=COUNT
        ENDIF
400     CONTINUE
C
C    CHECK TO SEE IF MINIMUM IS AT INITIAL POINT
C
      IF(MINIMUM.EQ.14) THEN
        IF((DX.LE.DXYMIN).AND.(DY.LE.DXYMIN).AND.(DB.LE.DBMIN))THEN
        GOTO 1000
      ELSE
        DX=DX/2
        DY=DY/2
        DB=DB/2
      ENDIF
      GOTO 220
```

```
      ELSE
        XCL=CRACKX(MINIMUM)
        YCL=CRACKY(MINIMUM)
        BETAL=CRACKB(MINIMUM)
      ENDIF
      IF(((XCL.GE.XMIN).AND.(XCL.LE.XMAX))
     &    .AND.((YCL.GE.YMIN).AND.(YCL.LE.YMAX))
     &    .AND.((BETAL.GE.BMIN).AND.(BETAL.LE.BMAX))) THEN
         GOTO 220
        ELSE
         GOTO 998
        ENDIF
C
C     998 IS AN ERROR ENDING
C
998   WRITE (*,1998)
      WRITE (IO,1998)
1998  FORMAT (' XCL, YCL, AND/OR BETAL OUT OF RANGE')
      GOTO 1000
C
C     999 IS AN ERROR ENDING
C
999   WRITE (*,1999)
      WRITE (IO,1999)
1999  FORMAT (' STOPPED BY OVER 100 ITERATIONS')
      GOTO 1000
C
C     1000 IS A NORMAL ENDING
C
1000   WRITE (*,2000)
      WRITE (IO,2000)
2000  FORMAT (' NORMAL EXIT')
      WRITE (IO,206) CRACKAO(MINIMUM)
      WRITE (*,206) CRACKAO(MINIMUM)
206   FORMAT (1X,' AO= ',E16.6)
      WRITE (IO,207) CRACKBO(MINIMUM)
      WRITE (*,207) CRACKBO(MINIMUM)
207   FORMAT (1X,' BO= ',E16.6)
      WRITE (IO,2207) CRACKC0(MINIMUM)
      WRITE (*,2207) CRACKC0(MINIMUM)
2207   FORMAT (1X,' C0= ',E16.6)
      WRITE (IO,208) CRACKA1(MINIMUM)
      WRITE (*,208) CRACKA1(MINIMUM)
208   FORMAT (1X,' A1= ',E16.6)
      WRITE (IO,2208) CRACKC1(MINIMUM)
      WRITE (*,2208) CRACKC1(MINIMUM)
2208   FORMAT (1X,' C1= ',E16.6)
      WRITE (IO,209) CRACKX(MINIMUM)
      WRITE (*,209) CRACKX(MINIMUM)
209   FORMAT (1X,' XCL= ',E16.6)
      WRITE (IO,210) CRACKY(MINIMUM)
      WRITE (*,210) CRACKY(MINIMUM)
210   FORMAT (1X,' YCL= ',E16.6)
      WRITE (IO,251) CRAW14(MINIMUM)
      WRITE (*,251) CRAW14(MINIMUM)
251   FORMAT (1X,' WRN14= ',E16.6)
      WRITE (IO,211) CRACKB(MINIMUM)
      WRITE (*,211) CRACKB(MINIMUM)
211   FORMAT (1X,' BETAL= ',E16.6,' radians')
```

```
      K1=SQRT(2*3.1415927)*CRACKAO(MINIMUM)
      WRITE (IO,212) K1
      WRITE (*,212) K1
212   FORMAT (1X,' K1= ',E16.6)
      K11=SQRT(2*3.1415927)*CRACKC0(MINIMUM)
      WRITE (IO,2212) K11
      WRITE (*,2212) K11
2212   FORMAT (1X,' K11= ',E16.6)
      BETAL=(180/3.1415927)*CRACKB(MINIMUM)
      WRITE (IO,213) BETAL
      WRITE (*,213) BETAL
213   FORMAT (1X,' BETAL= ',E16.6,' degrees')
      CLOSE (IN)
      CLOSE (IO)
      WRITE (*,1300)
      READ (*,1301) IN
1300  FORMAT (1X,'TYPE RETURN TO CONTINUE ')
1301  FORMAT (1X,I1)
      STOP
      END


SUBROUTINE FIT

c     This routine prepares data and calls MLLS
c     Modified 2/14/97 for mixed mode data
c     This routine is updated and valid 5/21/95.  It includes ONLY
c     fourth root of normalized weighted residuals.
c     This version is for 27 solutions.
c
c
C     Declare REAL Function and internal vectors and matrices
c
c
c     The first COMMON block contains the variables used for 27 solutions
c     of the MLLS problem, these are used by the main program, and the
c     subroutine FIT.  The crack tip offsets are stored here.
c
      COMMON/CMAIN/CRACKX,CRACKY,CRACKB,CRACKAO,CRACKBO,CRACKA1,CRACKC0
     &   ,CRACKC1,CRAW14,XCL,YCL,BETAL,DX,DY,DB,DXYMAX,DBMAX,DXYMIN
     &   ,DBMIN,XMAX,XMIN,YMAX,YMIN,BMAX,BMIN,COUNT
      REAL CRACKX(27),CRACKY(27),CRACKB(27),CRACKAO(27),CRACKBO(27)
     &   ,CRACKA1(27),CRACKC0(27),CRACKC1(27)
     &   ,XCL,YCL,BETAL,DX,DY,DB,DXYMAX,CRAW14(27)
     &   ,DBMAX,DXYMIN,DBMIN,XMAX,XMIN,YMAX,YMIN,BMAX,BMIN
      INTEGER COUNT
c
c
      COMMON/CFIT/XG,YG,ANB,STRN,MU,K,BETA,N,XC,YC,AO,BO,A1
     &   ,C0,C1,WGH14,STRNSUM
      REAL XG(80),YG(80),ANB(80),STRN(80),MU,K,BETA,XC,YC
      REAL AO,BO,A1,C0,C1,WGH14,STRNSUM
      INTEGER N
c
c     The COMMON block CMMLS contains the output from the MLLS routine for
c     the current case as the 27 cases are stepped through.  These
variables
c     are then placed in the 27 deep vectors in COMMON block CMAIN.
```

```
c
      COMMON/CMLLS/Y,X1,X2,X3,X4,SUMY2,SY2,SR2,FT1,FT2,BOGO,GO,R,THETA
     & ,ALPHA
      REAL Y(80),X1(80),X2(80),X3(80),X4(80),SUMY2,SY2,SR2,FT1,FT2
      REAL BOGO
      REAL GO,R(80),THETA(80),ALPHA(80)
      INTEGER I
      OPEN (30,FILE="FITOUT")
C
C     Initialize parameter and output variables
c
      STRNSUM=0.0
      DO 10 I=1,N
        R(I)=SQRT((XG(I)-CRACKX(COUNT))**2+(YG(I)-CRACKY(COUNT))**2)
        THETA(I)=ATAN2((-(XG(I)-CRACKX(COUNT))*SIN(CRACKB(COUNT))
     &      +(YG(I)-CRACKY(COUNT))*COS(CRACKB(COUNT))),
     &      ((XG(I)-CRACKX(COUNT))*COS(CRACKB(COUNT))
     &      +(YG(I)-CRACKY(COUNT))*SIN(CRACKB(COUNT))))
        ALPHA(I)=ANB(I)-CRACKB(COUNT)
        Y(I)=2*MU*STRN(I)
        X1(I)=(1./SQRT(R(I)))*(K*COS(THETA(I)/2)
     &      -0.5*SIN(THETA(I))*SIN(1.5*THETA(I))*COS(2*ALPHA(I))
     &      +0.5*SIN(THETA(I))*COS(1.5*THETA(I))*SIN(2*ALPHA(I)))
        X2(I)=SQRT(R(I))*COS(THETA(I)/2)*(K+
     &      SIN(THETA(I)/2)*SIN(THETA(I)/2)*COS(2*ALPHA(I))
     &      -0.5*SIN(THETA(I))*SIN(2*ALPHA(I)))
        X3(I)=(1./SQRT(R(I)))*(SIN(THETA(I)/2)*(-K-COS(2*ALPHA(I))*(1
     &         +COS(THETA(I)/2)*COS(1.5*THETA(I)))+SIN(2*ALPHA(I))*
     &         (COS(THETA(I)/2)-.5*SIN(THETA(I))*SIN(1.5*THETA(I))))
         X4(I)=SQRT(R(I))*(SIN(THETA(I)/2)*(K+COS(2*ALPHA(I))*
     &       (1+COS(THETA(I)/2)*COS(THETA(I)/2)))+SIN(2*ALPHA(I))*
     &       COS(THETA(I)/2)*(1+SIN(THETA(I)/2)*SIN(THETA(I)/2)))
        STRNSUM=STRNSUM+ABS(STRN(I))
       WRITE (30,200) X1(I),X2(I),X3(I),X4(I),STRNSUM
10      CONTINUE
      CALL MLLS
      GO=K+COS(2*ALPHA(1))
      BO=BOGO/GO
      WGH14=0.0
      DO 110 I=1,N
         WGH14=WGH14+SQRT(SQRT(ABS((2*MU*STRN(I)-AO*X1(I)-A1*X2(I)
     &  -C0*X3(I)-C1*X4(I)-BO*GO)*STRN(I)/(MU*STRNSUM))))
110   CONTINUE
200   FORMAT (1X,G12.6,1X,G12.6,1X,G12.6,1X,G12.6,1X,G12.6)
100   FORMAT (1X,I2,1X,G12.6,1X,G12.6,1X,G12.6)
       WRITE (*,100) N,AO,C0,WGH14
       WRITE (30,100) N,AO,C0,WGH14
C
      RETURN
      END



SUBROUTINE MLLS
c     Modified 2/97 for mixed modes
c     Least Square subroutine for search program
c
C     Declare REAL Function and internal vectors and matrices
```

```
c
c     The COMMON block CFIT contains the strain data as measured on the
c     hardware or FEM model in global coordinates and the current solution
c     from MLLS as the 27 cases are stepped through
c
      COMMON/CFIT/XG,YG,ANB,STRN,MU,K,BETA,N,XC,YC,AO,BO,A1
     &  ,C0,C1,WGH14,STRNSUM
      REAL XG(80),YG(80),ANB(80),STRN(80),MU,K,BETA,XC,YC
      REAL AO,BO,A1,C0,C1,WGH14,STRNSUM
      INTEGER N
c
c     The COMMON block CMMLS contains the output from the MLLS routine for
c     the current case as the 27 cases are stepped through.  These
variables
c     are then placed in the 27 deep vectors in COMMON block CMAIN.
c
      COMMON/CMLLS/Y,X1,X2,X3,X4,SUMY2,SY2,SR2,FT1,FT2,BOGO,GO,R,THETA
     &,ALPHA
      REAL Y(80),X1(80),X2(80),X3(80),X4(80),SUMY2,SY2,SR2,FT1,FT2
      REAL BOGO
      REAL GO,R(80),THETA(80),ALPHA(80)
      REAL X(80,5),B(5),X1AVE,X2AVE,X3AVE,X4AVE,Y2SUM,XTX(5,5)
      REAL XTXINV(5,5),XTY(5),BTXTY
      INTEGER I,J,L
      OPEN (31,FILE="MLLSOUT")
C
C     X(80,5) - centered set of data
C     B(5) - vector of estimation parameters
C     X1AVE - average of X1 values
C     X2AVE - average of X2 values
C     X3AVE - average of X3 values
C     X4AVE - average of X4 values
C     Y2SUM - sum of Y^2
C     XTX(5,5) - X transpose times X
C     XTXINV(5,5) - XTX inverse
C     XTY(5) - X transpose times Y
C     BTXTY - B transpose times XTY
C     I,J,L - general use index
C
C     Initialize parameter and output variables
c
100   FORMAT (1X,I2,1X,G12.6,1X,G12.6,1X,G12.6)
101   FORMAT (1X,G12.6,1X,G12.6,1X,G12.6,1X,G12.6,1X,G12.6,1X,G12.6)
      X1AVE=0.0
      X2AVE=0.0
      X3AVE=0.0
      X4AVE=0.0
      Y2SUM=0.0
      SUMY2=0.0
      DO 10 I=1,N
      X1AVE=X1AVE+X1(I)
      X2AVE=X2AVE+X2(I)
      X3AVE=X3AVE+X3(I)
      X4AVE=X4AVE+X4(I)
      Y2SUM=Y2SUM+Y(I)*Y(I)
      SUMY2=SUMY2+Y(I)
10    CONTINUE
C
      X1AVE=X1AVE/N
```

```
      X2AVE=X2AVE/N
      X3AVE=X3AVE/N
      X4AVE=X4AVE/N
      SUMY2=SUMY2**2.
C
C  create centered data in x matrix and initialize other arrays
C
      DO 20 I=1,N
         X(I,1)=1.0
         X(I,2)=X1(I)-X1AVE
         X(I,3)=X2(I)-X2AVE
         X(I,4)=X3(I)-X3AVE
         X(I,5)=X4(I)-X4AVE
       WRITE (31,200) X(I,1),X(I,2),X(I,3),X(I,4),X(I,5)
20       CONTINUE
      DO 25 I=1,5
         XTY(I)=0.0
         B(I)=0.0
         DO 26 J=1,5
            XTX(I,J)=0.0
            XTXINV(I,J)=0.0
26          CONTINUE
25       CONTINUE
      DO 30 I=1,5
         DO 40 J=1,5
            DO 50 L=1,N
               XTX(I,J)=XTX(I,J)+X(L,I)*X(L,J)
50           CONTINUE
40          CONTINUE
30       CONTINUE
c     Set zero values on XTX (remove roundoff error)
      DO 121 I=1,5
        WRITE (31,200) XTX(I,1),XTX(I,2),XTX(I,3),XTX(I,4),XTX(I,5)
121     CONTINUE
      DO 130 I=2,5
        XTX(1,I)=1.0E-20
        XTX(I,1)=1.0E-20
130     CONTINUE
      DO 120 I=1,5
        WRITE (31,200) XTX(I,1),XTX(I,2),XTX(I,3),XTX(I,4),XTX(I,5)
120     CONTINUE
      CALL INV2(XTX,XTXINV,5,5)
      DO 140 I=2,5
        XTXINV(1,I)=1.0E-20
        XTXINV(I,1)=1.0E-20
140     CONTINUE
      DO 60 I=1,5
         DO 70 J=1,N
            XTY(I)=XTY(I)+X(J,I)*Y(J)
70          CONTINUE
60       CONTINUE
      DO 80 I=1,5
         DO 90 J=1,5
            B(I)=B(I)+XTXINV(I,J)*XTY(J)
90          CONTINUE
80       CONTINUE
      BOGO=B(1)-B(2)*X1AVE-B(3)*X2AVE-B(4)*X3AVE-B(5)*X4AVE
      AO=B(2)
      A1=B(3)
```

```
      C0=B(4)
      C1=B(5)
      SY2=(Y2SUM-SUMY2/N)/(N-1)
      FT1=SUMY2/(N*SY2)
      BTXTY=B(1)*XTY(1)+B(2)*XTY(2)+B(3)*XTY(3)+B(4)*X3AVE+B(5)*X4AVE
      SR2=(BTXTY-(SUMY2)/N)/4
      S2=(Y2SUM-BTXTY)/(N-5)
200   FORMAT (1X,G12.6,1X,G12.6,1X,G12.6,1X,G12.6,1X,G12.6)
      RETURN
      END




      SUBROUTINE INV2 (A,Z,N,KR)
      REAL  A(KR,KR),Z(KR,KR)
      REAL SMAX,S,XOFF,X
      INTEGER N,KR,I,J,NIT,NOT,NERROR,IT,NM1,L
      INTEGER LA,K,JMAX,LS,M,M1,LMAX,IOFF,JOFF,JC
      REAL W(150),U(150),IV(150)
     + ,IRE(150),BIN(150)
      DATA  NIT,NOT/5,25/
C
C  MATRIX INVERSION  (A**-1 = Z).  RANK ANNIHILATION METHOD.
C  THE INVERSION CHECK Z*A IS CALCULATED AND PRINTED.
C  THE MAXIMUM SIZE IS
C    N=150
C  CODED BY CARL BODLEY.  FEBRUARY  1967.
C
C    SUBROUTINE ARGUMENTS
C  A  = INPUT MATRIX TO BE INVERTED.  SIZE(N,N).
C  Z  = OUTPUT RESULT MATRIX.  SIZE (N,N).
C  N  = INPUT SIZE OF MATRICES A,Z.  MAX = 150.
C  KR = INPUT ROW DIMENSION OF A,Z IN CALLING PROGRAM.
C
 2000 FORMAT  (// 10X,10(7X,1H(,I2,1H)))
 2001 FORMAT  (// 10X,41HSUBROUTINE INV2 HAS CALCULATED DATA BELOW)
 2002 FORMAT  (///10X,37HTHE (A**-1)*(A) INVERSION CHECK GIVES
     *      ///10X,25HTHE DIAGONAL ELEMENTS ARE // (13X,10F11.8))
 2003 FORMAT  (// 10X,35HTHE MAXIMUM OFF-DIAGONAL ELEMENT IS
     *                          E11.3, 2X, 4HAT ( I3, 1H, I3, 1H) )
C
c     OPEN (UNIT=25,FILE="INV2.DAT",STATUS="NEW")
                                    NERROR=1
      IF (N.GT.150)GO TO 999
C
                                    NERROR=2
C
C     GENERATE INITIAL ROW INDICES.
      IT=1
      GO TO 90
91    IT=2
90    DO 5 I=1,N
      IRE(I)=I
5     IV(I)=I
C
C     CONDITION A FOR MAXIMUM DIAGONAL ELEMENTS.
```

```
      NM1=N-1
      DO 6 L=1,NM1
      SMAX=0.0
      DO 8 J=L,N
      LA=IRE(J)
      I=L
      K=LA
      IF (IT.EQ.2) I=LA
      IF (IT.EQ.2) K=L
      IF (ABS(A(K,I)).LE.SMAX) GO TO 8
      JMAX=J
      SMAX=ABS(A(K,I))
8     CONTINUE
      LS=IRE(L)
      IRE(L)=IRE(JMAX)
6     IRE(JMAX)=LS
      DO 7 L=1,N
      LA=IRE(L)
      BIN(L)=A(LA,L)
      IF(IT.EQ.2) BIN(L)=A(L,LA)
7     IF (BIN(L).EQ.0.0) BIN(L)=1.0
C
C     GENERATE INITIAL Z AND ABAR.
      DO 10 L=1,N
      LA=IRE(L)
      I=L
      K=LA
      IF (IT.EQ.2) I=LA
      IF (IT.EQ.2) K=L
      DO 15 J=1,N
      M=J
      M1=LA
      IF(IT.EQ.2) M=LA
      IF (IT.EQ.2) M1=J
15    Z(M,M1)=0.0
      Z(I,K)=1.0/BIN(L)
10    A(K,I)=A(K,I)-BIN(L)
C
C     INVERSION LOOP, USES ROW OF ABAR WITH MAXIMUM S.
      DO 35 L=1,N
      SMAX=0.0
      DO 23 J=L,N
      LA=IV(J)
      S=1.0
      DO 26 K=1,N
26    S=S+A(LA,K)*Z(K,LA)
      IF (ABS(S).LE.SMAX) GO TO 23
      LMAX=J
      SMAX=ABS(S)
23    CONTINUE
      IF (SMAX.GT.1.0E-99) GO TO 60
                                                  NERROR=3
      IF (IT.EQ.2) GO TO 999
      GO TO 65
60    LS=IV(L)
      IV(L)=IV(LMAX)
      IV(LMAX)=LS
      LA=IV(L)
      DO 25 I=1,N
```

```
      W(I)=0.0
      DO 25 J=1,N
25    W(I)=W(I)+A(LA,J)*Z(J,I)
      S=1.0+W(LA)
      DO 30 I=1,N
30    U(I)=Z(I,LA)
      DO 35 I=1,N
      DO 35 J=1,N
35    Z(I,J)=Z(I,J)-U(I)*W(J)/S
C
C     RESTORE A.
65    DO 40 L=1,N
      LA=IRE(L)
      I=L
      K=LA
      IF (IT.EQ.2) I=LA
      IF (IT.EQ.2) K=L
40    A(K,I)=A(K,I)+BIN(L)
      IF (SMAX.LE.1.0E-99) GO TO 91
C
C     COMPUTE INVERSION CHECK Z*A.
      XOFF=0.0
      DO 50 J=1,N
      DO 45 I=1,N
      X=0.
      DO 46 K=1,N
46    X=X+Z(I,K)*A(K,J)
      IF (I.NE.J) GO TO 47
      U(I)=X
      GO TO 45
47    IF (ABS(X).LT.XOFF) GO TO 45
      XOFF=X
      IOFF=I
      JOFF=J
45    CONTINUE
50    CONTINUE
C
C     PRINT INVERSION CHECK AND MAXIMUM OFF-DIAGONAL ELEMENT.
c     WRITE (NOT,2000) (JC, JC=1,10)
c     WRITE (NOT,2001)
c     WRITE (NOT,2002) (U(I), I=1,N)
c     WRITE (NOT,2003) XOFF , IOFF , JOFF
c     WRITE (NOT,2020) ((A(I,J), I=1,N), J=1,N)
c     WRITE (NOT,2020) ((Z(I,J), I=1,N), J=1,N)
c2020 FORMAT(1X,E14.6)
      RETURN
98    Z(1,1)=1.0/A(1,1)
C
 999  WRITE (NOT,*) 'ERROR NUMBER',NERROR
c     CLOSE (25)
      END
```

APPENDIX C. EDM COMPACT TENSION FINITE ELEMENT MODEL LISTING

```
/prep7
/Title,EDM CT Specimen, Special Tip Mesh
mp,ex,1,9.9e6
mp,nuxy,1,.33
c***
c*** center keypoints
c***
k,1,,.05 $ ,2,.45,.05 $ ,3,1.125,.05 $ ,4,1.25 $ ,5,1.875
,6,3.5 $ ,7,3.5,1.1875 $ ,8,.45,1.1875 $ ,9,,1.1875
,10,.45,.55 $ ,11,.45,.55,1
circle,10,.25,11,8,,8
k,30,1.6 $ ,31,2.2005 $ ,32,2.4 $ ,33,1.6,.2485 $ ,34,1.885,.2485
,35,2.2005,.2463 $ ,36,2.4,.2463 $ ,37,1.6,.5 $ ,38,1.885,.5
,39,2.2005,.5 $ ,40,2.4,.5 $ ,41,1.6,1.1875 $ ,42,2.4,1.1875
k,50,3.5,.2463 $ ,51,3.5,.5 $ ,52,2.2005,1.1875 $ ,53,1.875,1.1875
,60,3.25,0 $ ,61,3.25,.2463 $ ,62,3.25,0.5 $ ,63,3.25,1.1875
c***
c*** surface keypoints
c***
k,101,,.05,.5 $ ,102,.45,.05,.5 $ ,103,1.125,.05,.5 $ ,104,1.25,,.5
,105,1.875,,.5 $ ,106,3.5,,.5 $ ,107,3.5,1.1875,.5 $ ,108,.45,1.1875,.5
,109,,1.1875,.5 $ ,110,.45,.55,.5 $ ,111,.45,.55,1
circle,110,.25,111,8,,8
k,130,1.6,,.5 $ ,131,2.2005,,.5 $ ,132,2.4,,.5 $ ,133,1.6,.2485,.5
,134,1.885,.2485,.5 $ ,135,2.2005,.2463,.5 $ ,136,2.4,.2463,.5
,137,1.6,.5,.5 $ ,138,1.885,.5,.5 $ ,139,2.2005,.5,.5 $ ,140,2.4,.5,.5
,141,1.6,1.1875,.5 $ ,142,2.4,1.1875,.5
k,150,3.5,.2463,.5 $ ,151,3.5,.5,.5 $ ,152,2.2005,1.1875,.5
,153,1.875,1.1875,.5 $ ,160,3.25,0,.5 $ ,161,3.25,.2463,.5
,162,3.25,0.5,.5 $ ,163,3.25,1.1875,.5
kmod,22,.2,.55,.490687
c***
c*** radius edge keypoints
c***
k,206,3.5,0,.25 $ ,250,3.5,0.2463,.25 $ ,251,3.5,0.5,.25
,207,3.5,1.1875,.25 $ ,201,0,.05,.226777 $ ,209,0,1.1875,.226777
,221,.273223,1.1875,.5 $ ,223,.273223,.05,.5
save
C***
c*** lines and areas on center plane
c***
l,1,2 $ ,2,3 $ ,3,4 $ ,4,30 $ ,8,9 $ ,9,1 $ ,8,12 $ ,16,2
,30,33 $ ,33,37 $ ,37,41 $ ,41,8
l,5,105,8 $ ,30,130,8 $ ,31,131,8 $ ,34,134,8
,35,135,8
,30,5,5 $ ,5,34,5 $ ,5,31,6
,130,105,5 $ ,105,134,5 $ ,105,131,6
save
kpsel,x,-.05,.46 $ kprse,z,-.1,.1 $ lskp,1
al,all
kpsel,x,.44,1.61 $ kprse,z,-.1,.1 $ lskp,1
al,all
kpall
lsall
arall
save
```

```
c***
c*** lines and areas on free surface
c***
l,102,103 $ ,103,104 $ ,104,130 $ ,141,108
,108,20 $ ,24,102
,130,133 $ ,133,137 $ ,137,141
,209,201
save
a,223,102,24,23
,21,20,108,221
kpsel,x,.44,1.61 $ kprse,z,0.45,1 $ lskp,1
al,all
kpall
lsall
local,15,1,.273223,0,.22677,0,0,-90
cscir,15,1
l,201,223 $ ,209,221
csys,0
kpse,x,0,.28 $ kprse,z,.2,.6 $ lskp,1 $ csys,15
al,all
csys,0
arall
kpall
save
c***
c*** lines and areas between center and free surface
c***
l,1,201 $ ,2,102 $ ,3,103 $ ,4,104 $ ,5,105
,8,108 $ ,9,209 $ ,12,20 $ ,16,24 $ ,14,22 $ ,18,26
save
a,1,9,209,201
save
kpsel,x,0,.46 $ kprse,y,0,.1 $ lskp,1
al,all
kpsel,x,0,.46 $ kprse,y,1,1.2 $ lskp,1
al,all
kpsel,x,.44,.46 $ kprse,y,0,.5 $ lskp,1
al,all
kpsel,x,.44,.46 $ kprse,y,.6,1.2 $ lskp,1
al,all
local,12,1,.45,.55
kpse,y,-5,95 $ kprse,x,.24,.26 $ lskp,1
al,all
kpse,y,-95,5 $ kprse,x,.24,.26 $ lskp,1
al,all
cscir,12,1
kpse,y,85,185 $ kprse,x,.24,.26 $ lskp,1
al,all
kpse,y,175,275 $ kprse,x,.24,.26 $ lskp,1
al,all
csys,0
kpsel,x,.44,1.15 $ kprse,y,0,.1 $ lskp,1
al,all
kpsel,x,1.1,1.3 $ kprse,y,0,.1 $ lskp,1
al,all
kpall
a,30,130,133,33
,33,133,137,37
,37,137,141,41
```

```
kpsel,x,1.2,1.65 $ kprse,y,0,.1 $ lskp,1
al,all
kpsel,x,.44,1.65 $ kprse,y,1.1,1.2 $ lskp,1
al,all
arall
kpall
save
c***
c***  Create all the volumes
c***
c*** clear areas to allow use of brick elements in meshing
kpse,x,1.55,2.5 $ kprse,y,0,.6 $ lskp,1 $ arls,1
adel,all
c*** adds back areas for volumes 1, 2 and 3
kpall $ arall $ lsall
a,37,38,138,137
a,38,39,139,138
a,39,40,140,139
a,30,33,133,130
a,33,37,137,133
save
c*** volume 1
kpse,x,0,.46 $ lskp,1 $ arls,1
va,all
save
c*** volume 2
kpse,x,.44,1.65 $ lskp,1 $ arls,1
va,all
kpall $ arall
c*** volume 3
v,37,38,53,41,137,138,153,141
c*** volume 4
v,33,34,38,37,133,134,138,137
c*** volume 5, above strain gage path
v,34,35,39,38,134,135,139,138
c*** volume 6
v,35,36,40,39,135,136,140,139
c*** volume 7, before crack tip
v,30,5,34,33,130,105,134,133
c*** volume 8, after crack tip
v,5,31,35,34,105,131,135,134
c*** volume 9
v,31,32,36,35,131,132,136,135
c*** volume 10
v,38,39,52,53,138,139,152,153
c*** volume 11
v,39,40,42,52,139,140,142,152
c*** volume 12
v,32,60,61,36,132,160,161,136
c*** volume 13
v,36,61,62,40,136,161,162,140
c*** volume 14
v,40,62,63,42,140,162,163,142
save
c*** volume 15
kpsel,x,3.25 $ kprse,z,.5 $ lskp,1 $ kpall
l,206,207
local,16,1,3.25,0,.25,0,0,-90
l,160,206 $ ,207,163
```

```
al,all
save
csys,0
a,6,7,207,206
a,63,7,207,163
a,60,6,206,160
kpsel,x,3.25,4 $ kprs,z,-.1,.1 $ lskp,1
al,all
kpsel,x,3.25,4 $ lskp,1 $ arls,1
va,all
kpall
lsall
save
c***
c*** Tip Mesh Nodes And Elements
c***
local,13,1,1.875
n,1
n,2,0.015625
ngen,9,1,2,2,1,0,22.5
n,11,0.0625
ngen,17,1,11,11,1,0,11.25
n,51,0,0,0.03125
n,61,0.0625,0,0.03125
ngen,9,1,61,61,1,0,22.5
ngen,8,100,all,,,0,0,0.0625
ngen,2,800,1,27,1,0,0,0.5
save
et,1,95
e,11,13,1,1,111,113,101,101
emore,12,3,1,2,112,103,101,102
emore,61,62,51,51
e,13,15,1,1,113,115,101,101
emore,14,4,1,3,114,104,101,103
emore,62,63,51,51
e,15,17,1,1,115,117,101,101
emore,16,5,1,4,116,105,101,104
emore,63,64,51,51
e,17,19,1,1,117,119,101,101
emore,18,6,1,5,118,106,101,105
emore,64,65,51,51
e,19,21,1,1,119,121,101,101
emore,20,7,1,6,120,107,101,106
emore,65,66,51,51
e,21,23,1,1,121,123,101,101
emore,22,8,1,7,122,108,101,107
emore,66,67,51,51
e,23,25,1,1,123,125,101,101
emore,24,9,1,8,124,109,101,108
emore,67,68,51,51
e,25,27,1,1,125,127,101,101
emore,26,10,1,9,126,110,101,109
emore,68,69,51,51save
egen,8,100,-8
save
csys,13
n,1001,0.09375
,1010,0.125
ngen,9,1,1001,1010,1,0,22.5
```

```
csys,0
n,1019,2.008,.088
,1020,2.00,.11
,1021,1.98,.13
,1022,1.78,.13
,1023,1.75,.11
,1024,1.74,.088
,1025,1.6
ngen,6,1,1025,1025,1,0,0.0497
n,1031,1.657
ngen,6,1,1031,1031,1,0,0.0497
n,1037,1.714
ngen,6,1,1037,1037,1,0,0.0497
n,1043,1.771,.1491
,1044,1.771,.1988
,1045,1.771,.2485
,1046,1.828,.1491
,1047,1.828,.1988
,1048,1.828,.2485
,1049,1.875,.1491
,1050,1.875,.1988
,1051,1.885,.2485
,1052,1.93758,.14778
,1053,1.93758,.19704
,1054,1.93758,.24813
,1055,1.9902,.14778
,1056,1.9902,.19704
,1057,1.9902,.24776
,1058,2.04275,0.0
ngen,5,1,1058,1058,1,0,0.04926
n,1063,2.04275,0.2474
,1064,2.09533,0.0
ngen,5,1,1064,1064,1,0,0.04926
n,1069,2.09533,0.24703
,1070,2.147917,0.0
ngen,5,1,1070,1070,1,0,0.04926
n,1075,2.147917,0.24667
,1076,2.2005
ngen,6,1,1076,1076,1,0,0.04926
ngen,9,1000,1001,1081,1,0,0,0.0625
save
c*** stif 45 elements
et,2,45
type,2
e,1025,1031,1032,1026,2025,2031,2032,2026
egen,5,1,-1
egen,2,6,-5
egen,8,1000,-10
e,1037,1018,1017,1038,2037,2018,2017,2038
e,1038,1017,1024,1039,2038,2017,2024,2039
e,1017,1016,1023,1024,2017,2016,2023,2024
e,1016,1015,1022,1023,2016,2015,2022,2023
e,1039,1024,1023,1040,2039,2024,2023,2040
e,1023,1022,1043,1040,2023,2022,2043,2040
e,1022,1015,1046,1043,2022,2015,2046,2043
e,1015,1014,1049,1046,2015,2014,2049,2046
egen,8,1000,-8
e,1040,1043,1044,1041,2040,2043,2044,2041
egen,2,1,-1
```

```
egen,5,3,-2
e,1055,1061,1062,1056,2055,2061,2062,2056
egen,2,1,-1
egen,8,1000,-12
e,1001,1010,1011,1002,2001,2010,2011,2002
egen,8,1,-1
egen,8,1000,-8
e,11,1001,1002,13,111,2001,2002,113
e,111,2001,2002,113,211,3001,3002,213
e,211,3001,3002,213,311,4001,4002,313
e,311,4001,4002,313,411,5001,5002,413
e,411,5001,5002,413,511,6001,6002,513
e,511,6001,6002,513,611,7001,7002,613
e,611,7001,7002,613,711,8001,8002,713
e,711,8001,8002,713,811,9001,9002,813
e,13,1002,1003,15,113,2002,2003,115
e,113,2002,2003,115,213,3002,3003,215
e,213,3002,3003,215,313,4002,4003,315
e,313,4002,4003,315,413,5002,5003,415
e,413,5002,5003,415,513,6002,6003,515
e,513,6002,6003,515,613,7002,7003,615
e,613,7002,7003,615,713,8002,8003,715
e,713,8002,8003,715,813,9002,9003,815
e,15,1003,1004,17,115,2003,2004,117
e,115,2003,2004,117,215,3003,3004,217
e,215,3003,3004,217,315,4003,4004,317
e,315,4003,4004,317,415,5003,5004,417
e,415,5003,5004,417,515,6003,6004,517
e,515,6003,6004,517,615,7003,7004,617
e,615,7003,7004,617,715,8003,8004,717
e,715,8003,8004,717,815,9003,9004,817
e,17,1004,1005,19,117,2004,2005,119
e,117,2004,2005,119,217,3004,3005,219
e,217,3004,3005,219,317,4004,4005,319
e,317,4004,4005,319,417,5004,5005,419
e,417,5004,5005,419,517,6004,6005,519
e,517,6004,6005,519,617,7004,7005,619
e,617,7004,7005,619,717,8004,8005,719
e,717,8004,8005,719,817,9004,9005,819
e,19,1005,1006,21,119,2005,2006,121
e,119,2005,2006,121,219,3005,3006,221
e,219,3005,3006,221,319,4005,4006,321
e,319,4005,4006,321,419,5005,5006,421
e,419,5005,5006,421,519,6005,6006,521
e,519,6005,6006,521,619,7005,7006,621
e,619,7005,7006,621,719,8005,8006,721
e,719,8005,8006,721,819,9005,9006,821
e,21,1006,1007,23,121,2006,2007,123
e,121,2006,2007,123,221,3006,3007,223
e,221,3006,3007,223,321,4006,4007,323
e,321,4006,4007,323,421,5006,5007,423
e,421,5006,5007,423,521,6006,6007,523
e,521,6006,6007,523,621,7006,7007,623
e,621,7006,7007,623,721,8006,8007,723
e,721,8006,8007,723,821,9006,9007,823
e,23,1007,1008,25,123,2007,2008,125
e,123,2007,2008,125,223,3007,3008,225
e,223,3007,3008,225,323,4007,4008,325
e,323,4007,4008,325,423,5007,5008,425
```

```
e,423,5007,5008,425,523,6007,6008,525
e,523,6007,6008,525,623,7007,7008,625
e,623,7007,7008,625,723,8007,8008,725
e,723,8007,8008,725,823,9007,9008,825
e,25,1008,1009,27,125,2008,2009,127
e,125,2008,2009,127,225,3008,3009,227
e,225,3008,3009,227,325,4008,4009,327
e,325,4008,4009,327,425,5008,5009,427
e,425,5008,5009,427,525,6008,6009,527
e,525,6008,6009,527,625,7008,7009,627
e,625,7008,7009,627,725,8008,8009,727
e,725,8008,8009,727,825,9008,9009,827
e,1010,1058,1059,1011,2010,2058,2059,2011
e,1011,1059,1060,1019,2011,2059,2060,2019
e,1011,1019,1020,1012,2011,2019,2020,2012
egen,2,1,-1
e,1019,1060,1061,1020,2019,2060,2061,2020
e,1020,1061,1055,1021,2020,2061,2055,2021
e,1013,1021,1055,1052,2013,2021,2055,2052
e,1014,1013,1052,1049,2014,2013,2052,2049
egen,8,1000,-8
e,1058,1064,1065,1059,2058,2064,2065,2059
egen,5,1,-1
egen,3,6,-5
egen,8,1000,-15
save
c*** change stif 45 into stif 95
type,1
esel,stif,45
emodif,all
emid
merge,0.001
save
c***
c*** Mesh Volumes
c***
et,3,95
type,3
elsize,.075
vmesh,8
save
vmesh,5
vmesh,7
vmesh,9
save
elsize,.1
vmesh,4
vmesh,6
save
elsize,.125
vmesh,3
vmesh,10,14
save
et,4,92
type,4
elsize,.16
vmesh,2
elsize,.1
vmesh,1
```

```
save
vmesh,15
save
c***
c*** modify mesh to incorporate tip mesh
c***
modmsh,deta
nsel,x,1.59,2.201
nrse,y,0,0.249
enode,1
erse,type,3
edel,all
eall
nelem
ninv
ndel,all
nall
eall
merge,.001
c***
c*** Constraints
c***
nsel,z,-.1,.001
d,all,uz,0.
nsel,y,-.1,.005
nrse,x,1.874,4.
d,all,uy,0.
nrse,x,1.874,1.876
d,all,ux,0.
c***
c*** Pressure to apply 1000 pound load at hole
c***
csys,12
cscir,12
nsel,x,0.23,0.27
nrse,y,-.1,180
psf,all,,,2000.
csys,0
nall
eall
c***
c*** search for best wavefront
c***
save
waves
wsort,x
,y
,z
afwri
fini
c***/check
/input,27
fini
/eof
/eof
```

APPENDIX D. MIXED MODE PLATE FINITE ELEMENT MODEL LISTING

```
/batch
/filnam,plate1
/PREP7
/TITLE, MIXED MODE PLATE, load case 1
MP,EX,1,9.9E6
,NUXY,1,.33
ET,1,plane2,,,3
R,1,.25
nread,plnodes
eread,plelem
WSORT,X
SAVE
c*** loadsteps for mixed mode plate
c*** written 4-23-91
/com,  load case 1
f,4902,fy,704.
,4903,fy,497.7
,4904,fy,650.3
,6783,fy,497.7
,6785,fy,650.3
d,4902,ux,0.
,6606,ux,0.
,6606,uy,0.
,6604,uy,0.
,6607,uy,0.
,8588,uy,0.
,8589,uy,0.
save
fini
/solution
solve
fini
/post1
/title, load case 1 , plate1
set,1
prrf
c*** nodes 36 to 26 are top gages 1 to 10
lpath,36,26
pdef,gagex,epel,x
pdef,gagey,epel,y
prpath,gagex,gagey
c*** nodes 585 to 586 are bottom gages 1 to 10
lpath,585,586
pdef,gagex,epel,x
pdef,gagey,epel,y
prpath,gagex,gagey
local,20,0,0,5
lpath,1,98,97,652,651
kcalc,1,1,3,1
kcalc,0,1,3,1
/eof
/eof
```

REFERENCES CITED

1. Pratt & Whitney, "SSME Alternate Turbopump Program Fracture Control Plan", FR-19793-3, February, 1995.

2. Marshall Space Flight Center, "Standard NDE Guidelines and Requirements for Fracture Control Programs", MSFC-STD-1249, September, 1985.

3. Pratt & Whitney, "Standard Flight Life Limit Deviation Approval Request (DAR) for the Space Shuttle Main Engine (SSME) Alternate Turbopump Program", PWA-SP-36184, June, 1995.

4. Johnson Space Flight Center, "Fatigue Crack Growth Computer Program "NASA/FLAGRO" Version 2.0", JSC-22267A, May, 1994.

5. Dally, J. W. and Sanford, R. J., "Strain-Gage Methods for Measuring the Opening-Mode Stress-Intensity Factor, KI", Experimental Mechanics, Volume 27 Number 4, pages 381-388, 1987.

6. Dally, J. W. and Berger, J. R., "An Overdeterministic Approach for Measuring K1 Using Strain Gages", Exp. Mech. Volume 28 Number 4, pages 142, 1988.

7. Dally, J. W. and Berger, J. R., "A Strain Gage Method for Determining KI and KII in a Mixed Mode Stress Field", Spring Conf. on Exp. Mech. 603-612 (June 1986).

8. Sanford, R. J. and Dally, J. W., "A General Method for Determining Mixed-Mode Stress Intensity Factors From Isochromatic Fringe Patterns", Engineering Fracture Mechanics Vol. 11 pages 621-633, 1979.

9. Dally, J. W. and Riley, W. F., "Experimental Stress Analysis, Second Edition", McGraw-Hill Book Company 1978.

10. Sanford, R. J., Chona, R., Forney, W. L., and Irwin, G. R., "A Photoelastic Study of the Influence of Non Singular Stresses in Fracture Test Specimens", NUREG/CR-2179, ORNL/Sub-7778/2, August 1981.

11. Sanford, R. J., "Determining Fracture Parameters with Full-Field Optical Methods", Experimental Mechanics, p 241-247, September 1989.

12. Dally, J. W., and Etheridge, J. M., "A Three Parameter Method for Determining Stress Intensity Factors From Isochromatic Fringe Loops", Journal of Strain Analysis Vol. 13, No 2, p 91-95, 1978.

13. Paris, F., Picon, R. Marin, J. and Canas, J., "Photoelastic Determination of KI and KII: A Numerical Study on Experimental Data", Experimental Mechanics, Vol. 37, No. 1, p. 45-55, 1997.

14. MacKenzie, P. McA., Walker, C. A., and Giannettoni, R., "A Technique for Experimental Evaluation of Mixed Mode Stress Intensity Factors", International Journal of Fracture, No 62, p 139-148, 1993.

15. Post, D. and Baracat, W. A., "High-Sensitivity Moire Interferometry - A Simplified Approach", Experimental Mechanics, Vol 21, p 100-104, March 1981.

16. Weissman, E. M. and Post, D., "Moire Interferometry Near the Theoretical Limit", Applied Optics, Vol 21, No 9, p 1621-1623, May 1982.

17. Post, D., "Moire Interferometry", Engineering Applications of Optical Measurements, Presented at the 1982 Fall Meting of the Society for Experimental Mechanics, p 1-8, 1982.

18. Younis, N. T., "Study of Mixed Mode Stress Intensity Factors Using the Experimental Method of Caustics", Ph. D. Dissertation, Iowa State University, 1988.

19. Theocaris, P. S. and Gdoutios, E. G., "An Optical Method for Determining Opening Mode and Edge-Sliding Mode Stress Intensity Factors", Journal of Applied Mechanics, 39, p91-97, 1972.

20. Theocaris, P. S. and Papadopoulas, G. A., "Stress Intensity Factors from Reflected Caustics in Birefringent Plates with Cracks", Journal of Strain Analysis, 16, p29-36, 1981.

21. Theocaris, P. S., "Local Yielding Around a Crack Tip in Plexiglas", Journal of Applied Mechanics, Transactions of the ASME, p. 409-415, 1970.

22. Nigam, H. and Shukla, A., "Comparison of the Techniques of Caustic and Photoelasticty as Applied to Fracture", Proceedings of the 1986 SEM Spring Conference on Experimental Mechanics, p760-766, 1986.

23. Sanford, R. J., "Determining Fracture Parameters with Full Field Optical Methods", Proceedings of the VI International Congress on Experimental Mechanics, p. 975-981, 1988.

24. Perry, C. C. and Lissner, H. R., "The Strain Gage Primer, Second Edition", McGraw-Hill Book Company,1962.

25. Dally, J. W. and Sanford, R. J., "Measuring the Stress Intensity factor for Propagating Cracks with Strain Gages", Journal of Testing and Evaluation, JTEVA, Vol. 18, No. 4, p 240-249, July 1990.

26. Dally, J. W. and Sanford, R. J., "On Measuring the Instantaneous Stress Intensity Factor for Propagating Cracks", Advances in Fracture Research, Proceedings of the 7th International Conference on Fracture, p 3223-3230, 1989.

27. Sanford, R. J., Dally, J. W., and Berger, J. R., "An Improved Strain Gage Method for Measuring KID for a Propagating Crack", Proceedings of the 1989 SEM Spring Conference on Experimental Mechanics, p 655-661.

28. Dally, J. W. and Berger, J. R., "The Role of the Electrical Resistance Strain Gauge in Fracture Mechanics", Experimental Techniques in Fracture, SEM, p. 1-39, 1993.

29. Swanson, G. R. and Zachary, L. W., "Measurement of Crack Tip Location, Orientation, and Mixed Mode Stress Intensity Factors Using Near Crack Tip Strain Gages", Post Conference Proceedings of the 1996 VIII International Congress on Experimental Mechanics, p. 421-428, 1996.

30. Tada, H., Paris, P. C. and Irwin, G. R., "The Stress Analysis of Cracks Handbook", Del Research Corporation, Hellertown, Pennsylvania, 1973.

31. Rooke, D. P. and Cartwright, D. J., "Compendium of Stress Intensity Factors", The Hillingdon Press, Uxbridge, England, 1976.

32. Parker, A. P., "The Mechanics of Fracture and Fatigue", E. & F. N. Spon, NY, NY, 1981.

33. Wilson, C. D., "Linear Elastic Fracture Mechanics Primer", NASA TM - 103591, July 1992.

34. Solecki, J. S., "Fracture Mechanics, A Revision 4.4 Tutorial", Swanson Analysis Systems, Inc. 1989.

35. Cox, C. P., "A Handbook of Introductory Statistical Methods", J. Wiley & Sons, New York, 1987.

36. Berger, J. R. and Dally, J. W., "An Overdterministic Approach for Measuring the Opening Mode Stress Intensity Factor Using Strain Gages", Proceedings of the 1986 SEM Spring Conference on Experimental Mechanics, p 597-502, 1986.

37. Wolfe, C. M., Rust, B. W., Dunn, J. H. and Brown, I. E., "An Interactive Nonlinear Least Squares Program", NBS Technical Note 1238, July 1987.

38. Barnett, S., "Matrices Methods and Applications", Clarendon Press, Oxford, 1990.

39. Hornbeck, R. W., "Numerical Methods", Quantum Publishers, Inc., New York, 1975.

40. Jefferys, W. H., Fitzpatrick, M. J., McArthur, B. E., McCartney, J. E., "GAUSSFIT: A System for Least Squares and Robust Estimation", COSMIC Program # MFS-26108, 1988.

41. Berger, J. R., Dally, J. W., and Sanford, R. J., "Extent of Validity of Three-Parameter Crack-Tip Strain Fields", Proceedings, 1991 SEM Spring Conference on Experimental Mechanics, p 572-577, 1991.

42. Gerstle, W. H. and Abdalla, J. E. Jr., "Finite Element Meshing Criteria for Crack Problems", Fracture Mechanics Twenty First Symposium, ASTM STP 1074, J. P. Gudas, J. A. Joyce, and E. M. Hackett, Eds., American Society for Testing and Materials, Philadelphia, pp. 509-521, 1990.

43. Liebowitz, H. and Moyer, E. T. Jr., "Finite Element Methods in Fracture Mechanics", Computers and Structures, Vol 31, No1, p 1-9, 1989.

44. Mikkola, T. P. J. and Niemi, H., "Quality Assurance for Fracture Mechanical Finite Element Analysis", Computers and Structures, Vol 40, No 2, p271-279, 1991.

45. "SSME Incident Report, John C. Stennis Spce Center, Test Stand A-1, Test 901-666, 24 July 1991, Engine 0215, High Pressure Fuel TurboPump Second Stage Turbine Blade Failure", Rockwell International, Rocketdyne Division, Report RSS-8591-45, 1991.

46. "SSME EO215 Turbine Blade Corrective Action Summary", Rockwell International, Rocketdyne Division summary presentation, unpublished, 1992.

47. Lee, H., "Space Shuttle Main Engine High Pressure Fuel TurboPump Turbine Blade Cracking", NASA TM-100327, 1988.

48. Wilson, C., "Crack Growth in HPFTP Second Stage Turbine Blades", unpublished presentation, 1992.

ACKNOWLEDGMENTS

I wish to express my deep gratitude to Dr. Loren W. Zachary for his assistance and patience during this research.

I am thankful for Dr. James L. Cornette's suggestions and insights which led to the selection of weighting functions.

To Dr. Otto Buck, who assisted in obtaining and preparing the specimens, I thank you.

To Dr. Ambar K. Mitra and Dr. Frederick M. Graham, I thank you for your service on the program of study committee.

Dr. Jerald M. Vogal has my appreciation for agreeing to substitute on the program of study committee after the sad occasion of Dr. Frederick M. Graham's death.

I also wish to thank the National Aeronautics and Space Administration's Marshall Space Flight Center for sponsoring my graduate studies.

Finally, this would not have been possible without the love, support, and encouragement of my wife, Kay.